AD 407 055

CIVIL ENGINEERING STUDIES

STRUCTURAL RESEARCH SERIES NO. 266

A NUMERICAL PROCEDURE FOR THE ANALYSIS OF CONTAINED PLASTIC FLOW PROBLEMS

by
G. N. HARPER
and
A. ANG

Approved by
N. M. NEWMARK

Issued as a Technical Report
to the
DEFENSE ATOMIC SUPPORT AGENCY
DEPARTMENT OF DEFENSE
Contract DA-49-146-XZ-104

DEPARTMENT OF CIVIL ENGINEERING
UNIVERSITY OF ILLINOIS
URBANA, ILLINOIS
JUNE 1963

(4) #910 (5) 427.100

(6) A NUMERICAL PROCEDURE FOR THE ANALYSIS OF CONTAINED PLASTIC FLOW PROBLEMS

(7-9) NA
(11) June 63,
(12) 95 p.
(13) NA
(14) Reviewed
(16-19) NA
(50) 2
(51) Doctoral Thesis

(10) By

G. N. Harper

and

A. Ang

Approved by

N. M. Newmark

Issued as a Technical Report
to the

Defense Atomic Support Agency
Department of Defense
(15) Contract DA-49-146-XZ-104

Department of Civil Engineering
UNIVERSITY OF ILLINOIS
URBANA, ILLINOIS

June 1963

ACKNOWLEDGEMENT

This report was prepared as a doctoral thesis by Mr. G. N. Harper, Research Associate in Civil Engineering, and submitted to the Graduate College of the University of Illinois in partial fulfillment of the requirements for the Ph.D. degree. The work was done under the general direction of Dr. N. M. Newmark, Professor and Head of the Department of Civil Engineering, and the immediate supervision of Dr. A. Ang, Associate Professor of Civil Engineering.

The investigation was undertaken as part of a research program of the Department of Civil Engineering with the sponsorship of the Defense Atomic Support Agency under Contract No. DA-49-146-XZ-104.

The helpful cooperation of the staff of the Digital Computer Laboratory in the operation and use of the IBM 7090-1401 computer system (partially supported by a National Science Foundation grant, NSF-GP700) is gratefully acknowledged.

TABLE OF CONTENTS

LIST OF FIGURES

LIST OF FIGURES (Cont'd.)

I. INTRODUCTION

1.1 Object and Scope

~~The object of this investigation is~~ the development of a systematic numerical procedure for determining the displacements, strains, and stresses within a plane continuum is presented wherein certain regions have been strained beyond an elastic yield limit. Such a procedure should make possible the observation of the development of the stress and strain patterns around regions of high stress intensity~~, such as regions around notches, holes, and points of concentrated loads~~.

The procedure is restricted to plane, static problems; and the example problems are further restricted to plane strain conditions. The procedure itself is applicable to plane stress problems if the relations between stress and strain for plane stress conditions are substituted for those of plane strain. The material of the continuum is considered to be isotropic and elastic-perfectly-plastic and the problems are solved for continuously increasing external loads. Unloading from a plastically strained state is not considered.

The numerical procedure is essentially a relaxation technique applied to a discrete physical model composed of suitably arranged stress points and mass points. Plastic yielding and flow in the solid is characterized by the corresponding yielding and flow of the stress points of the model. Introduction of the discrete model reduces the problem of the continuum with an infinite number of degrees of freedom to a problem in particle mechanics with a finite number of degrees of freedom. The primary advantage of such a technique is that it makes possible the solution of

problems not tractable by ordinary mathematical analysis, particularly problems involving partial loadings and complicated boundary conditions. The basic disadvantage of the discrete model approach is its very finiteness--stresses and displacements are defined only at a finite number of points. Hence frequently the finite model can furnish only a rough quantitative measure of the true but unknown solution in the continuum. To gain some notion of the accuracy of the model used in this investigation, a problem in plane elasticity for which there is an analytic solution is solved by using the model and the results compared to the analytic solution.

Once the level of external loading has been raised to a sufficiently high level, the more highly stressed regions of the continuum begin to yield, or flow plastically. The initiation of yielding is determined by the Mises-Hencky yield criterion. Thereafter, yielded regions are assumed to obey the plastic stress-strain relations postulated by the Prandtl-Reuss theory. Two examples of problems wherein plastic flow has taken place over a finite region are included to demonstrate the application of the numerical procedure.

The entire procedure for handling plane problems of contained plastic flow in elastic-perfectly-plastic continua has been coded for use on the IBM 7090 digital computer. Only the two numerical solutions mentioned above are included in the thesis; an extensive investigation of the various problems of interest in contained plastic flow falls outside the scope of this work.

1.2 Historical Notes

This brief review of the literature is by no means intended to be complete. Only a few of the more important publications related to the present study are discussed. Several of these references (6), (8), (15), (22)[1] contain

1 Numbers in parentheses refer to corresponding entries in the Bibliography.

extensive bibliographies or footnotes through which more detailed access to the literature may be obtained.

The idea of replacing plane elastic continua with discrete models began to attract researchers' interest in the early 1940's--about the same time that Southwell (19) (20) developed efficient and practical relaxational techniques for the solution of highly complex systems. It is not at all surprising that the development of finite models should have awaited more efficient methods of computation, since by their very nature solutions determined with the use of models involve systems with a large number of simultaneous equations. Hrennikoff (10) and McHenry (13) were perhaps among the earliest of those who introduced "frameworks" or "lattice analogies" to solve problems in plane elasticity. Using hexagonal and square patterns as the basic module in the discrete model, Austin (3) and Dauphin (5) made informative comparisons of the model solution to the exact analytic solution for several problems in plane elasticity. Newmark (15) gives a good discussion of the use of models in several areas of structural analysis.

More recently, there has been a renewed interest in the development of models; this is partly prompted by more efficient computational devices. The advent of high-speed digital computers has induced many analysts to seek discrete models suitable for digital computation. The work of Clough (4) and Gaus (7) is typical of the model approach now being adopted in order to solve continuum problems on computers. It is interesting to note that none of the writers above make any mention of attempts to extend their models beyond the elastic range. Schnobrich (18) has indicated that considerations for future extension into plastic behavior influenced the selection of his model, though his work presents only elastic results.

The scientific study of the theory of plasticity seems to be much older than any serious study of finite models, for it extends back at least

to Coulomb and his study of yielding in soils in 1773. Any number of readable texts in the elementary theory (8), (9), (16), (17) are available, though the presentation here follows most closely that in Prager and Hodge (17) and Hoffman and Sachs (9). The only successful numerical solutions of problems in contained plastic flow known to the author are those presented by Allen and Southwell (1) and Jacobs (11). Their solutions are obtained by a rather tedious manual relaxation technique which yields values of the stress function from which the stresses are computed.

In summary then, it appears that both the theory of plasticity and the theory of models have attracted the efforts of able researchers, though there have been few, if any, attempts to apply the theory directly to a discrete model. Accordingly, it is the purpose of this investigation to develop a numerical procedure for solving problems of contained plastic flow with the use of a discrete model.

1.3 Notation

The following notation has been adopted for use in this thesis.

x	direction of axis
y	direction of axis
z	direction of axis (perpendicular to the plane of analysis)
u	displacement in x direction
v	displacement in y direction
η,h	displacement in horizontal direction
ξ,v	displacement in vertical direction
E	Young's modulus
ν	Poisson's ratio
G	shear modulus = $\frac{E}{2(1+\nu)}$

K	bulk modulus $= \frac{E}{3(1-2\nu)}$
k	yield stress in simple shear
S^T	total stress tensor
S^S	spherical stress tensor
S^D	deviator stress tensor
E^T	total strain tensor
E^S	spherical strain tensor
E^D	deviator strain tensor
s	mean normal stress $= \frac{1}{3}(\sigma_x + \sigma_y + \sigma_z)$
s_x	normal component of S^D in x direction $= \sigma_x - s$
s_y	normal component of S^D in y direction $= \sigma_y - s$
s_z	normal component of S^D in z direction $= \sigma_z - s$
e	mean normal strain $= \frac{1}{3}(\epsilon_x + \epsilon_y + \epsilon_z)$
e_x	normal component of E^D in x direction $= \epsilon_x - e$
e_y	normal component of E^D in y direction $= \epsilon_y - e$
e_z	normal component of E^D in z direction $= \epsilon_z - e$
s_1	principal normal component of stress deviation $= \sigma_1 - s$
s_2	principal normal component of stress deviation $= \sigma_2 - s$
s_3	principal normal component of stress deviation $= \sigma_3 - s$
e_1	principal normal component of strain deviation $= \epsilon_1 - e$
e_2	principal normal component of strain deviation $= \epsilon_2 - e$
e_3	principal normal component of strain deviation $= \epsilon_3 - e$
J_1	first invariant $= s_1 + s_2 + s_3$
J_2	second invariant $= \frac{1}{2}(s_1^2 + s_2^2 + s_3^2)$
J_3	third invariant $= \frac{1}{3}(s_1^3 + s_2^3 + s_3^3)$
W	work performed by stresses during a plastic distortion

F	axial force component at a stress point
S	shear force component at a stress point
X	body force per unit volume
Y	body force per unit volume
I	moment of inertia of a unit width of the reinforcing frame
A	cross-sectional area of a unit width of the reinforcing frame
σ_x	element of the total stress tensor
σ_y	element of the total stress tensor
σ_z	element of the total stress tensor
τ_{xy}	element of the total stress tensor
τ_{xz}	element of the total stress tensor
τ_{yz}	element of the total stress tensor
σ_1	principal normal stress
σ_2	principal normal stress
σ_3	principal normal stress
ϵ_x	element of the total strain tensor
ϵ_y	element of the total strain tensor
ϵ_z	element of the total strain tensor
$\frac{1}{2}\gamma_{xy}$	element of the total strain tensor
$\frac{1}{2}\gamma_{xz}$	element of the total strain tensor
$\frac{1}{2}\gamma_{yz}$	element of the total strain tensor
ϵ_1	principal normal strain
ϵ_2	principal normal strain
ϵ_3	principal normal strain
λ	factor of proportionality between stress and strain rate, horizontal or vertical distance between mass points

δ	distance along x or y axis between mass points
σ_{el}	level of external load at which first yielding begins
f	flexibility coefficient
P	concentrated external load

II. DESCRIPTION OF THE MODEL

2.1 Criteria for Selection of a Model

Historically, there have been at least two distinct criteria for selecting a finite mechanical model to replace a continuum. Hrennikoff (10) and Clough (4) both demand equality of deformation between model and continuum under similar loading conditions. It is interesting in this regard to quote Hrennikoff (10).

> It is now possible to formulate the basic principle governing determination of the framework pattern. The necessary and sufficient condition for equivalence of infinitesimal framework and solid material is equality in deformability of the two...

Hrennikoff's application of this criterion is questionable, since several of his simple framework patterns deform as does the continuum only if Poisson's ratio has the value 1/3. Michell (14) shows, however, that at least for simply connected regions the values of the elastic constants do not affect the computation of the stresses if the boundary conditions are specified by loading conditions rather than by displacement conditions. Nevertheless, any criterion which restricts the value of a material constant to a specific value cannot be completely satisfactory for treatment of the most general problems.

A second criterion that is sometimes used in the selection of a model was mentioned by Newmark (15) and attempted by Gaus (7), and was explicitly proposed by Ang (2) in the development of the model which is used in this thesis. The criterion is that there be a mathematical consistency between the finite equations governing the behavior of the model and the differential equations governing the behavior of the continuum. By this is meant that the equations for strains, stresses, equilibrium, and compatibility which are derived directly from the model should be the same as a set of finite difference equations of the corresponding differential relations governing the

continuum. If this requirement is met the requirement of equal deformability of a model and the corresponding continuum will automatically be satisfied, and no restriction need be placed on the value of Poisson's ratio or of any other elastic constant.

2.2 Description of the Model

The model used in this investigation possesses all the requirements of the second criterion cited above. The essential characteristics of the model are shown in Fig. 1, wherein a square grid has been superposed on the continuum. The mass of the continuum is concentrated at the intersections of the grid lines. Each of the mass points is connected through stress points to the neighboring mass points. Three components of stresses and strains are defined at each stress point (two perpendicular axial components and a shear component). Displacements in the continuum are defined only at the mass points while stresses and strains are defined only at the stress points. Modifications of the model to include a stiffened rectangular opening are also shown in Fig. 1.

There are two important advantages of the model configuration described above. First, all elements of the strain tensor and the stress tensor are defined at the same point. This is an important characteristic of the model, especially in extending its use to problems of plasticity. Second, horizontal and vertical boundaries of the model contain only mass points. Thus boundary conditions given in terms of either external tractions acting on the mass points or prescribed displacements of these mass points can be applied with equal ease.

2.3 Relation of the Model to Finite Difference Equations of the Continuum

The material presented in this section follows closely that given by Ang (2). For purposes of illustration the following notation is used. Superscript letters refer to stress point locations. Subscript letters x and y refer to the directions of the axes. Subscript numbers refer to mass point locations. Displacement components in the x and y directions are given by u and v, respectively. Sign convention is that established by Timoshenko (21).

The components of the strains at a typical stress point "a" are defined, with reference to Fig. 1, as follows:

$$\epsilon_x^a = \frac{u_{54}-u_{43}}{\delta}$$

$$\epsilon_y^a = \frac{v_{53}-v_{44}}{\delta} \qquad (1)$$

$$\gamma_{xy}^a = \frac{u_{53}-u_{44}}{\delta} + \frac{v_{54}-v_{43}}{\delta}$$

These strains, which are derived directly from the model, are identical to the finite difference expressions for the differential strain-displacement relations of the classical theory for plane continua under small deformations:

$$\epsilon_x = \frac{\partial u}{\partial x}$$

$$\epsilon_y = \frac{\partial v}{\partial y} \qquad (2)$$

$$\gamma_{xy} = \frac{\partial u}{\partial y} + \frac{\partial v}{\partial x}$$

The equation of equilibrium, in the x direction, for a typical interior mass point at "43" is (see Fig. 2)

$$(F_x^a - F_x^c) + (S_{xy}^b - S_{xy}^d) + \frac{X\delta^2}{2} = 0 \tag{3}$$

where X is the body force per unit volume. The volume of a parallelepiped of unit thickness and area $\lambda^2 = \frac{\delta^2}{2}$ is considered concentrated at each mass point. If the thickness of the model is taken as unity in the z direction, forces at the stress point "a" are obtained from the stresses as follows:

$$\begin{aligned} F_x^a &= \sigma_x^a \cdot \frac{\delta}{2} \\ F_y^a &= \sigma_y^a \cdot \frac{\delta}{2} \\ S_{xy}^a &= \tau_{xy}^a \cdot \frac{\delta}{2} \end{aligned} \tag{4}$$

Using Eqs. (4) in Eq. (3), the following equation of equilibrium, in terms of stresses, is obtained:

$$\frac{\sigma_x^a - \sigma_x^c}{\delta} + \frac{\tau_{xy}^b - \tau_{xy}^d}{\delta} + X = 0 \tag{5a}$$

A similar equation is obtained in the y direction:

$$\frac{\sigma_y^b - \sigma_y^d}{\delta} + \frac{\tau_{xy}^a - \tau_{xy}^c}{\delta} + Y = 0 \tag{5b}$$

These equilibrium equations, (5a) and (5b), are identical to the finite difference expressions for the differential equations of equilibrium governing the corresponding continuum:

$$\frac{\partial \sigma_x}{\partial x} + \frac{\partial \tau_{xy}}{\partial y} + X = 0 \tag{6a}$$

$$\frac{\partial \sigma_y}{\partial y} + \frac{\partial \tau_{xy}}{\partial x} + Y = 0 \tag{6b}$$

The strains in the model will necessarily satisfy the compatibility relation, since strain compatibility is essentially a requirement placed on the three components of strain in order to insure that the three strain components correspond to a physically possible displacement configuration. The model deals directly with displacements, and the strains are defined directly in terms of these displacements. Hence, it can be expected that the strains derived from the displacements of the model will identically satisfy the compatibility condition.

It is also possible to express the equations of equilibrium in terms of displacements. This is done below for a linearly elastic solid in plane strain. Similar relations exist for plane stress conditions. For this purpose it is necessary to express the three force components at the stress point "a" in terms of displacements, as follows:

$$F_x^a = \frac{E}{(1+\nu)(1-2\nu)}\left[(1-\nu)\,\frac{u_{54}-u_{43}}{\delta} + \nu\,\frac{v_{53}-v_{44}}{\delta}\right]\frac{\delta}{2}$$

$$F_y^a = \frac{E}{(1+\nu)(1-2\nu)}\left[(1-\nu)\,\frac{v_{53}-v_{44}}{\delta} + \nu\,\frac{u_{54}-u_{43}}{\delta}\right]\frac{\delta}{2} \qquad (7)$$

$$S_{xy}^a = \frac{E}{2(1+\nu)}\left[\frac{u_{53}-u_{44}}{\delta} + \frac{v_{54}-v_{43}}{\delta}\right]\frac{\delta}{2}$$

Eqs. (7) are essentially Hooke's stress-strain relationships for plane strain. Substitution of these and similar relations for the forces originating at the other stress points into Eq. (3) results in the following equation of equilibrium in the x direction, in terms of displacements:

$$\frac{E}{(1+\nu)(1-2\nu)}\left[2(1-\nu)\left(\frac{u_{54}-2u_{43}+u_{32}}{\delta^2}\right) + (1-2\nu)\left(\frac{u_{52}-2u_{43}+u_{34}}{\delta^2}\right) + \frac{(v_{53}-v_{42})-(v_{44}-v_{33})}{\delta^2}\right] + X = 0 \qquad (8)$$

A similar equation exists for equilibrium in the y direction. Note that this equation is identically the same as a finite difference equation for the differential equation of equilibrium, Eq. (9), governing the continuum.

$$\frac{E}{(1+\nu)(1-2\nu)}\left[2(1-\nu)\frac{\partial^2 u}{\partial x^2}+(1-2\nu)\frac{\partial^2 u}{\partial y^2}+\frac{\partial^2 v}{\partial x \partial y}\right]+X=0 \qquad (9)$$

2.4 Boundary Conditions

In general, boundary conditions (for either continua or discrete models) can be of two types: either the forces acting along some boundary or the displacements on the boundary are prescribed. As pointed out earlier, either type of condition can be imposed on the model. A few examples are given below to indicate how boundary conditions are prescribed for the model.

For greater flexibility and ease in programming, an extra line of mass points has been included on each of the four sides of the rectangular model, as indicated in Fig. 1 by dotted lines. Thus if the continuum being simulated is to be ten λ high and eight λ wide (demanding a grid of eleven rows and nine columns), there will actually be thirteen rows and eleven columns in the complete description of the model. Suppose that the continuum is known to possess symmetry about a vertical axis through a column of mass points. The boundary condition on the right edge of the model (see Fig. 1) is specified as follows:

$$\begin{aligned} u_{i6} &= v_{i4} \\ v_{i6} &= u_{i4} \end{aligned} \qquad i = 1, 2, \ldots, 6 \qquad (10)$$

If an external load is to be applied to the top surface of the continuum, the model will have equivalent concentrated loads applied at the

second row of mass points, and the extra top row of mass points will be neglected completely. If it is desired to hold the base of the continuum fixed against displacement, the bottom row of extra mass points is simply given a zero displacement.

In problems for which the model is being used to simulate an infinite half-space, the problem of what boundary conditions to impose on the left-most column of extra mass points arises. For vertical loadings which are symmetric about the center line, it has been assumed that the horizontal displacements of this left-most column are zero and that the vertical displacements of this left-most column of mass points will be equal to the vertical displacements of the column of mass points immediately to the right of this boundary column. When these vertical and horizontal motions are resolved into displacements in the x and y directions, the boundary conditions become

$$\begin{aligned} u_{i1} &= \frac{1}{2}(u_{i2} + v_{i2}) \\ v_{i1} &= \frac{1}{2}(u_{i2} + v_{i2}) \end{aligned} \qquad i = 1, 2, \ldots, 6 \qquad (11)$$

These examples indicate the manner in which boundary conditions are prescribed for the model. A variety of practically significant conditions can be conceived, and several different sets of boundary conditions were actually investigated during preparation of the numerical examples. An extensive treatment of the effect of various boundary conditions on the stress and displacement patterns is beyond the scope of the present work.

2.5 Modification of the Model to Include Interior Rectangular Openings

An example of the adaptability of the model approach to structural analysis is given in the problem of determining the stress pattern within a

plane solid around a rectangular opening, which opening may or may not be reinforced. In the general case, it is supposed that the opening is reinforced. If the opening is to be a cavity only, the modulus of elasticity of the reinforcing material is set equal to zero.

The reinforcement, if any, in the continuum is replaced in the model by a system of moment and axial springs. As shown in Fig. 1, the moment springs are located at the mass points, and the axial springs span from mass point to mass point in either a vertical or a horizontal direction. By means of the moment springs, shear forces due to moments in the reinforcing continuum can be simulated; axial springs simulate the direct tensile or compressive forces in the reinforcing continuum. Tensile forces in the axial springs are taken as positive. Sign convention for positive moments is basically dictated by the requirements for positive shears arising as a result of these moments. This sign convention is shown in Fig. 3.

The vertical or horizontal shearing forces acting on each mass point (depending on whether the mass point is on a horizontal or vertical reinforcing section, respectively) can be calculated from the differences in the moments acting at three consecutive mass points. Until a moment spring begins to yield, the moment can be computed directly from the displacements (Fig. 4) as follows:

$$M_{15} = \frac{-EI}{\sqrt{2}\lambda^2}\left[(u_{34}+v_{34}) - 2(u_{35}+v_{35}) + (u_{36}+v_{36})\right] \qquad (12)$$

where E is the modulus of elasticity of the reinforcing material, modified for plane strain, and I is the moment of inertia of a unit width of reinforcement. After a moment spring has reached its yield limit, it is assumed to hold the yield moment, even though the rotation of the section may increase considerably.

The vertical or horizontal axial forces acting on each mass can be determined as the algebraic difference of the axial springs acting on each side of the mass point. Until an axial spring yields, the force in a single axial spring can be computed from the displacements (Fig. 4) as follows:

$$F_{15} = \frac{AE}{\sqrt{2\lambda}} \left[(u_{36}-v_{36}) - (u_{35}-v_{35}) \right] \tag{13}$$

where A is the cross-sectional area of the reinforcement, E is the modulus of elasticity of the reinforcing material, modified for plane strain conditions. After an axial spring has reached its yield limit, it is assumed that the axial force maintains this yield level regardless of the values of the surrounding displacements.

Once the horizontal and vertical forces acting on a mass point as a result of the reinforcement are determined, they are resolved into x and y components and handled in the same way as the forces in the rest of the solid.

It is evident that a mass point which lies on an interior opening will have forces acting on it that are different from the forces acting on a general interior mass point. It is also evident that the forces acting on mass points which lie on the opening will vary depending on whether the mass point is on the top, bottom, side, or corner of the opening. For this reason a set of operators has been developed which computes the forces acting on a mass point, given the location of the mass point.

III. CONSTITUTIVE RELATIONS FROM THE THEORY OF PERFECT PLASTICITY

3.1 General Remarks on the Theory and Its Limitations

Any constitutive relationships of the theory of plasticity may be divided into the following three parts:

(1) stress-strain relations for the elastic region,

(2) yield criterion to define the initiation of yielding,

(3) stress-strain relations for the plastic region.

These three major divisions of the theory will be discussed in turn, after the associated assumptions and limitations are listed and after a set of notation that will be useful in the discussion of the theory is introduced.

There are three main assumptions underlying the theory of perfectly plastic material used in this investigation. These can be stated as follows:

(1) It is assumed that the Mises-Hencky yield condition accurately determines the beginning of yield. General considerations of isotropy and symmetry can furnish only the general form of the yield condition. Beyond this, any yield condition is a hypothesis which only tests can justify.

(2) It is assumed that there is no permanent volume change. This assumption, justified on the basis of experimental evidence for metals, leads to the result that the plastic strain is equal to the plastic deviator strain.

(3) During plastic flow, it is assumed that the deviator strain rate tensor is proportional to the instantaneous deviator stress. This is the familiar Prandtl-Reuss postulate.

In addition to these three main assumptions, it is possible to list several other restrictions on the theory:

(4) The material must be isotropic. This condition is used in developing the general form of the yield condition.

(5) There is no work hardening, and the material follows the stress-strain diagram of Fig. 5 when subjected to simple tension or compression.

(6) No unloading occurs. Once a stress point has yielded, it remains yielded under successive increments of external load.

(7) Time effects of loading, such as creep, are ignored.

(8) Displacements are small so that the small deformation theory of elasticity applies.

3.2 Definitions and Notation

The following definitions and notation are introduced for the purpose of describing the pertinent constitutive relationships used in this work.

$$\text{Total Stress Tensor} = S^{T} = \begin{matrix} \sigma_x & \tau_{xy} & \tau_{xz} \\ \tau_{xy} & \sigma_y & \tau_{yz} \\ \tau_{xz} & \tau_{yz} & \sigma_z \end{matrix} \tag{14}$$

$$\text{Spherical Stress Tensor} = S^{S} = \begin{matrix} s & 0 & 0 \\ 0 & s & 0 \\ 0 & 0 & s \end{matrix} \tag{15}$$

$$\text{Deviator Stress Tensor} = S^D = \begin{matrix} s_x & \tau_{xy} & \tau_{xz} \\ \tau_{xy} & s_y & \tau_{yz} \\ \tau_{xz} & \tau_{yz} & s_z \end{matrix} \tag{16}$$

where

$$s = \text{mean normal stress} = \frac{1}{3}(\sigma_x + \sigma_y + \sigma_z) \tag{17}$$

$$\begin{aligned} s_x &= \text{normal x-component of } S^D = \sigma_x - s \\ s_y &= \text{normal y-component of } S^D = \sigma_y - s \\ s_z &= \text{normal z-component of } S^D = \sigma_z - s \end{aligned} \tag{18}$$

With these notations, it is obvious that

$$S^T = S^S + S^D \tag{19}$$

$$s_x + s_y + s_z = \sigma_x + \sigma_y + \sigma_z - 3s = 0 \tag{20}$$

Principal normal stresses are designated by σ_1, σ_2, σ_3, (21)

Principal normal components of the stress deviator are

$$\begin{aligned} s_1 &= \sigma_1 - s \\ s_2 &= \sigma_2 - s \\ s_3 &= \sigma_3 - s \end{aligned} \tag{22}$$

A completely similar notation exists for strains.

$$\text{Total Strain Tensor} = E^T = \begin{matrix} \epsilon_x & \frac{1}{2}\gamma_{xy} & \frac{1}{2}\gamma_{xz} \\ \frac{1}{2}\gamma_{xy} & \epsilon_y & \frac{1}{2}\gamma_{yz} \\ \frac{1}{2}\gamma_{xz} & \frac{1}{2}\gamma_{yz} & \epsilon_z \end{matrix} \tag{23}$$

$$\text{Spherical Strain Tensor} = E^S = \begin{matrix} e & 0 & 0 \\ 0 & e & 0 \\ 0 & 0 & e \end{matrix} \tag{24}$$

$$\text{Deviator Strain Tensor} = E^D = \begin{matrix} e_x & \frac{1}{2}\gamma_{xy} & \frac{1}{2}\gamma_{xz} \\ \frac{1}{2}\gamma_{xy} & e_y & \frac{1}{2}\gamma_{yz} \\ \frac{1}{2}\gamma_{xz} & \frac{1}{2}\gamma_{yz} & e_z \end{matrix} \tag{25}$$

where

$$e = \text{mean normal strain} = \frac{1}{3}(\epsilon_x + \epsilon_y + \epsilon_z) \tag{26}$$

$$\begin{aligned} e_x &= \text{normal x-component of } E^D = \epsilon_x - e \\ e_y &= \text{normal y-component of } E^D = \epsilon_y - e \\ e_z &= \text{normal z-component of } E^D = \epsilon_z - e \end{aligned} \tag{27}$$

With these notations it is obvious that

$$E^T = E^S + E^D \tag{28}$$

$$e_x + e_y + e_z = \epsilon_x + \epsilon_y + \epsilon_z - 3e = 0 \tag{29}$$

Principal normal strains are designated as ϵ_1, ϵ_2, ϵ_3. (30)

Principal normal components of the strain deviator are

$$\begin{aligned} e_1 &= \epsilon_1 - e \\ e_2 &= \epsilon_2 - e \\ e_3 &= \epsilon_3 - e \end{aligned} \tag{31}$$

3.3 Elastic Stress-Strain Relations

In the elastic range the relationship between the elements of the stress and strain tensors is assumed to be that of Hooke's law. It is convenient to express this linear relationship in terms of the elements of the deviator stress and deviator strain tensors as follows:

$$\begin{aligned} s_x &= 2Ge_x & s_y &= 2Ge_y & s_z &= 2Ge_z \\ \tau_{xy} &= G\gamma_{xy} & \tau_{xz} &= G\gamma_{xz} & \tau_{yz} &= G\gamma_{yz} \end{aligned} \tag{32}$$

$$\sigma_x + \sigma_y + \sigma_z = 3K(\epsilon_x + \epsilon_y + \epsilon_z) \tag{33}$$

where

$$G = \frac{E}{2(1+\nu)} \tag{34}$$

$$K = \frac{E}{3(1-2\nu)} \tag{35}$$

Eqs. (32) can be expressed more concisely as

$$S^D = 2GE^D \tag{36}$$

Note that Eqs. (32) or Eqs. (36) are not six independent relations, since addition of $s_x + s_y + s_z = 0$ gives an identity. Accordingly, Eq. (33) is needed to give a complete statement of Hooke's law.

3.4 Yield Criterion

A yield criterion can be defined as a condition defining the limit of elasticity under any possible combination of stresses (8). The following considerations of isotropy and symmetry show what the general form of the

yield criterion must be. The Mises criterion is then presented and reduced for the plane strain condition.

Since Hooke's law is presumed to be valid in the elastic range, the strain at the very first instant of plastic deformation is uniquely determined by the stresses. Thus for this very first occurence of plastic straining, the yield condition can be written as a function of the stresses alone.

$$f(\sigma_x, \sigma_y, \sigma_z, \tau_{xy}, \tau_{xz}, \tau_{yz}) = 0 \tag{37}$$

Since the material is assumed to be isotropic, the value of f must not change if the coordinate axes are rotated. In other words, f must be an invariant of the stress tensor. The form of f can be further restricted by noting that mere hydrostatic pressure does not produce appreciable plastic deformation in metals (8). Therefore f is restricted to be an invariant of the deviator stress tensor.

Let the deviator stress tensor be referred to its principal axes. The following three linearly independent stress invariants are then chosen.

$$\begin{aligned} J_1 &= s_1 + s_2 + s_3 \\ J_2 &= \tfrac{1}{2}(s_1^2+s_2^2+s_3^2) = \tfrac{1}{2}(s_x^2+s_y^2+s_z^2) + \tau_{xy}^2 + \tau_{xz}^2 + \tau_{yz}^2 \\ J_3 &= \tfrac{1}{3}(s_1^3 + s_2^3 + s_3^3) \end{aligned} \tag{38}$$

Now any invariant of the deviator stress tensor can be expressed in terms of these three linearly independent stress invariants (17). But f is an invariant of the deviator stress tensor. Therefore it must be possible to express f from Eq. (37) in terms of J_2 and J_3:

$$F(J_2, J_3) = 0 \tag{39}$$

The yield criterion which is used in this investigation is that of Mises-Hencky and follows the general form above:

$$J_2 - k^2 = 0 \tag{40}$$

where k is the yield limit in simple shear. Note that this criterion depends only on J_2. For equivoluminal plane strain conditions, Eq. (40) reduces to

$$\left(\frac{\sigma_x - \sigma_y}{2}\right)^2 + \tau_{xy}^2 - k^2 = 0 \tag{41}$$

Eq. (41) is the form of the yield condition actually used in the model.

3.5 Plastic Stress-Strain Relations

In order to relate stress and strain in a material which is submitted to plastic flow, it is convenient to express the strain tensor in terms of elastic and plastic components. Single primes will be used to denote an elastic component, and double primes will denote a plastic component. Dots will denote rate of change with respect to increment of external load.

The essential nature of the relations between stress and strain during plastic flow is contained in assumptions (2) and (3) of section 3.1. The assumption that there is no permanent change of volume is expressed mathematically by Eq. (42).

$$e'' = \frac{1}{3}(\epsilon_x'' + \epsilon_y'' + \epsilon_z'') = 0 \tag{42}$$

This implies that the plastic strain deviation is identical to the plastic strain, or,

$$e_x'' = \epsilon_x'' \qquad e_y'' = \epsilon_y'' \qquad e_z'' = \epsilon_z'' \tag{43}$$

Assumption (3) of section 3.1 states that during plastic flow the deviator strain rate tensor is proportional to the instantaneous deviator stress tensor. This is expressed mathematically by Eq. (44) below:

$$\begin{aligned} 2G\dot{e}''_x &= \lambda s_x & 2G\dot{e}''_y &= \lambda s_y & 2G\dot{e}''_z &= \lambda s_z \\ G\dot{\gamma}''_{xy} &= \lambda \tau_{xy} & G\dot{\gamma}''_{xz} &= \lambda \tau_{xz} & G\dot{\gamma}''_{yz} &= \lambda \tau_{yz} \end{aligned} \tag{44}$$

where λ is a proportionality factor. Eqs. (44) are in the same form as the elastic stress-strain relations given in Eqs. (32).

The basic relationships which are assumed during plastic flow have now been presented. It is now necessary to apply these relations, along with the yield criterion Eq. (40) and the elastic relations of Eqs. (32) and (33) in order to develop the final relationships between the stress rates (incremental stresses), strain rates (incremental strains), and the instantaneous stresses.

The plastic strain rates have been expressed in terms of stresses by Eqs. (44). Similarly, the elastic strain rates are expressed in terms of stress rates by differentiating Eqs. (32):

$$\begin{aligned} 2G\dot{e}'_x &= \dot{s}_x & 2G\dot{e}'_y &= \dot{s}_y & 2G\dot{e}'_z &= \dot{s}_z \\ G\dot{\gamma}'_{xy} &= \dot{\tau}_{xy} & G\dot{\gamma}'_{xz} &= \dot{\tau}_{xz} & G\dot{\gamma}'_{yz} &= \dot{\tau}_{yz} \end{aligned} \tag{45}$$

Combining the elastic and plastic strain rates gives the total strain rate.

$$\begin{aligned} 2G\dot{e}_x &= 2G\dot{e}'_x + 2G\dot{e}''_x = \dot{s}_x + \lambda s_x \\ 2G\dot{e}_y &= 2G\dot{e}'_y + 2G\dot{e}''_y = \dot{s}_y + \lambda s_y \\ 2G\dot{e}_z &= 2G\dot{e}'_z + 2G\dot{e}''_z = \dot{s}_z + \lambda s_z \\ G\dot{\gamma}_{xy} &= G\dot{\gamma}'_{xy} + G\dot{\gamma}''_{xy} = \dot{\tau}_{xy} + \lambda \tau_{xy} \\ G\dot{\gamma}_{xz} &= G\dot{\gamma}'_{xz} + G\dot{\gamma}''_{xz} = \dot{\tau}_{xz} + \lambda \tau_{xz} \\ G\dot{\gamma}_{yz} &= G\dot{\gamma}'_{yz} + G\dot{\gamma}''_{yz} = \dot{\tau}_{yz} + \lambda \tau_{yz} \end{aligned} \tag{46}$$

Note that these relations apply only during plastic flow, i.e., when

$$J_2 = k^2 \quad \text{and} \quad \dot{J}_2 = 0 \tag{47}$$

In order to eliminate the proportionality factor λ from Eqs. (46), it is convenient to introduce the notation

$$\dot{W} = s_x\dot{e}_x + s_y\dot{e}_y + s_z\dot{e}_z + \tau_{xy}\dot{\gamma}_{xy} + \tau_{xz}\dot{\gamma}_{xz} + \tau_{yz}\dot{\gamma}_{yz} \tag{48}$$

where $\dot{W}$ may be interpreted as the rate at which stresses do work during a change of shape and to note that

$$\dot{J}_2 = s_x\dot{s}_x + s_y\dot{s}_y + s_z\dot{s}_z + 2\tau_{xy}\dot{\tau}_{xy} + 2\tau_{xz}\dot{\tau}_{xz} + 2\tau_{yz}\dot{\tau}_{yz} \tag{49}$$

By multiplying the first three of Eqs. (46) by s_x, s_y, s_z and the last three of Eqs. (46) by $2\tau_{xy}$, $2\tau_{xz}$, $2\tau_{yz}$, respectively, and adding, there results

$$\begin{aligned} 2G\dot{W} &= s_x\dot{s}_x + \lambda s_x^2 + s_y\dot{s}_y + \lambda s_y^2 + s_z\dot{s}_z + \lambda s_z^2 \\ &+ 2\tau_{xy}\dot{\tau}_{xy} + 2\lambda\tau_{xy}^2 + 2\tau_{xz}\dot{\tau}_{xz} + 2\lambda\tau_{xz}^2 + 2\tau_{yz}\dot{\tau}_{yz} + 2\lambda\tau_{yz}^2 \\ &= \dot{J}_2 + \lambda(s_x^2 + s_y^2 + s_z^2 + 2\tau_{xy}^2 + 2\tau_{xz}^2 + 2\tau_{yz}^2) \\ &= \dot{J}_2 + 2\lambda J_2 \end{aligned} \tag{50}$$

But during plastic flow,

$$J_2 = k^2 \quad \text{and} \quad \dot{J}_2 = 0 \tag{47}$$

Hence,

$$2G\dot{W} = 2\lambda k^2 \tag{51}$$

and,

$$\lambda = \frac{G\dot{W}}{k^2} \tag{52}$$

Substituting this value of λ into Eqs. (46), it is possible to solve for the deviator stress rates, which gives the following:

$$\begin{aligned}
\dot{s}_x &= 2G(\dot{e}_x - \frac{\dot{W}}{2k^2} s_x) & \dot{\tau}_{xy} &= G(\dot{\gamma}_{xy} - \frac{\dot{W}}{k^2} \tau_{xy}) \\
\dot{s}_y &= 2G(\dot{e}_y - \frac{\dot{W}}{2k^2} s_y) & \dot{\tau}_{xz} &= G(\dot{\gamma}_{xz} - \frac{\dot{W}}{k^2} \tau_{xz}) \\
\dot{s}_z &= 2G(\dot{e}_z - \frac{\dot{W}}{2k^2} s_z) & \dot{\tau}_{yz} &= G(\dot{\gamma}_{yz} - \frac{\dot{W}}{k^2} \tau_{yz})
\end{aligned} \tag{53}$$

To obtain the total stress rates it is necessary to add the deviator stress rates from Eqs. (53) to the spherical stress rate which can be obtained by differentiating Eq. (33):

$$\dot{s} = 3K\dot{e} \tag{54}$$

Adding Eqs. (53) and (54) results in the total stress rates, as follows:

$$\begin{aligned}
\dot{\sigma}_x &= \dot{s}_x + \dot{s} = 2G(\dot{e}_x - \frac{\dot{W}}{2k^2} s_x) + 3K\dot{e} & \dot{\tau}_{xy} &= G(\dot{\gamma}_{xy} - \frac{\dot{W}}{k^2} \tau_{xy}) \\
\dot{\sigma}_y &= \dot{s}_y + \dot{s} = 2G(\dot{e}_y - \frac{\dot{W}}{2k^2} s_y) + 3K\dot{e} & \dot{\tau}_{xz} &= G(\dot{\gamma}_{xz} - \frac{\dot{W}}{k^2} \tau_{xz}) \\
\dot{\sigma}_z &= \dot{s}_z + \dot{s} = 2G(\dot{e}_z - \frac{\dot{W}}{2k^2} s_z) + 3K\dot{e} & \dot{\tau}_{yz} &= G(\dot{\gamma}_{yz} - \frac{\dot{W}}{k^2} \tau_{yz})
\end{aligned} \tag{55}$$

Eqs. (55) give the desired relationships between the stress rates, strain rates, and instantaneous stresses.

3.6 An Incremental Form of the Plasticity Relations for Application to the Model

In general, the application of the plasticity relations to the model is closely associated with the three stages of material behavior presented in sections 3.3 through 3.5. The applications of Hooke's law and the Mises-Hencky yield criterion to the model are straightforward, since the strains can be

computed from the displacements by relations similar to Eqs. (1) and the stresses (or forces) at a stress point can be computed directly from the displacements by relations similar to Eqs. (7). Accordingly, the discussion which follows is concerned with the development of an incremental form of the Prandtl-Reuss relations for application to the model.

Eqs. (55) are first reduced to an incremental form. Note that for plane problems the number of relations is reduced from six to three. Therefore,

$$\begin{aligned} \Delta\sigma_x &= \Delta s_x + \Delta s \\ \Delta\sigma_y &= \Delta s_y + \Delta s \\ \Delta\tau_{xy} &= G\left(\Delta\gamma_{xy} - \frac{\Delta W}{k^2}\tau_{xy}\right) \end{aligned} \tag{56}$$

For plane strain conditions, Eqs. (53) are reduced to

$$\begin{aligned} \Delta s_x &= 2G\left(\Delta e_x - \frac{\Delta W}{2k^2} s_x\right) \\ \Delta s_y &= 2G\left(\Delta e_y - \frac{\Delta W}{2k^2} s_y\right) \\ \Delta\tau_{xy} &= G\left(\Delta\gamma_{xy} - \frac{\Delta W}{k^2}\tau_{xy}\right) \end{aligned} \tag{57}$$

and Eq. (54) becomes

$$\Delta s = 3K\Delta e = K(\Delta\epsilon_x + \Delta\epsilon_y) \tag{58}$$

The incremental $\dot{W}$ becomes

$$\Delta W = s_x\Delta e_x + s_y\Delta e_y + s_z\Delta e_z + \tau_{xy}\Delta\gamma_{xy} \tag{59}$$

But

$$s_z = \sigma_z - \frac{1}{3}(\sigma_x + \sigma_y + \sigma_z) \tag{60}$$

Where, for plane strain,

$$\sigma_z = \nu\ (\sigma_x + \sigma_y) \tag{61}$$

and during plastic flow

$$\nu = 1/2 \tag{62}$$

Hence,

$$s_z = \frac{1}{2}\ (\sigma_x + \sigma_y) - \frac{1}{3}\ (\sigma_x + \sigma_y + \frac{\sigma_x+\sigma_y}{2}) = 0 \tag{63}$$

Thus,

$$\begin{aligned}
s_x &= \sigma_x - \frac{1}{3}\ (\sigma_x + \sigma_y + \frac{\sigma_x+\sigma_y}{2}) = \frac{\sigma_x-\sigma_y}{2} \\
s_y &= \sigma_y - \frac{1}{3}\ (\sigma_y + \sigma_x + \frac{\sigma_x+\sigma_y}{2}) = \frac{\sigma_y-\sigma_x}{2} = -s_x \\
e_x &= \epsilon_x - \frac{1}{3}\ (\epsilon_x + \epsilon_y) = \frac{2\epsilon_x-\epsilon_y}{3} \\
\Delta e_x &= \frac{2\Delta\epsilon_x - \Delta\epsilon_y}{3} \\
e_y &= \epsilon_y - \frac{1}{3}\ (\epsilon_x + \epsilon_y) = \frac{2\epsilon_y-\epsilon_x}{3} \\
\Delta e_y &= \frac{2\Delta\epsilon_y - \Delta\epsilon_x}{3}
\end{aligned} \tag{64}$$

Substituting these values, Eqs.(64), into Eq. (59) yields an incremental ΔW, which reads,

$$\Delta W = \frac{1}{2}\ (\sigma_x - \sigma_y)(\Delta\epsilon_x - \Delta\epsilon_y) + \tau_{xy}\Delta\gamma_{xy} \tag{65}$$

Using the expressions for ΔW, Δe_x, and s_x from Eqs. (64) and (65) in Eq. (56), $\Delta\sigma_x$ becomes

$$\Delta\sigma_x = 2G\left[\frac{2\Delta\epsilon_x - \Delta\epsilon_y}{3} - \frac{\frac{1}{2}(\sigma_x - \sigma_y)(\Delta\epsilon_x - \Delta\epsilon_y) + \tau_{xy}\Delta\gamma_{xy}}{2k^2}\left(\frac{\sigma_x - \sigma_y}{2}\right)\right] + K(\Delta\epsilon_x + \Delta\epsilon_y) \tag{66}$$

Collecting terms gives

$$\Delta\sigma_x = \Delta\epsilon_x\left[\frac{4G + 3K}{3} - \frac{G}{k^2}\left(\frac{\sigma_x - \sigma_y}{2}\right)^2\right] + \Delta\epsilon_y\left[\frac{-2G + 3K}{3} + \frac{G}{k^2}\left(\frac{\sigma_x - \sigma_y}{2}\right)^2\right] + \Delta\gamma_{xy}\left[\frac{-G\tau_{xy}}{k^2}\left(\frac{\sigma_x - \sigma_y}{2}\right)\right] \tag{67}$$

Similar expressions are obtained for $\Delta\sigma_y$ and $\Delta\tau_{xy}$, as follows:

$$\Delta\sigma_y = \Delta\epsilon_x\left[\frac{-2G + 3K}{3} + \frac{G}{k^2}\left(\frac{\sigma_x - \sigma_y}{2}\right)^2\right] + \Delta\epsilon_y\left[\frac{4G + 3K}{3} - \frac{G}{k^2}\left(\frac{\sigma_x - \sigma_y}{2}\right)^2\right] + \Delta\gamma_{xy}\left[\frac{G}{k^2}\tau_{xy}\left(\frac{\sigma_x - \sigma_y}{2}\right)\right] \tag{68}$$

$$\Delta\tau_{xy} = \Delta\epsilon_x\left[\frac{-G}{k^2}\tau_{xy}\left(\frac{\sigma_x - \sigma_y}{2}\right)\right] + \Delta\epsilon_y\left[\frac{G}{k^2}\tau_{xy}\left(\frac{\sigma_x - \sigma_y}{2}\right)\right] + \Delta\gamma_{xy}\left[G\left(1 - \frac{\tau_{xy}^2}{k^2}\right)\right] \tag{69}$$

These last three equations are the incremental relationships with which the incremental stress components in a plastic region are computed.

These incremental stress components are added to the existing stress components at a stress point to obtain the total stresses acting at a yielded stress point.

In order to compute the quantities $\Delta\epsilon_x$, $\Delta\epsilon_y$, $\Delta\gamma_{xy}$ which appear in Eqs. (67) through (69), two sets of displacements corresponding to two consecutive load levels are required. One set of displacements is the set which is being generated for the current level of external load; the other set is that computed for the previous external load level. The quantities $\Delta\epsilon_x$, $\Delta\epsilon_y$, $\Delta\gamma_{xy}$ are computed as the differences in strains determined from these two sets of displacements.

IV. SYSTEMATIC RELAXATION PROCEDURE FOR DETERMINING DISPLACEMENTS

4.1 Preliminary Remarks

When a problem in continuum mechanics is replaced by a corresponding problem in particle mechanics involving a discrete model, the question of how to determine the equilibrium displacements in the model arises. Perhaps the most obvious solution is to write and solve the set of simultaneous linear algebraic equations (equations similar to Eq. (8)) for the unknown displacement components u_i and v_i. Such an approach has significant disadvantages, however. The preparation of the equations, whether it be done by hand or by an intricate program for the computer, involves a considerable amount of labor. In addition, even with machines as large as the IBM 7090 the number of equations which can be solved by the standard library subroutines is limited to about 150. And perhaps most important, the changes in the coefficients for the displacements resulting from yielding of one or more stress points are not at all easy to determine.

A more flexible and practical approach to the problem is the relaxation procedure described below. Such an approach eliminates completely the preparation of simultaneous equations, and can handle a very large number of displacement components (of the order of several thousand). An additional advantage of the relaxation method is the physical meaning that can be attached to each step of the procedure. This is of considerable help in determining plastic stresses and strains.

4.2 The Relaxation Procedure

The relaxation procedure used for determining the displacements can be graphically summarized by means of the flow diagram presented in Fig. 6.

All mass points of the model are initially in equilibrium with zero displacements and no external load. The first increment of external load is then applied to the boundary mass points (or other specified mass points), thus destroying the equilibrium of the loaded mass points. The following operations are then performed for each mass point of the model.

The forces acting on a mass point are determined as follows. External forces acting on the mass point are given as a part of the loading pattern applied to the model. Internal forces, originating at the stress points, are determined uniquely in the elastic range from the displacements surrounding the stress points by equations similar to Eqs. (7). After a stress point has yielded, the force components at that stress point are determined both by the surrounding displacements and the past history of that particular stress point. Incremental plastic forces are determined from the incremental plastic stresses given by Eqs. (67), (68), and (69). These incremental plastic forces are then added to the last set of equilibrium forces at the stress point to obtain the current total plastic forces acting at the yielded stress point.

After the forces acting on a given mass point are determined, a summation of all the forces acting in the x direction is made. In general, this will result in a residual force which is an indication of the amount by which the mass point is out of equilibrium in the x direction. The mass point is then displaced through a small distance in the x direction equal to the product of the residual and a flexibility coefficient.

Similar operations are performed for the y direction. This places the current mass point in equilibrium, though in general it will destroy the equilibrium of surrounding mass points by a small amount. The procedure is repeated for each mass point until every mass point has been moved once in

the x direction and once in the y direction, thus completing one cycle of relaxation.

After every relaxation cycle, each mass point is inspected to determine if it is in equilibrium. If not, the relaxation process is repeated until all mass points are in equilibrium to within a prescribed allowable error. When all mass points are in equilibrium, then all the stress points are inspected for yielding by the Mises-Hencky yield criterion, Eq. (41), and the yielded regions are recorded. All the displacements and stresses for the equilibrium configuration just obtained are also recorded. If desired, the external load is given a new increment and the complete procedure is repeated for each load increment in order to trace the development of plastic yielding from one stress point to another. The following example demonstrates the manner in which the computations are performed.

4.3 A Computational Example

Consider the elementary example shown in Fig. 7. Only mass points "43" and "53" are free to move; due to symmetry about a vertical line through these mass points, the u and v displacements at a mass point are equal:

$$\begin{aligned} u_{43} &= v_{43} \\ u_{53} &= v_{53} \end{aligned} \tag{70}$$

Hence there are only two unknown displacements in the problem, u_{43} and u_{53}. Using the material constants, dimensions, and loading shown in Fig. 7, it is possible to write two simultaneous linear algebraic equations (similar to Eq. (8)) for the elastic behavior of the system in terms of the two unknowns, u_{43} and u_{53}. Solution of these two equations yields

$$\begin{aligned} u_{43} = v_{43} &= 1.010 \times 10^{-3} \text{ inches} \\ u_{53} = v_{53} &= .252 \times 10^{-3} \text{ inches} \end{aligned} \tag{71}$$

Converting these displacements to elastic stress components by means of Eqs. (7) and (4) gives

$$\begin{aligned} \sigma_x^a &= -.7857 \text{ ksi} & \sigma_x^m &= -.2143 \text{ ksi} \\ \sigma_y^a &= -.0714 \text{ ksi} & \sigma_y^m &= -.0714 \text{ ksi} \\ \tau_{xy}^a &= -.2143 \text{ ksi} & \tau_{xy}^m &= -.0714 \text{ ksi} \end{aligned} \tag{72}$$

These values will now be used to measure the progress of the relaxation procedure.

Before beginning the systematic relaxation procedure, it is first necessary to convert external pressures to concentrated loads for application at the mass points and to determine the flexibility coefficients for each mass point. For example, if an external vertical pressure of 1 ksi is acting on the top surface of the model shown in Fig. 7, the concentrated vertical force acting on mass point "43", which arises from this pressure acting over a distance of $\lambda/2 = 1/2$ inch on either side of mass point "43", is

$$P_v = (1 \text{ ksi})\left(\frac{1"}{2} + \frac{1"}{2}\right)(1") = 1 \text{ kip} \tag{73}$$

where the thickness of the model is taken to be one inch. This vertical force is then resolved into components in the x and y directions for application at mass point "43":

$$\begin{aligned} P_x &= .707 \text{ kip} \\ P_y &= .707 \text{ kip} \end{aligned} \tag{74}$$

The flexibility coefficient for a mass point is obtained from a consideration of the effect of a unit force acting on the mass point. For example, a unit external force of one kip applied in the x direction at mass point "43" is resisted by internal force components acting at stress points "a" and "b."

$$\text{External Load} = 1 \text{ kip} = -(F_x^a + S_{xy}^b) \tag{75}$$

Expressing F_x^a and S_{xy}^b in terms of displacements by means of equations similar to Eqs. (7) and noting that all displacement components except u_{43} are held fixed gives.

$$1 = -\frac{E}{(1+\nu)(1-2\nu)}(1-\nu)\left(\frac{-u_{43}}{\delta}\right)\frac{\delta}{2} - \frac{E}{2(1+\nu)}\left(\frac{-u_{43}}{\delta}\right)\frac{\delta}{2} \tag{76}$$

Solving Eq. (76) for u_{43} yields the flexibility coefficient in the x direction:

$$u_{43} = f_x^{43} = \frac{4(1+\nu)(1-2\nu)}{(3-4\nu)E} \tag{77}$$

Because of the symmetrical arrangement of the force components acting on mass point "43", the flexibility coefficient in the y direction is equal to f_x^{43}:

$$f_y^{43} = f_x^{43} = \frac{4(1+\nu)(1-2\nu)}{(3-4\nu)E} \tag{78}$$

A similar derivation gives the flexibility coefficients for mass point "53":

$$f_y^{53} = f_x^{53} = \frac{2(1+\nu)(1-2\nu)}{(3-4\nu)E} \tag{79}$$

If E and ν take on the values 1000 ksi and 0.25, respectively, as shown in Fig. 7, then these flexibility coefficients become

$$\begin{aligned} f_x^{43} &= f_y^{43} = .001250 \text{ inches/kip} \\ f_x^{53} &= f_y^{53} = .000625 \text{ inches/kip} \end{aligned} \tag{80}$$

With these values for the concentrated external loads and flexibility coefficients, it is possible to begin the relaxation procedure. The following step numbers make reference to the flow diagram of Fig. 6.

Step	Operation
1	Set $u_{43} = v_{43} = u_{53} = v_{53} = 0$. Also set force components = 0.
2	Apply the increment of external load to mass point "43". $P_x = .707$ kips $P_y = .707$ kips
3	Begin with mass point "43".
4	No stress point has yet yielded, since all stress components are initially = 0. Go to 5b.
5b	On the first cycle all force components are computed as zero, since no mass point has yet been moved.
6	On the first cycle, only external forces are non-zero. Hence, $\sum F_x = P_x = +.707$ kips $\sum F_y = P_y = +.707$ kips
7	New u_{43} = old $u_{43} + f_x^{43} (\sum F_x)$ $u_{43} = 0 + .00125\ (.707) = .884 \times 10^{-3}$ inches Similarly, $v_{43} = 0 + .00125\ (.707) = .884 \times 10^{-3}$ inches Note that these displacements of mass point "43" destroy the equilibrium of mass point "53".
8	The current mass point, "43", is not the last mass point. Go to 9.
9	Take mass point "53". Got to 4.
4	Again no stress point has yielded, since yielding can occur only after an equilibrium configuration has been reached. Go to 5b.

Step	Operation

5b Force components at stress points "a" and "b" are computed from Eqs. (7), taking account of the evanescence of all displacement components except $u_{43} = v_{43}$, $u_{53} = v_{53}$. Note that only those components acting on mass point "53" are computed.

$$F_y^a = \frac{E}{(1+\nu)(1-2\nu)} \left[(1-\nu)\frac{v_{53}}{\delta} - \nu \frac{u_{43}}{\delta}\right] \frac{\delta}{2}$$

$$= \frac{1000}{(1+.25)(1-.50)} \left[(1-.25)(0) - .25(.000884)\right] \frac{1}{2}$$

$$= -.177 \text{ kips}$$

$$S_{xy}^a = \frac{E}{2(1+\nu)} \left[\frac{u_{53}}{\delta} - \frac{v_{43}}{\delta}\right] \frac{\delta}{2}$$

$$= \frac{1000}{2(1+.25)} \left[0 - .000884\right] \frac{1}{2} = -.177 \text{ kips}$$

$$F_x^b = \frac{E}{(1+\nu)(1-2\nu)} \left[(1-\nu)\frac{u_{53}}{\delta} - \nu \frac{v_{43}}{\delta}\right] \frac{\delta}{2}$$

$$= \frac{1000}{(1+.25)(1-.50)} \left[(1-.25)(0) - .25(.000884)\right] \frac{1}{2}$$

$$= -.177 \text{ kips}$$

$$S_{xy}^b = \frac{E}{2(1+\nu)} \left[-\frac{u_{43}}{\delta} + \frac{v_{53}}{\delta}\right] \frac{\delta}{2}$$

$$= \frac{1000}{2(1+.25)} \left[-.000884 + 0\right] \frac{1}{2} = -.177 \text{ kips}$$

Note that for the first cycle, mass point "53" has not yet been moved. Hence $u_{53} = v_{53} = 0$ and all force components

Step | Operation

at "m" and "n" = 0. From considerations of symmetry, it can also be concluded that

$$F_y^a = F_x^b$$

$$S_{xy}^a = S_{xy}^b$$

The equality of the shearing forces and the axial forces at a stress point on this first cycle is purely coincidental.

6 Following the sign convention of Fig. 2 for positive forces,

$$\sum F_x = -S_{xy}^a - F_x^b + S_{xy}^n + F_x^m$$

$$= + .177 + .177 + 0 + 0 = + .354 \text{ kips}$$

$$\sum F_y = - F_y^a - S_{xy}^b + F_y^n + S_{xy}^m$$

$$= + .177 + .177 + 0 + 0 = +.354 \text{ kips}$$

7 New u_{53} = old u_{53} + f_x^{43} ($\sum F_x$)

$$u_{53} = 0 + .000625\ (.354) = .221 \times 10^{-3} \text{ inches}$$

Similarly,

$$v_{53} = 0 + .000625\ (.354) = .221 \times 10^{-3} \text{ inches}$$

Note that these displacements of mass point "53" destroy the equilibrium of mass point "43".

8 This is the last mass point and the end of the first cycle of relaxation. Go to 10.

10 All mass points are not in equilibrium, since the displacements u_{53} and v_{53} under step 7 above destroyed the equilibrium of mass point "43". Hence there must be a second cycle of

relaxation, beginning at step 3. Note, however, that in only one cycle of relaxation the displacement components have attained nearly 90 percent of their final values.

The operations listed above demonstrate the procedure for elastic behavior. Suppose that a sufficient number of relaxation cycles has been performed to bring both mass points to within an acceptable error in the equilibrium equations. The following discussion indicates how the yield criterion is applied (step 11 of Fig. 6) and how the force components at a yielded stress point (step 5a of Fig. 6) are computed.

To illustrate the application of the yield criterion, assume that the yield stress in simple tension for the material is 35 ksi. Then the yield stress in simple shear is

$$k^2 = \left(\frac{\sigma_{yield}}{2}\right)^2 = \left(\frac{35}{2}\right)^2 = 306 \tag{81}$$

Applying the yield criterion, Eq. (41), to stress point "a" gives

$$\begin{aligned} &\left(\frac{-.7856 + .0714}{2}\right)^2 + (-.2142)^2 - 306 < 0 \\ &0.174 - 306 < 0 \end{aligned} \tag{82}$$

and to stress point "m" gives

$$\begin{aligned} &\left(\frac{-.214 + .071}{2}\right)^2 + (-.071)^2 - 306 < 0 \\ &0.010 - 306 < 0 \end{aligned} \tag{83}$$

Obviously both stress points are far from yield at an external pressure of only 1 ksi. Indeed, first yielding will take place at stress point "a" at an external vertical pressure of

$$\sqrt{\frac{306}{.174}}\ 1\ \text{ksi} = 42\ \text{ksi} \tag{84}$$

Note that this value of external stress is considerably greater than the yield stress in simple tension or compression of 35 ksi assumed for the material. This is characteristic of failure or yielding in two dimensional stress systems, and will be evident again in the numerical problems presented in Chapter V.

Until the load level has reached 42 ksi, all stresses and displacements increase linearly. When this elastic limit has been reached, the corresponding displacements and stresses are 42 times those of Eqs. (71) and (72):

$$\begin{aligned}
u_{43} &= v_{43} = 4.242 \times 10^{-2}\ \text{inches} \\
u_{53} &= v_{53} = 1.058 \times 10^{-2}\ \text{inches} \\
\sigma_x^a &= -33.00\ \text{ksi} \qquad \sigma_x^m = -9.00\ \text{ksi} \\
\sigma_y^a &= -3.00\ \text{ksi} \qquad \sigma_y^m = -3.00\ \text{ksi} \\
\tau_{xy}^a &= -9.00\ \text{ksi} \qquad \tau_{xy}^m = -3.00\ \text{ksi}
\end{aligned} \tag{85}$$

These values are recorded, and are used to determine the total displacements and stresses for the first load increment above the 42 ksi load level.

Suppose now that the load level is increased to five percent above this elastic limit, i.e., to 1.05 (42) = 44.1 ksi. As a first approximation to the final displacements at this new load level, the displacements of Eqs. (85) are also increased by five percent.

$$\begin{aligned}
u_{43} &= v_{43} = 4.454 \times 10^{-2}\ \text{inches} \\
u_{53} &= v_{53} = 1.111 \times 10^{-2}\ \text{inches}
\end{aligned} \tag{86}$$

Note that two sets of displacements are available: the last set of equilibrium displacements, Eqs. (85), and the current set of displacements, Eqs. (86)

(which in general are not compatible with the condition of equilibrium). These two sets of displacements are necessary in order to compute the incremental plastic stress components according to the discussion in section 3.6.

In order to compute the incremental plastic stress components, it is necessary to compute first the strains at the stress point "a", for both levels of external load, by Eqs. (1):

For load level = 42 ksi:

$$\epsilon_x^a = -\frac{u_{43}}{\delta} = -\frac{.04242}{1.414} = -.03000$$

$$\epsilon_y^a = \frac{v_{53}}{\delta} = \frac{.01058}{1.414} = +.00749$$

$$\gamma_{xy}^a = \frac{u_{53}-v_{43}}{\delta} = \frac{.01058 - .04242}{1.414}$$

$$= -.02252 \qquad (87)$$

For load level = 44.2 ksi:

$$\epsilon_x^a = -\frac{.04454}{1.414} = -.03150$$

$$\epsilon_y^a = \frac{.01111}{1.414} = +.00786 \qquad (88)$$

$$\gamma_{xy}^a = \frac{.01111-.04454}{1.414} = -.02364$$

The incremental strains in Eqs. (67), (68), and (69) are obtained by subtracting Eqs. (87) from Eqs. (88):

$$\Delta\epsilon_x = -.03150 + .03000 = -.00150$$

$$\Delta\epsilon_y = .00786 - .00749 = +.00037 \qquad (89)$$

$$\Delta\gamma_{xy} = -.02364 + .02252 = -.00112$$

Before computing $\Delta\sigma_x$, $\Delta\sigma_y$, and $\Delta\tau_{xy}$, it is convenient to compute the numerical values for G and K:

$$G = \frac{E}{2(1+\nu)} = \frac{1000}{2(1+.25)} = 400$$
$$K = \frac{E}{3(1-2\nu)} = \frac{1000}{3(1-.50)} = 667 \qquad (90)$$

Note that instantaneous values of the stress components are required in Eqs. (67), (68), and (69) in order to compute the incremental stress components. For small increments in the external loading, the instantaneous stresses are very nearly equal to the stresses at the last equilibrium configuration, Eqs. (85).

Substitution of Eqs. (85), (89), and (90) into Eqs. (67), (68), and (69) gives the following:

$$\begin{aligned}
\Delta\sigma_x^a &= (-.00150)\left[\frac{4(400)+3(667)}{3} - \frac{400}{306}\left(\frac{-33+3}{2}\right)^2\right] \\
&\quad + (.00037)\left[\frac{-2(400)+3(667)}{3} + \frac{400}{306}\left(\frac{-33+3}{2}\right)^2\right] \\
&\quad + (-.00112)\left[\frac{-400(-9)}{306}\left(\frac{-33+3}{2}\right)\right] \\
&= -.90 \text{ ksi} \\
\Delta\sigma_y^a &= (-.00150)\left[\frac{-2(400)+3(667)}{3} + \frac{400}{306}\left(\frac{-33+3}{2}\right)^2\right] \\
&\quad + (.00037)\left[\frac{4(400)+3(667)}{3} - \frac{400}{306}\left(\frac{-33+3}{2}\right)^2\right] \\
&\quad + (-.00112)\left[\frac{400}{306}(-9)\left(\frac{-33+3}{2}\right)\right] \\
&= -.90 \text{ ksi}
\end{aligned} \qquad (91)$$

$$\Delta\tau_{xy}^{a} = (-.00150)\left[\frac{-400}{306}(-9)\left(\frac{-33+3}{2}\right)\right]$$
$$+ (.00037)\left[\frac{400}{306}(-9)\left(\frac{-33+3}{2}\right)\right]$$
$$+ (-.00112)\left[400\left(1 - \frac{(-9)^2}{306}\right)\right]$$
$$= 0$$

Two important observations can be made immediately from inspection of Eqs. (91). First, the stress components at the yielded stress point "a" are not increasing linearly. Second, the stresses at the yielded stress point "a" are increasing in such a fashion that the yield condition, Eq. (41), remains satisfied. This is a consequence of the fact that the yield condition is used to eliminate the factor of proportionality λ in the Prandtl-Reuss plastic stress-strain relations, Eqs. (44).

To obtain a first approximation to the stresses and forces at stress point "a" at the load level 44.1 ksi, it is necessary to add the incremental stresses, Eqs. (91), to the last set of stresses, Eqs. (85):

$$\begin{aligned}
\sigma_x^a &= -.90-33.00 = -33.90 \text{ ksi} & F_x^a &= \sigma_x^a \tfrac{\delta}{2} = -23.95 \text{ kips} \\
\sigma_y^a &= -.90- 3.00 = - 3.90 \text{ ksi} & F_y^a &= \sigma_y^a \tfrac{\delta}{2} = - 2.76 \text{ kips} \\
\tau_{xy}^a &= 0 - 9.00 = - 9.00 \text{ ksi} & S_{xy}^a &= \tau_{xy}^a \tfrac{\delta}{2} = - 6.36 \text{ kips}
\end{aligned} \qquad (92)$$

Eqs. (93) correspond to step 5a in Fig. 6, wherein the forces acting at a yielded stress point are computed. Once these "plastic" forces are known, the relaxation technique proceeds in the same manner as before. For example, summing forces acting on mass point "43" gives the result

$$\begin{aligned}
\sum F_x &= P_x+F_x^a+S_{xy}^b = +31.20-23.95-6.36 = +0.89 \text{ kip} \\
\sum F_y &= P_y+F_y^b+S_{xy}^a = +31.20-23.95-6.36 = +0.89 \text{ kip}
\end{aligned} \qquad (93)$$

Hence the second approximation to the displacement of mass point "43" is obtained by adding Eqs. (86) to the incremental displacements resulting from the unbalanced forces of Eqs. (93):

$$u_{43} = .0445 + .00125(.89) = .0456 \text{ inch}$$
$$v_{43} = .0445 + .00125(.89) = .0456 \text{ inch} \tag{94}$$

where .00125 is the flexibility coefficient, Eq. (77), for mass point "43". Accordingly, one observes that the displacements, as well as the stresses, are no longer linear functions of the external load after plastic yielding has begun.

V. THE NUMERICAL PROBLEMS

5.1 Problem 1: A Comparison of Theoretical and Model Solutions

Problem 1, shown diagrammatically in Fig. 8, is presented in order to demonstrate the measure of accuracy obtainable with the model used in this investigation. The theoretical solution is obtained from that given by Timoshenko (21) for a single concentrated load acting vertically on the surface of a half-space. To obtain the approximate theoretical solution for the linearly distributed vertical pressure shown in Fig. 8, the effects of seven concentrated loads, located symmetrically with respect to the vertical center line, are superposed.

As an approximation to the semi-infinite half-space of the theoretical solution, the following boundary conditions are used for the model. The left boundary is assumed to have a zero horizontal displacement and a vertical displacement equal to that of the material spaced a horizontal distance λ from the left boundary. The lower boundary is assumed to be completely fixed. The boundary on the right is established as a line of symmetry. These boundary conditions are indicated graphically in Fig. 8. It should be recognized that these boundary conditions on the left edge and at the base of the model only approximate the true boundary conditions in the half-space. Accordingly, exact agreement between the theoretical and model solutions cannot be expected, especially in the regions near the boundaries.

The basic solution obtained from the model is a set of displacements and stresses in the x and y directions oriented as shown in Fig. 1. For presentation, however, all displacements and stresses are resolved into horizontal and vertical components. Figures 9, 10, and 11 give these

displacement and stress components for Problem 1. The displacement components within a square refer to the displacements of the mass point located at the upper left corner of the square. The stress components refer to the stresses at the stress point located in the center of the square.

To facilitate comparison of theoretical and model solutions, plots of the vertical stresses and displacements at various depths in the half-space are given in Figs. 12 and 13, and a plot of vertical deflections at the center line is given in Fig. 14. Note the very good agreement of the two solutions for vertical stresses in Fig. 12. Only near the lower boundary is there any observable difference between model and theory; this difference most likely arises from the different boundary conditions along the lower boundary for the two solutions. The pattern of vertical displacements (Fig. 13) appears quite reasonable, and the comparison of these deflections at the center line with the corresponding theoretical solution (Fig. 14) shows a good agreement in the pattern of the deflections, with only minor discrepancies in the magnitudes of the deflections. Again, this difference in the magnitudes of the deflections obtained from the model and from the theory of elasticity is attributed to the differences in the boundary conditions for the two solutions, particularly the condition along the lower boundary.

5.2 Problem 2: Notched Bar Under Tension

As an example of a type of problem in contained plastic flow which can be solved using a discrete model and a systematic relaxation procedure, a bar with a long rectangular notch, or slit, is shown in Fig. 15. In the finite model, the notch actually has a width of λ, though for practical purposes the notch may be thought of as having infinitesimal width. A

uniform tension is applied at the upper edge of the bar, the left edge of the bar being free of external stress. The bar is assumed symmetrical about a vertical axis through its center and symmetrical about a horizontal axis through the notch. Hence the boundary conditions, on the right and lower edges of the bar are those of zero shear on the boundaries and zero displacement perpendicular to the boundaries.

As mentioned earlier, the basic solution obtained from the model is a set of displacement and stress components. However, once successive sets of displacements are known, the stresses can be computed. Further, it has been observed that the general pattern of stresses does not vary appreciably as the level of external loading is increased, even though portions of the material may be undergoing plastic flow. Accordingly, only the basic solutions in terms of displacement components (Figs. 16-19) are given for each load level above the load level which initiates plastic yielding. For this elastic limit load level (σ_{el}), a complete set of stress components is given in Figs. 20 and 21, and plots of the vertical stresses and vertical displacements for various depths at this load level are given in Figs. 22 and 23.

In the discussion of problems in contained plastic flow, a very useful concept is that of an "equivalent shear stress", defined as follows:

$$\text{Equivalent Shear Stress} = \sqrt{J_2} = \sqrt{\left(\frac{\sigma_x - \sigma_y}{2}\right)^2 + \tau_{xy}^2} \qquad (95)$$

Note that this is actually the largest shear stress existing on any plane passing through a given point at which σ_x, σ_y, and τ_{xy} are defined. If this equivalent shear stress is divided by the yield stress in simple shear, k, the ratio represents the percentage of the yield capacity of the state of stress at a given point. Figures 24, 25, and 26 present values of the

equivalent shear stress, expressed as a percentage of its maximum value k, for three levels of external load: σ_{el}, $1.46\sigma_{el}$, and $1.58\sigma_{el}$.

It is of some interest to trace the development of the yielded region as the level of external load increases. The first stress point to yield is the one at the very end of the notch (Fig. 24). It is of significance (Fig. 20 or 22) that the vertical stress component at this stress point when yielding begins is 47.4 ksi -- considerably greater than the assumed yield limit of 35 ksi in simple tension or compression. As mentioned previously, this is characteristic of yielding in two-dimensional stress systems; the yield condition depends upon a combination of the stress components rather than on the value of any single component.

To be strictly correct, the external load increments after this first stress point has yielded should be applied in very small increments. Initial investigations indicate, however, that the displacements and stresses are very nearly linear between yielding of two successive stress points, particularly if the yielded region is of small extent. Hence the next two stress points were yielded by relatively large increments of external load.

At an external load level of $1.22\sigma_{el}$, the second stress point, immediately above the first yielded stress point, begins to yield. As the load is increased to $1.46\sigma_{el}$, a third stress point yields (Fig. 25). Note that the yielding is not taking place along a horizontal line at the waist of the specimen, as one might at first be led to expect, but is progressing vertically upward and to the right. The material has now been highly enough stressed so that only a small increase in external load is necessary to propagate the yielded region completely across the bar (Fig. 26). In problems of this type which involve local concentrations of stress, the specimen can actually withstand a considerably greater external stress than that causing

initial local yielding. Figure 27 summarizes the progression of plastic yielding at several levels of external load.

This pattern of plastic yielding shows remarkably good agreement with results presented by Jacobs (11), who used a modified stress function approach and a relaxation technique developed by Allen and Southwell (1). As Allen and Southwell (1) have remarked, this type of plastic yielding may indicate the mechanical behavior behind the type of fracture commonly known as "cup and cone". The first stages of failure may involve slipping along planes at roughly 45 degrees to the vertical. Eventually the tensile stress across the elastic portion of the waist of the specimen becomes great enough to cause a breakdown in cohesion, resulting in a horizontal tensile fracture across the reduced waist of the specimen.

Figure 28 illustrates graphically that displacements are no longer linear functions of the applied loading after plastic yielding has begun. Load deflection curves are given for mass points located at "a", "b", and "c" of Fig. 15. Mass point "a" is immediately above the end of the notch; mass points "b" and "c" are at a horizontal distance $\lambda/2$ from the vertical center line and at vertical distances $5\text{-}1/2\ \lambda$ and $2\text{-}1/2\ \lambda$ from the horizontal center line, respectively. Note that the load deflection curves differ, depending on the location of the mass point, and that the load deflection curve for the material within the elastic core at the center of the specimen (mass point "c") remains nearly elastic.

5.3 Problem 3: A Partially Loaded Half-Space

As a second example of a problem in contained plastic flow, the problem of a partially loaded half-space is shown in Fig. 29. Such a problem might represent the effect of a footing on soil, or a machine part bearing against another part of much larger dimensions.

The boundary conditions for the problem are the same as those for Problem 1, and the elastic solutions, Figs. 30 and 34 through 37, is quite similar to the elastic solution of Problem 1. Preliminary investigation of plastic yielding under the triangular loading of Problem 1 indicates quite different yield patterns for the two problems, however. It might be mentioned at this point that the loading pattern shown in Fig. 29 purposely introduces the linearly varying stress distribution at the left edge of the loading pattern. This type of external stress distribution reduces significantly the oscillation in displacements and stresses which occurs in the model solution if the external stress distribution drops abruptly from a finite value to zero.

The concept of an equivalent shear stress is again used as a measure of the closeness to yield. Figure 38 shows values of this equivalent shear stress as a percentage of its maximum value k for the elastic load limit (σ_{el}) which initiates plastic yielding. In marked contrast to the large increments of external load demanded by Problem 2 in order to yield a second and third stress point, it was found that only a small increase of two percent of the elastic limit load was required to initiate yielding at several other stress points. An increase of six percent (Fig. 39) in the external loading σ_{el} extended the yielded zone over a circular arc which almost intersected the surface of the half-space. Figures 30-33 give the basic solutions in terms of displacements for each load level, and Fig. 41 summarizes the progression of plastic yielding at these load levels. This pattern of plastic yielding under a partial load agrees very well with the trajectories of maximum shear under a footing given by Jurgenson (12).

Note again (Fig. 36) that there are regions within the material where a single component of stress (vertical stress immediately beneath the

load, for example) can have a value considerably greater than the yield stress of 35 ksi in simple tension or compression.

The non-linear relation of load and displacement at specific points within the material is also evident in this problem. The load-deflection curves for the three mass points "a", "b", and "c" of Fig. 29 are shown in Fig. 41. All three mass points are on the vertical center line; "a" is at the surface, and "b" and "c" are at depths of 5λ and 8λ below the surface. The surface mass point, "a", departs greatly from the linear behavior, since it feels the cumulative displacements of all the material beneath. Mass point "b" is located within the yielded zone and also shows a non-linear behavior. Mass point "c" is beneath the yielded zone and exhibits even less than linear deflections. This seems to indicate that the increments in external load are not being transmitted directly through the yielded zone, but rather are being carried around this zone by a redistribution of the stresses.

VI. SUMMARY AND CONCLUSION

The object of the thesis is the development of a numerical procedure for the solution of problems in contained plastic flow of plane continua. To accomplish this, a discrete model is introduced to replace the physical continuum. The equations governing the behavior of the model are shown to be identical with a set of finite difference equations for the differential equations governing the plane continuum.

The Mises-Hencky yield criterion and the Prandtl-Reuss stress-strain relations for plastic straining are given, and a finite form of these relations is developed for application to the model. A systematic relaxation technique for the computation of displacements and stresses within the model is developed. The relaxation technique applies to both elastic and plastic behavior, and is well adapted for use on large, high-speed computers.

Three numerical example problems are solved by means of the relaxation procedure. The first example indicates the measure of accuracy obtainable using the model. The last two examples illustrate the application of the procedure to problems of plastic straining.

Results of the example problems indicate that the numerical procedure developed herein can be used successfully for the solution of a wide range of interesting and practical problems in contained plastic flow.

VII. BIBLIOGRAPHY

1. Allen, D. N. de G., and Southwell, R. V., "Relaxation Methods Applied to Engineering Problems - XIV Plastic Straining in Two Dimensional Stress Systems", Philosophical Transactions of the Royal Society of London, Series (A), Vol. 242, 1950.

2. Ang, A., "Mathematically Consistent Discrete Models for Simulating Solid Continua", in Computation of Underground Structural Response, Compiled by A. Ang and N. M. Newmark, Final Report to the Defense Atomic Support Agency, Contract No. DA-49-146-XZ-104, June, 1963.

3. Austin, W. J., "A Framework Analogy for Plane Problems in Elasticity", M.S. Thesis, University of Illinois, 1946.

4. Clough, R. W., "The Finite Element Method in Plane Stress Analysis", Second Conference on Electronic Computation, American Society of Civil Engineers, 1960.

5. Dauphin, E. L., "Framework Analogies for Plane Stress Problems in Elasticity", M.S. Thesis, University of Illinois, 1947.

6. Drucker, D. C., "Stress-Strain Relations in the Plastic Range--A Survey of Theory and Experiments", Brown University ONR Report, Contract Number ONR-358, 1950.

7. Gaus, M. P., "A Numerical Solution for the Transient Strain Distribution in a Rectangular Plate with a Propagating Crack", Ph.D. Thesis, University of Illinois, 1959.

8. Hill, R., The Mathematical Theory of Plasticity, Oxford University Press, London, 1950.

9. Hoffman, O., and Sachs, G., Introduction to the Theory of Plasticity for Engineers, McGraw-Hill Book Co., New York, 1953.

10. Hrennikoff, A., "Solution of Problems in Elasticity by Framework Method", Journal of Applied Mechanics, Vol. 8, No. 4, December, 1941.

11. Jacobs, J. A., "Relaxation Methods Applied to Problems of Plastic Flow", Philosophical Magazine, Vol. 41, 1950.

12. Jurgenson, L., "The Application of Theories of Elasticity and Plasticity to Foundation Problems", Journal of the Boston Society of Engineers, Vol. 21, 1934.

13. McHenry, D., "Lattice Analogue for Solution of Stress Problems", Journal of the Institute of Civil Engineers, Vol. 21, December, 1943.

14. Michell, J. H., "On the Direct Determination of Stress in an Elastic Solid, with Application to the Theory of Plates", London Mathematical Society Proceedings, Vol. 31, 1899.

15. Newmark, N. M., "Numerical Methods of Analysis of Bars, Plates and Elastic Bodies", in Numerical Methods of Analysis in Engineering, ed. L. E. Grinter, MacMillan Co., New York, 1949.

16. Phillips, A., Introduction to Plasticity, Ronald Press Company, New York, 1956.

17. Prager, W., and Hodge, P. G., Jr., Theory of Perfectly Plastic Solids, John Wiley and Sons, New York, 1951.

18. Schnobrich, W. C., "A Physical Analogue for the Numerical Analysis of Cylindrical Shells", Ph.D. Thesis, University of Illinois, 1962.

19. Southwell, R. V., Relaxation Methods in Engineering Science, Oxford University Press, London, 1940.

20. Southwell, R. V., Relaxation Methods in Theoretical Physics, Vols. 1 and 2, Oxford University Press, London, 1946 and 1956.

21. Timoshenko, S., and Goodier, J. N., Theory of Elasticity, Second Edition, McGraw-Hill Book Co., New York, 1951.

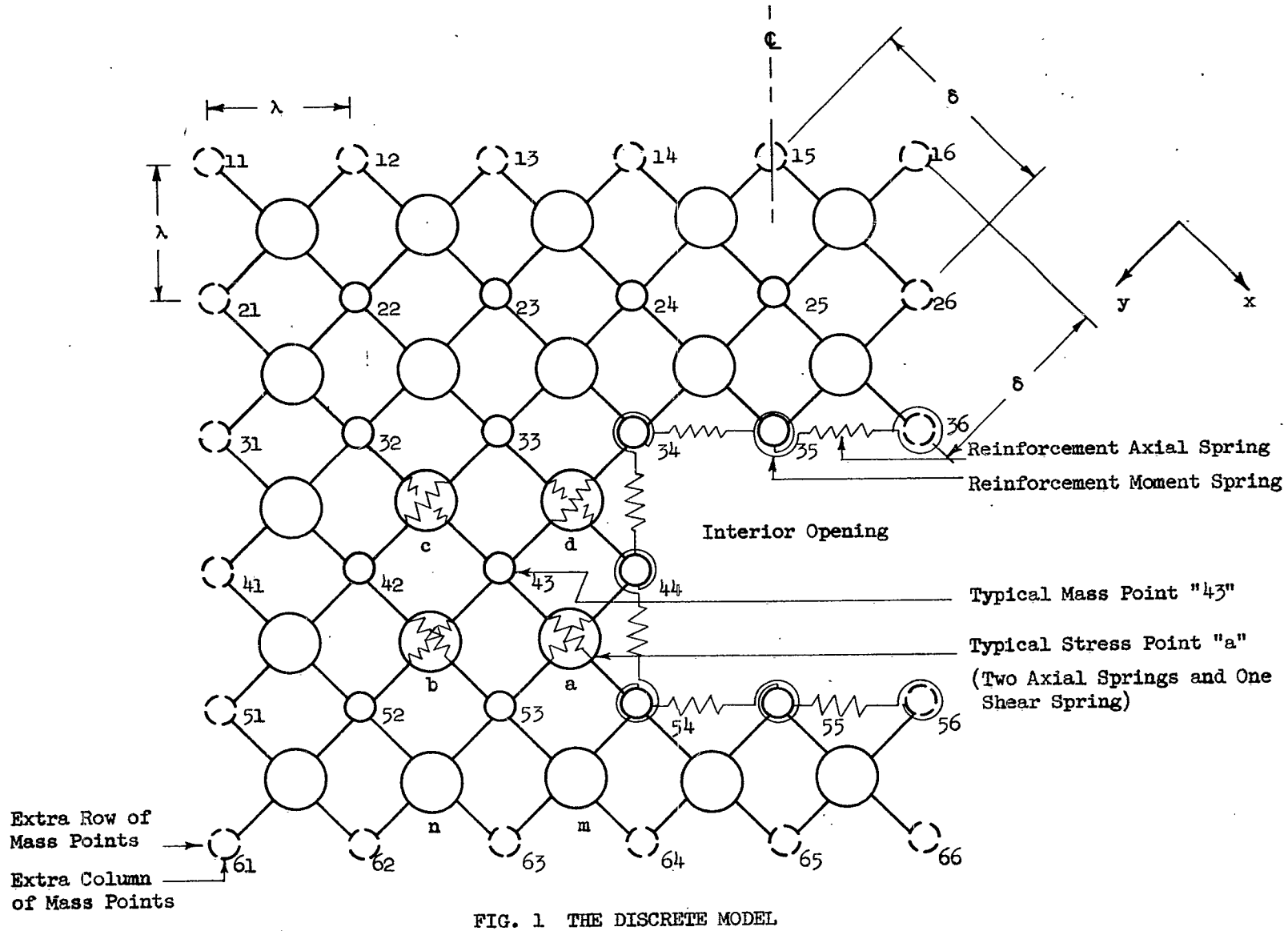

FIG. 1 THE DISCRETE MODEL

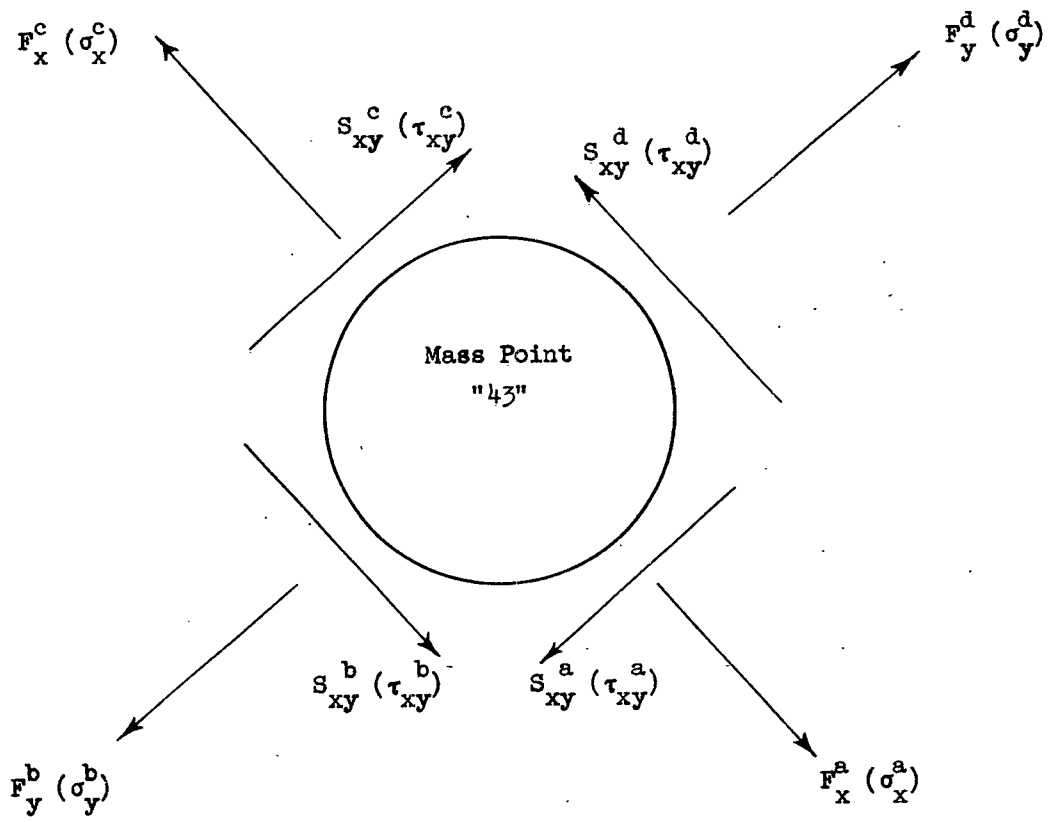

FIG. 2 FORCES (STRESSES) ACTING ON MASS POINT "43"

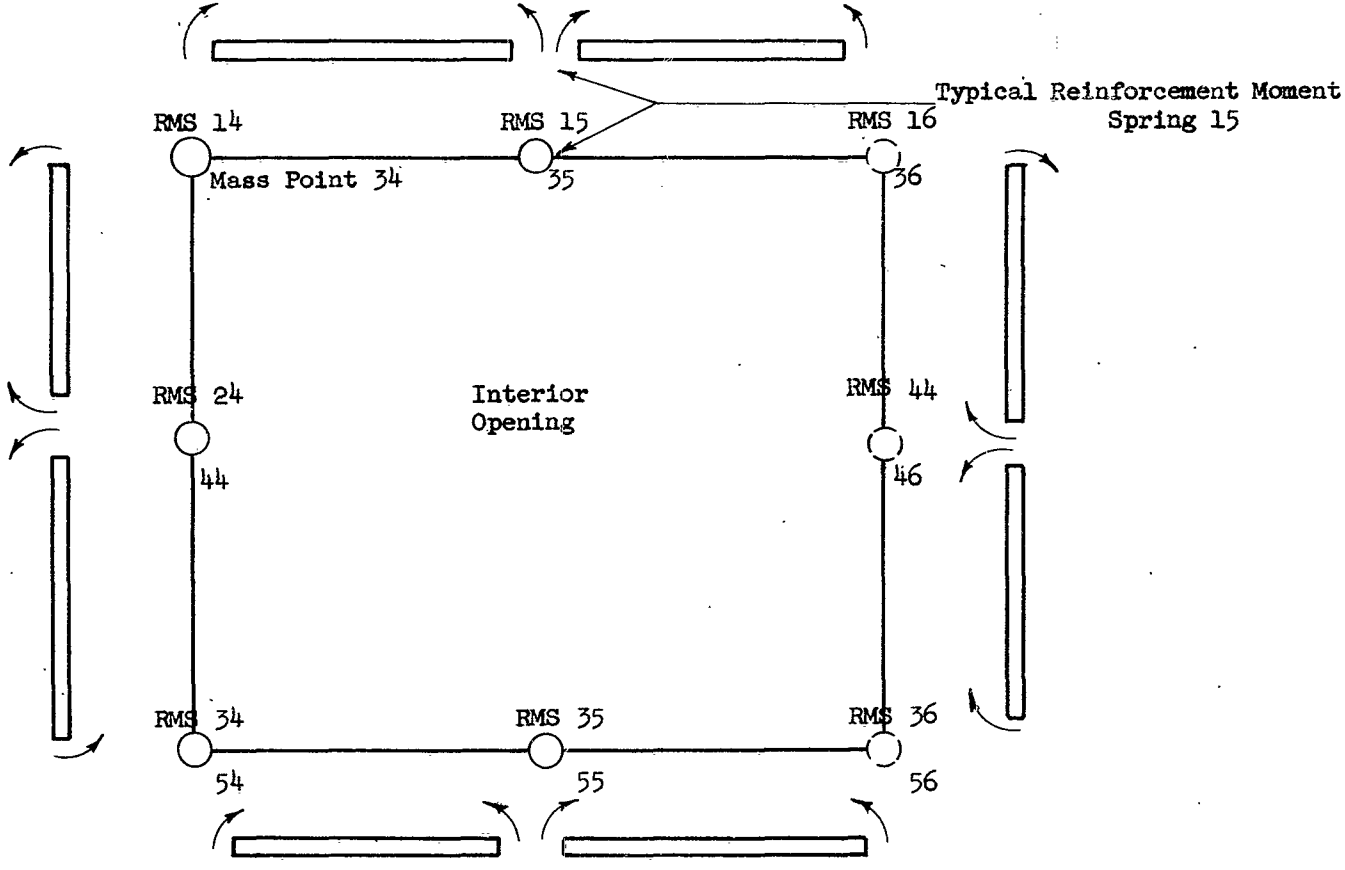

FIG. 3 NOMENCLATURE AND SIGN CONVENTION FOR POSITIVE MOMENT IN REINFORCEMENT AROUND A CAVITY

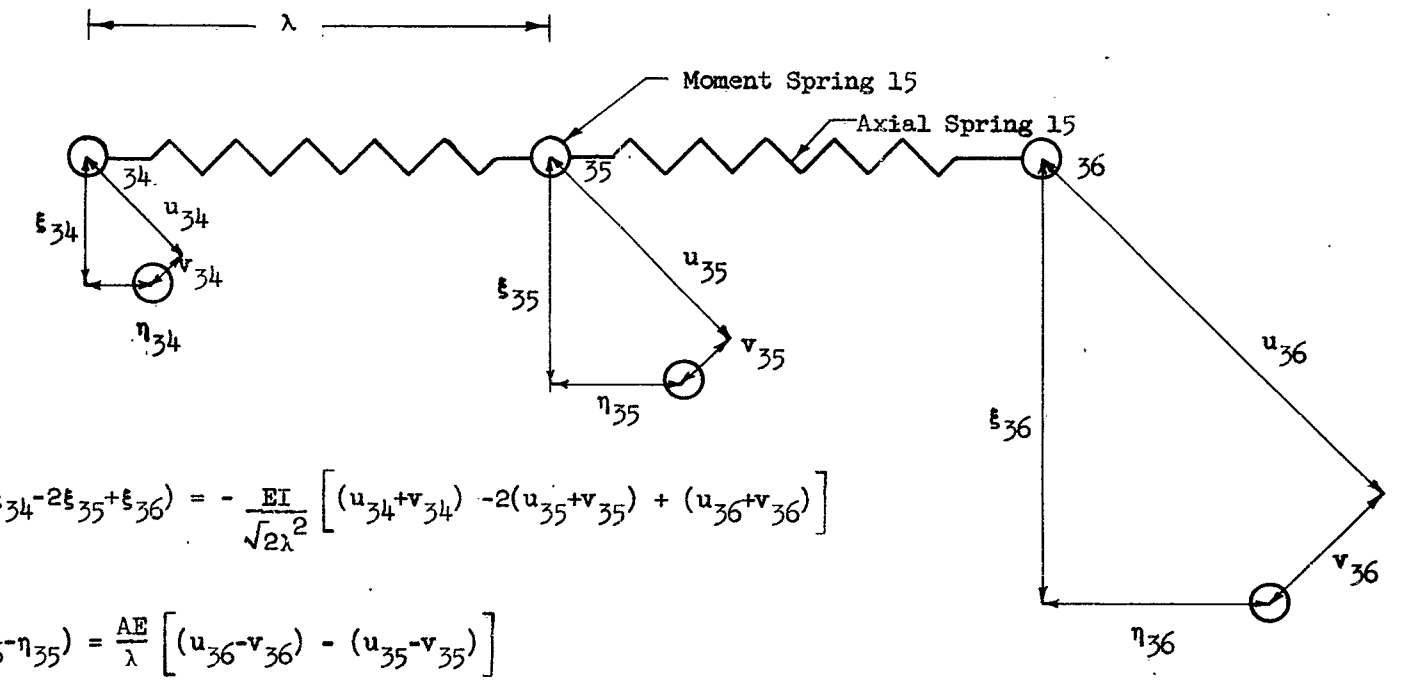

$$M_{15} = -\frac{EI}{\lambda^2}(\xi_{34}-2\xi_{35}+\xi_{36}) = -\frac{EI}{\sqrt{2}\lambda^2}\left[(u_{34}+v_{34}) -2(u_{35}+v_{35}) + (u_{36}+v_{36})\right]$$

$$F_{15} = \frac{AE}{\lambda}(\eta_{36}-\eta_{35}) = \frac{AE}{\lambda}\left[(u_{36}-v_{36}) - (u_{35}-v_{35})\right]$$

FIG. 4 COMPUTATION OF MOMENTS AND AXIAL FORCES FROM DISPLACEMENTS

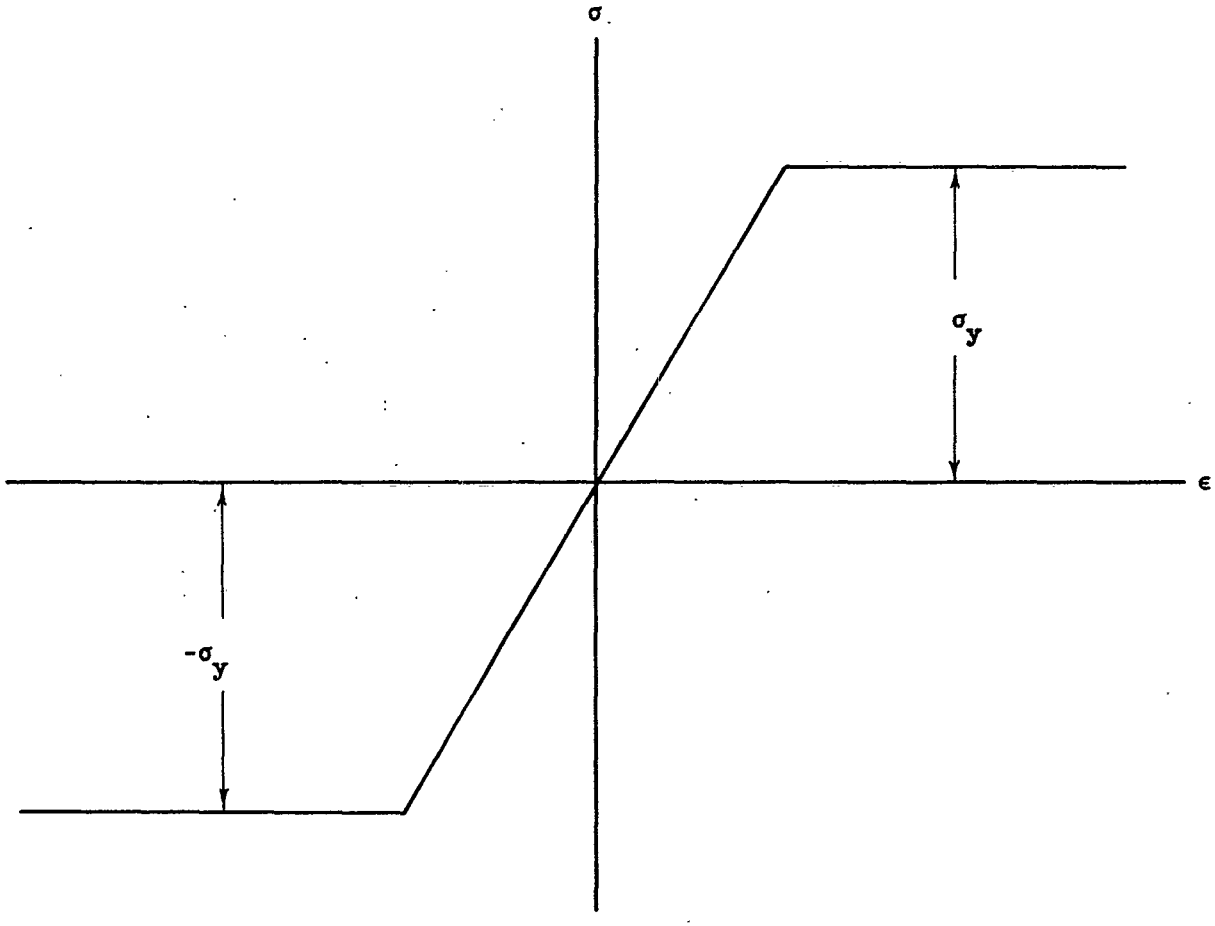

FIG. 5 STRESS-STRAIN CURVE FOR ELASTIC-PERFECTLY-PLASTIC MATERIAL IN SIMPLE TENSION OR COMPRESSION

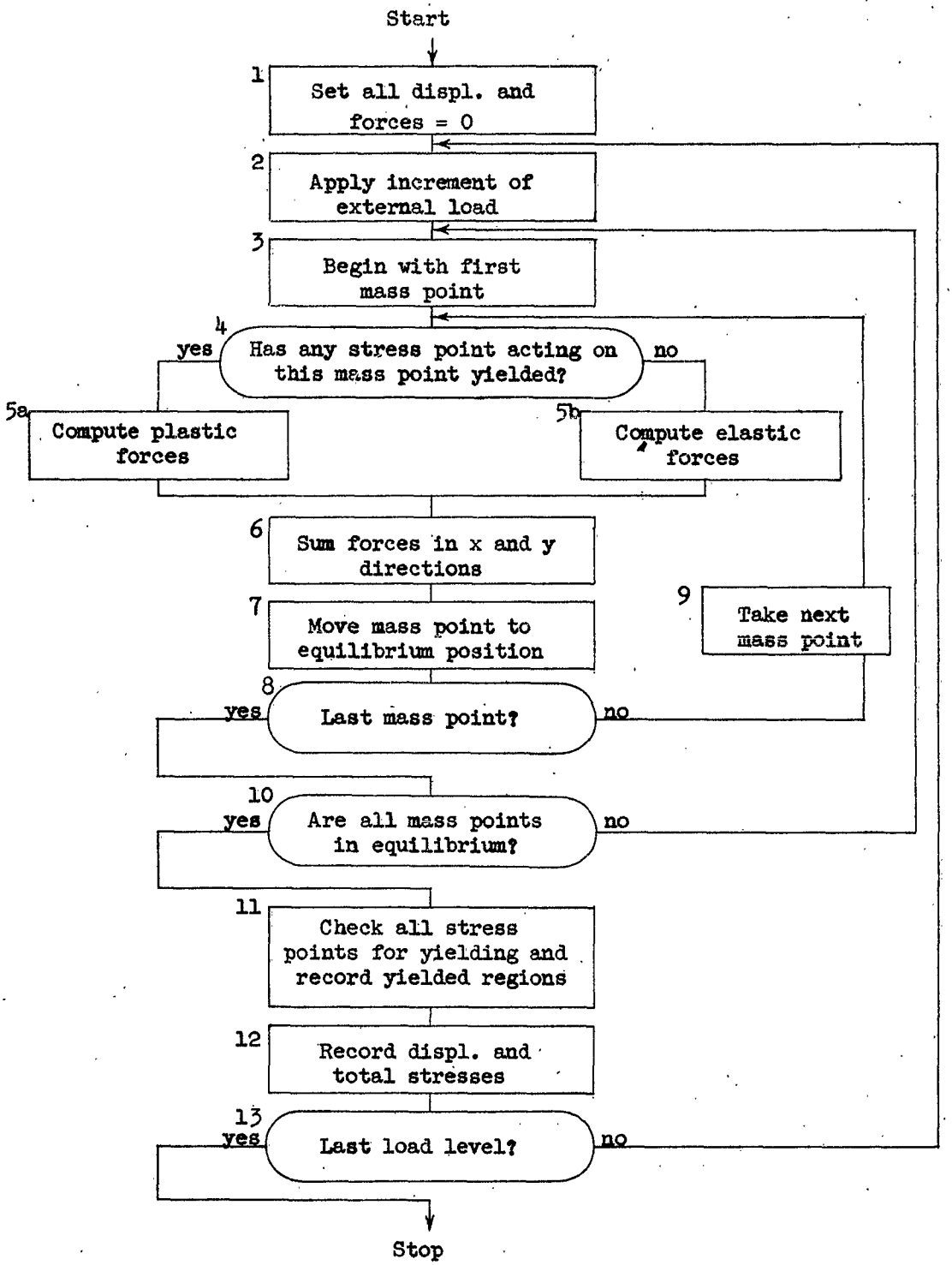

FIG. 6 FLOW DIAGRAM FOR RELAXATION PROCEDURE

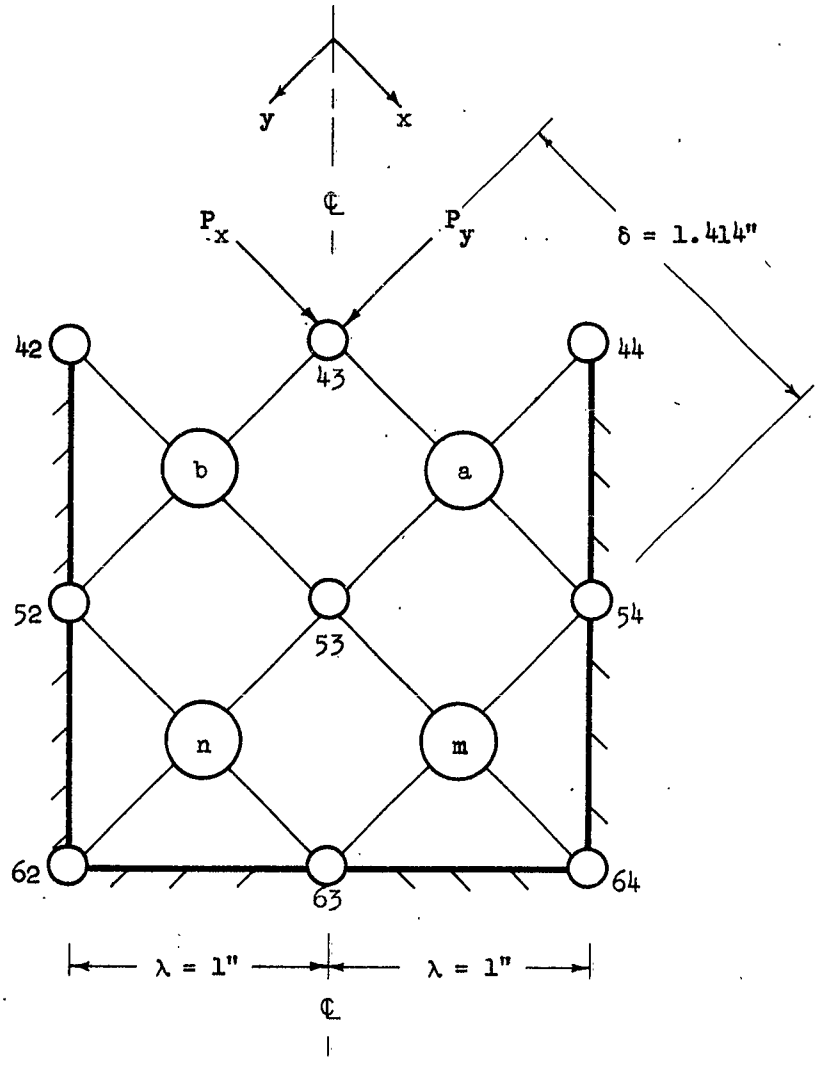

E = 1000 ksi ν = 0.25

$P_x = P_y = .707$ kip

FIG. 7 DIAGRAM FOR COMPUTATIONAL EXAMPLE

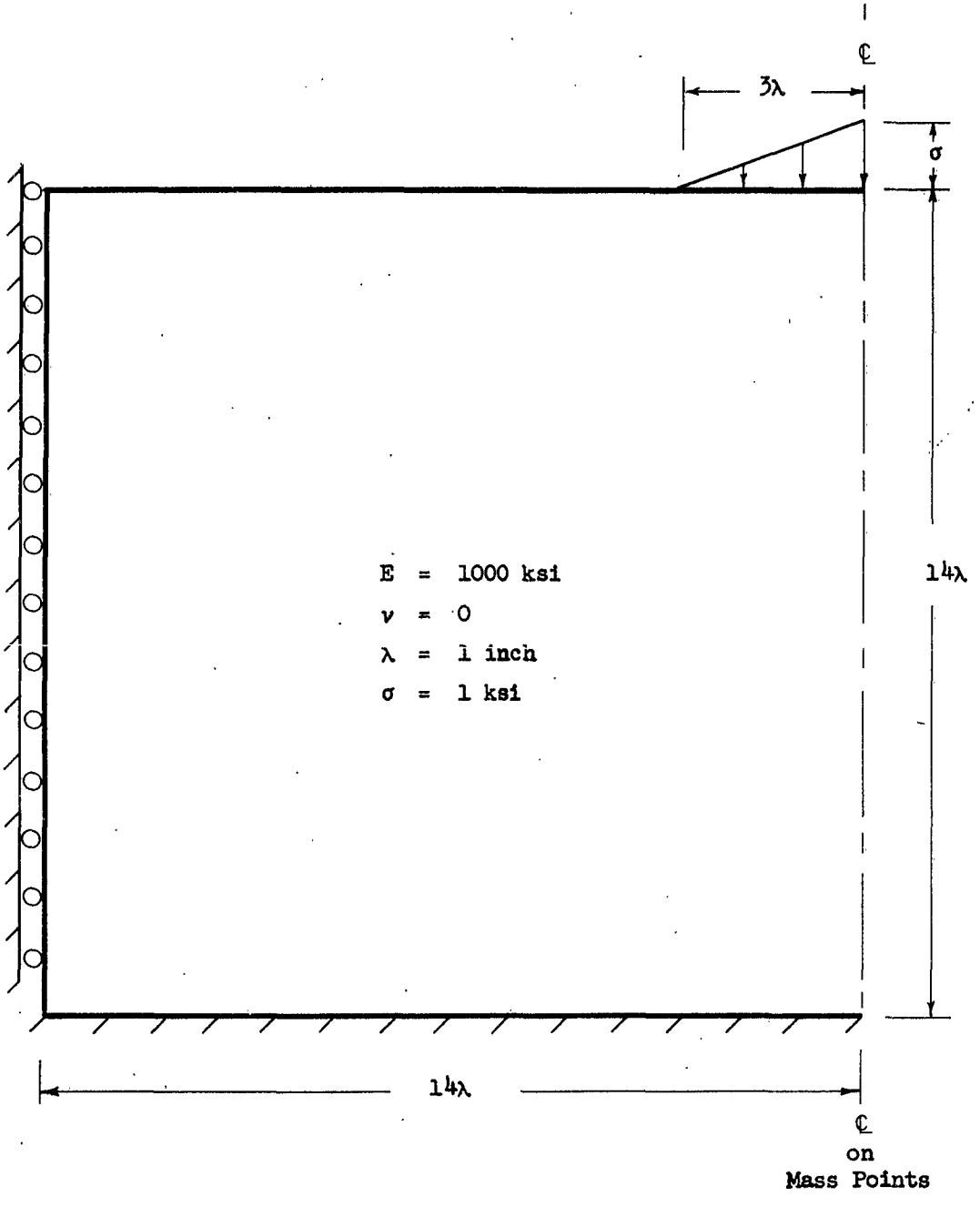

FIG. 8 DIAGRAM FOR PROBLEM 1: A COMPARISON OF THEORETICAL AND MODEL SOLUTIONS

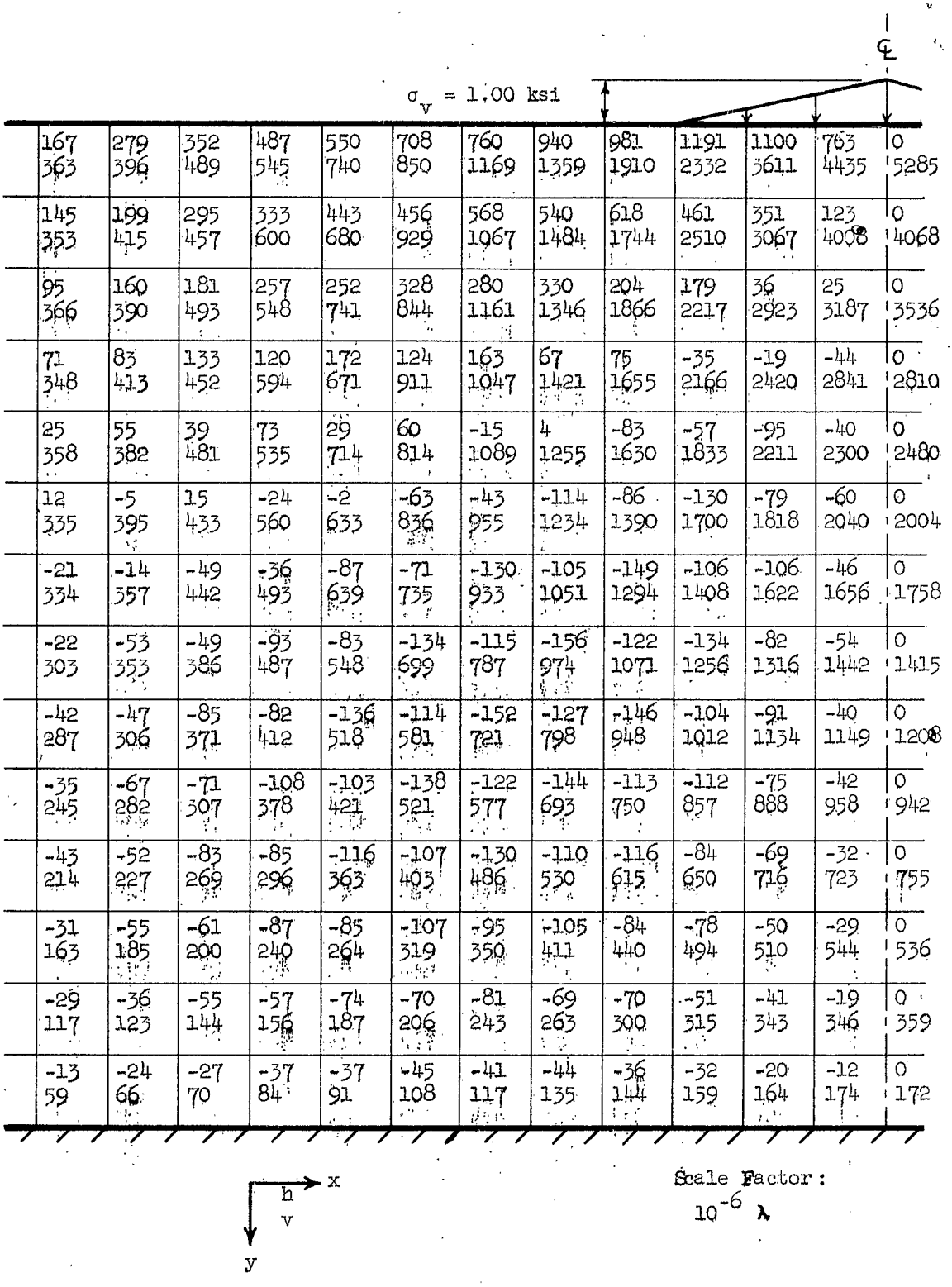

FIG. 9 HORIZONTAL AND VERTICAL DISPLACEMENTS

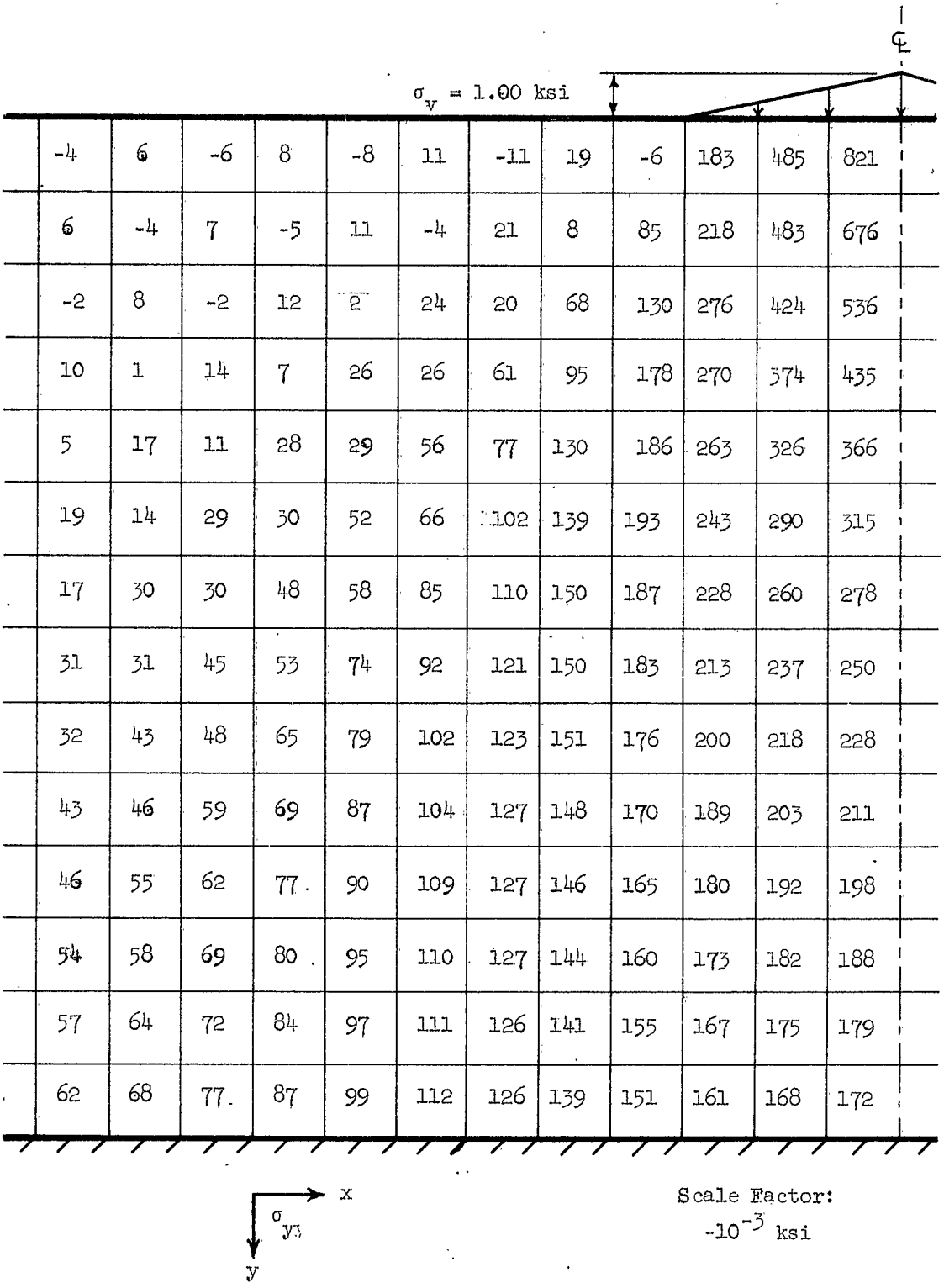

FIG. 10 VERTICAL STRESSES

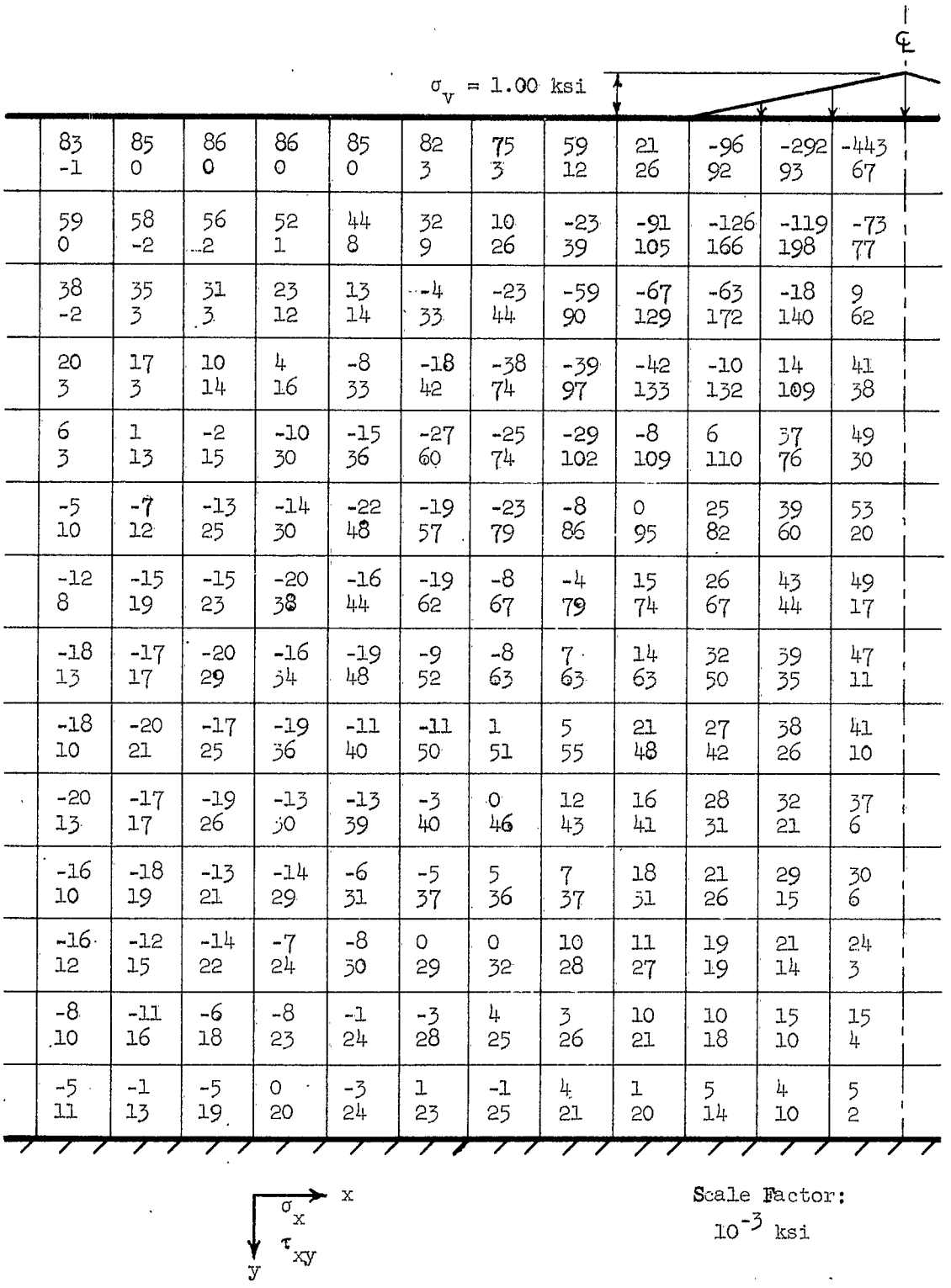

FIG. 11 HORIZONTAL AND SHEAR STRESSES

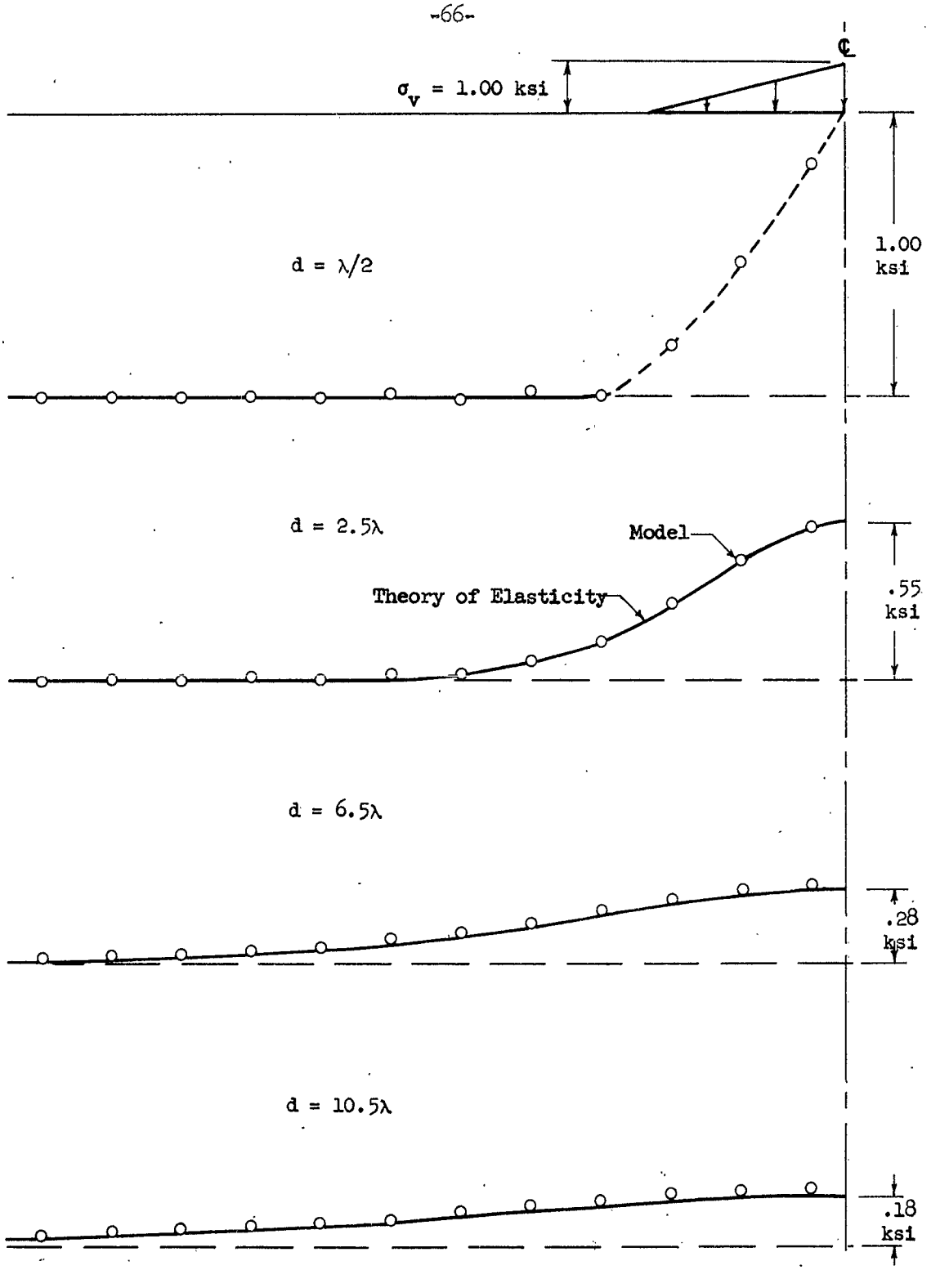

FIG. 12 VERTICAL STRESSES AT VARIOUS DEPTHS

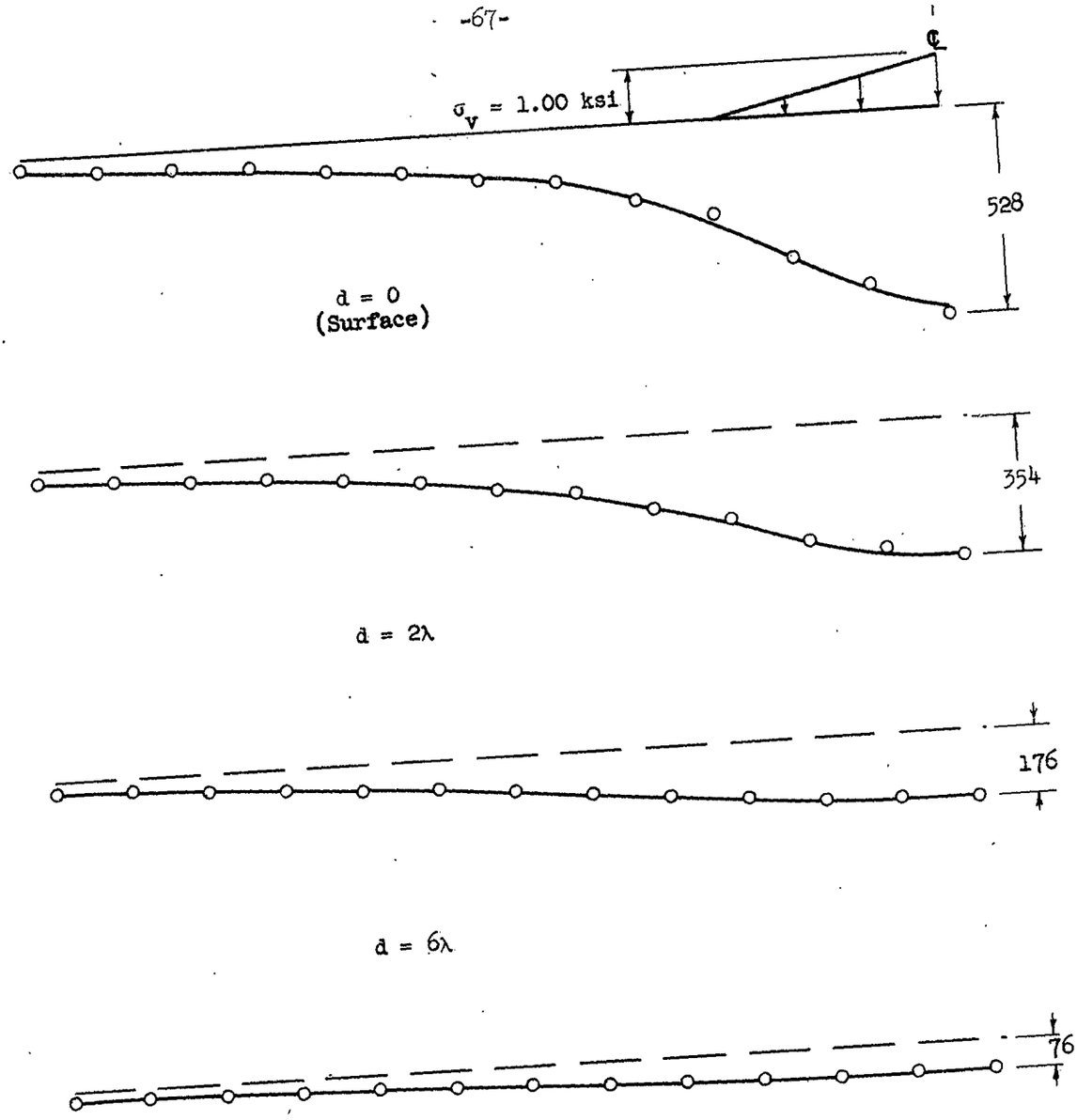

FIG. 13 VERTICAL DISPLACEMENTS AT VARIOUS DEPTHS

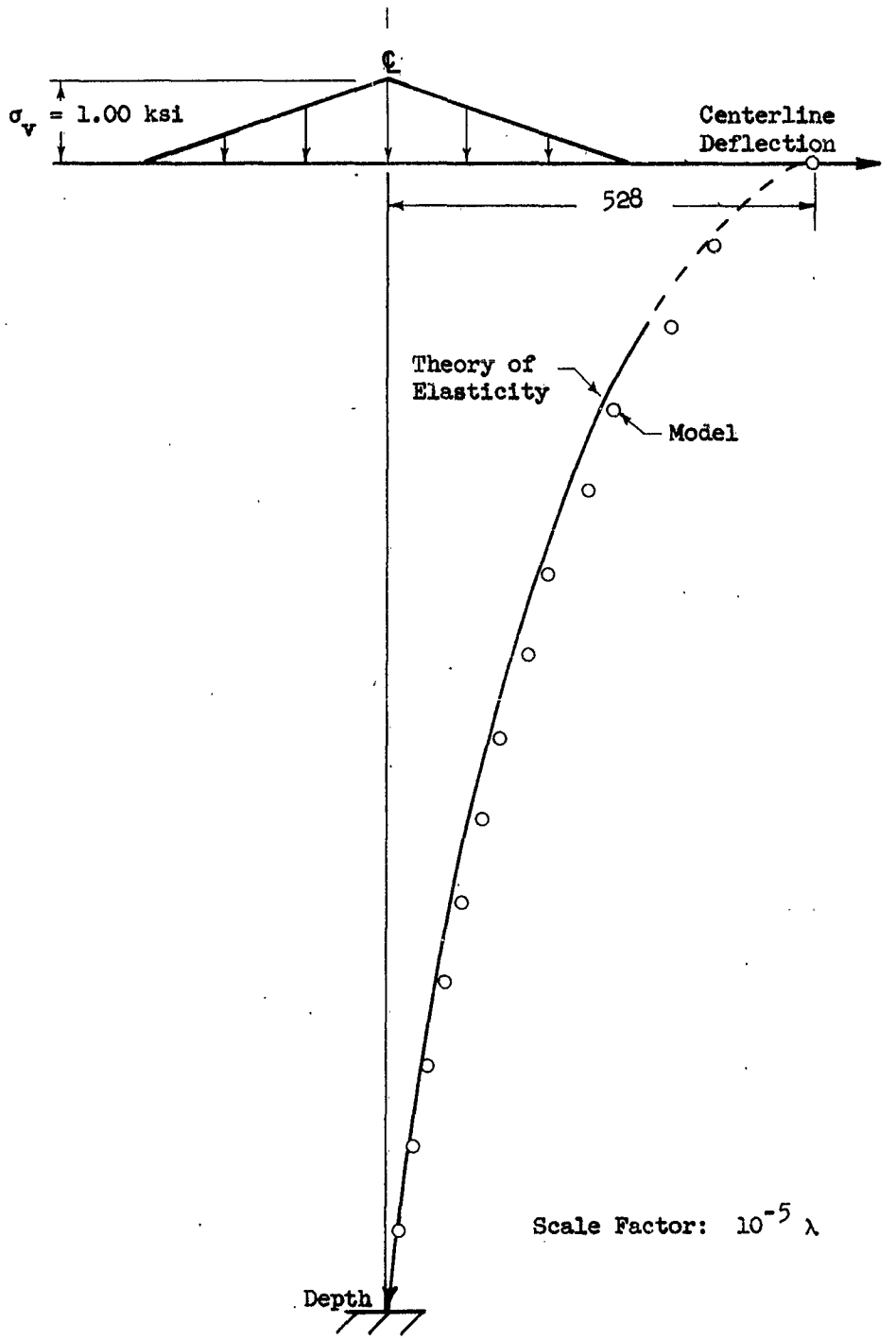

FIG. 14 DEFLECTIONS AT CENTERLINE VS. DEPTH

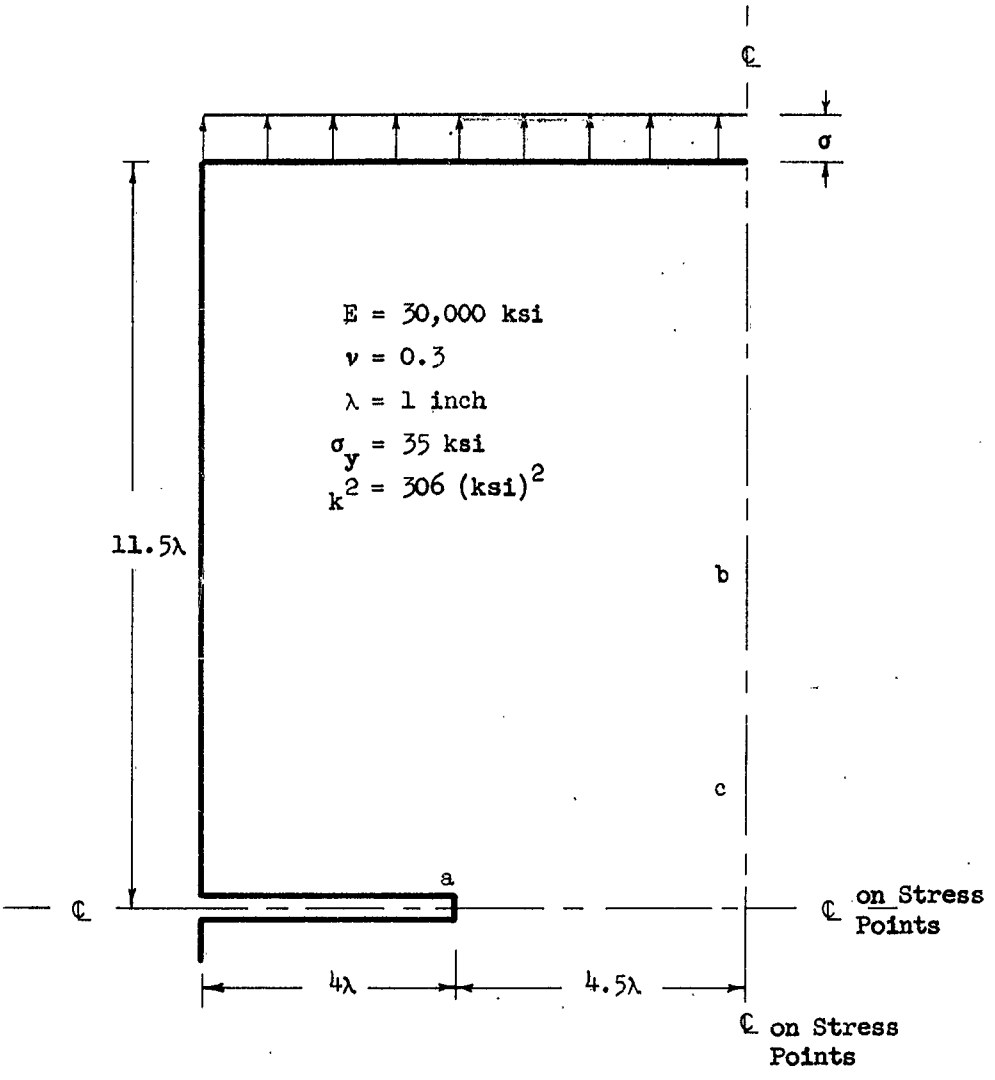

FIG. 15 DIAGRAM FOR PROBLEM 2: NOTCHED BAR UNDER TENSION

$\sigma = \sigma_{el} = 14.3$ ksi

2232 7583	2637 7638	1908 7230	2173 7230	1491 6798	1546 6755	878 6422	758 6385	933 6261
2690 7348	1911 7011	2246 6987	1540 6590	1697 6493	1054 6121	1029 6021	428 5798	293 5757
1938 6767	2351 6749	1619 6406	1876 6284	1219 5897	1283 5741	696 5439	614 5335	68 5222
2456 6482	1688 6242	2058 6116	1373 5736	1538 5532	936 5169	915 4993	380 4776	254 4708
1736 6054	2218 5975	1494 5642	1781 5399	1150 4990	1209 4736	664 4423	567 4267	75 4152
2322 5816	1550 5612	1988 5349	1314 4923	1485 4580	916 4179	871 3914	380 3686	230 3589
1494 5624	2117 5375	1384 4994	1715 4553	1105 4077	1147 3675	644 3333	519 3108	83 2993
2102 5453	1290 5227	1842 4677	1176 4173	1368 3592	838 3127	761 2733	336 2509	189 2381
937 5637	1773 4954	1026 4543	1481 3736	907 3146	929 2499	494 2145	368 1861	44 1789
1402 5365	537 5201	1358 4165	716 3565	1002 2522	534 1942	412 1408	113 1292	97 1212
-139 5887	774 4718	-17 4598	884 3057	359 2129	292 1032	-13 812	60 730	-27 697
190 5289	-733 5325	22 3940	-857 3768	-57 1081	-297 194	-120 302	-97 221	-13 229

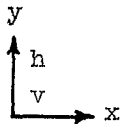

Scale Factor:
10^{-6} inches

FIG. 16 HORIZONTAL AND VERTICAL DISPLACEMENTS

$\sigma = 1.22\ \sigma_{el} = 17.4$ ksi

2653 9324	3302 9404	2259 8891	2734 8904	1753 8362	1965 8321	1005 7903	998 7864	458 7708
3366 9050	2261 8625	2823 8608	1811 8110	2150 8003	1219 7537	1331 7422	456 7142	427 7095
2294 8329	2952 8318	1905 7888	2370 7749	1419 7264	1642 7082	7839 6703	820 6581	16 6439
3080 7992	1989 7688	2593 7546	1606 7069	1956 6831	1077 6373	1190 6167	400 5892	378 5812
2047 7459	2789 7375	1752 6957	2256 6672	1336 6157	1555 5858	749 5459	762 5277	29 5129
2916 7179	1820 6920	2511 6612	1533 6078	1898 5675	1055 5162	1139 4853	408 4554	342 4441
1753 6933	2667 6642	1615 6168	2183 5646	1281 5043	1487 4572	733 4120	7016 3861	51 3703
2646 6735	1503 6450	2339 5799	1360 5168	1769 4483	964 3874	1010 3417	371 3101	280 2955
1088 6935	2251 6133	1175 5620	1915 4666	1033 3914	1239 3155	564 2657	509 2331	30 2207
1799 6635	602 6401	1760 5185	785 4439	1352 3208	590 2432	590 1805	128 1587	136 1496
-200 7213	1053 5865	-70 5660	1209 3860	325 2712	502 1404	-33 1008	73 890	-40 858
340 6563	-922 6526	160 4941	-1084 4637	163 1552	-473 348	-196 319	-143 294	-23 272

y
h
v
x

Scale Factor:
10^{-6} inches

FIG. 17 HORIZONTAL AND VERTICAL DISPLACEMENTS

$\sigma = 1.46\ \sigma_{el} = 20.9$ ksi

3132 11314	4008 11464	2677 10797	3313 10862	2088 10165	2376 10154	1204 9618	1204 9593	55 9393
4092 11033	2670 10485	3427 10503	2149 9870	2604 9772	1456 9183	1606 9066	549 8712	512 8662
2701 10138	3589 10151	2252 9609	2875 9468	1690 8862	1987 8661	942 8189	987 8049	24 7872
3751 9754	2342 9375	3152 9222	1906 8635	2372 8363	1292 7799	1439 7555	488 7216	451 7120
2401 9107	3397 9010	2068 8507	2741 8174	1599 7550	1887 7190	911 6703	921 6477	44 6296
3563 8763	2134 8467	3056 8098	1823 7470	2309 6979	1281 6362	1387 5972	508 5608	412 5461
2041 8484	3260 8115	1904 7588	2661 6951	1549 6245	1818 5649	914 5104	861 4758	74 4564
3268 8183	1755 7925	2866 7119	1627 6423	2169 5567	1203 4849	1252 4235	4821 3849	348 3637
1269 8486	2802 7461	1384 6977	2360 5795	1279 4957	1539 3963	744 3355	649 2873	41 2717
2327 7993	736 7888	2236 6332	936 5638	1680 4099	806 3183	757 2260	162 1961	176 1830
-188 8831	1465 7088	0 7049	1630 4764	442 3730	600 1908	-58 1251	82 1099	-63 1042
673 7865	-991 8065	440 6004	-1104 5844	602 2183	-628 458	-302 428	-215 342	-37 335

℄ ℄ ℄ ℄

Scale Factor: 10^{-6} inches

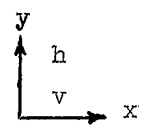

FIG. 18 HORIZONTAL AND VERTICAL DISPLACEMENTS

$\sigma = 1.58\ \sigma_{el} = 22.6$ ksi

3369 12362	4340 12584	2894 11811	3570 11940	2279 11140	2542 11173	1340 10561	1264 10557	102 10328
4443 12106	2882 11478	3706 11540	2338 10823	2797 10755	1609 10091	1703 9536	638 9588	511 9541
2909 11104	3895 11147	2443 10543	3102 10419	1857 9746	2123 9546	1063 9022	1028 8879	73 8682
4084 10705	2531 10290	3415 10142	2083 9502	2551 9220	1442 8604	1527 8343	579 7971	444 7866
2588 9999	3697 9897	2249 9365	2964 9010	1770 8342	2022 7948	1043 7421	963 7166	98 6969
3902 9605	2311 9319	3323 8913	2006 8262	2493 7720	1448 7067	1482 6620	614 6227	406 6052
2203 9335	3572 8901	2084 8391	2891 7681	1737 6959	1963 6279	1069 5704	916 5280	133 5070
3623 8928	1917 8756	3151 7830	1814 7161	2354 6198	1394 5468	1356 4726	599 4312	357 4025
1400 9349	3127 8145	1547 7776	2616 6409	1483 5608	1667 4481	912 3838	693 3171	64 3019
2673 8659	872 8748	2532 6926	1098 6396	1903 4584	1064 3741	765 2530	174 2184	182 2034
-104 9749	1762 7691	137 7890	1909 5244	621 4455	703 2141	-65 1345	66 1252	-69 1160
963 8975	-914 8975	682 6533	-969 6703	922 2579	-681 493	-316 477	-219 377	-41 382

Scale Factor: 10^{-6} inches

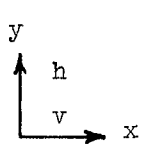

FIG. 19 HORIZONTAL AND VERTICAL DISPLACEMENTS

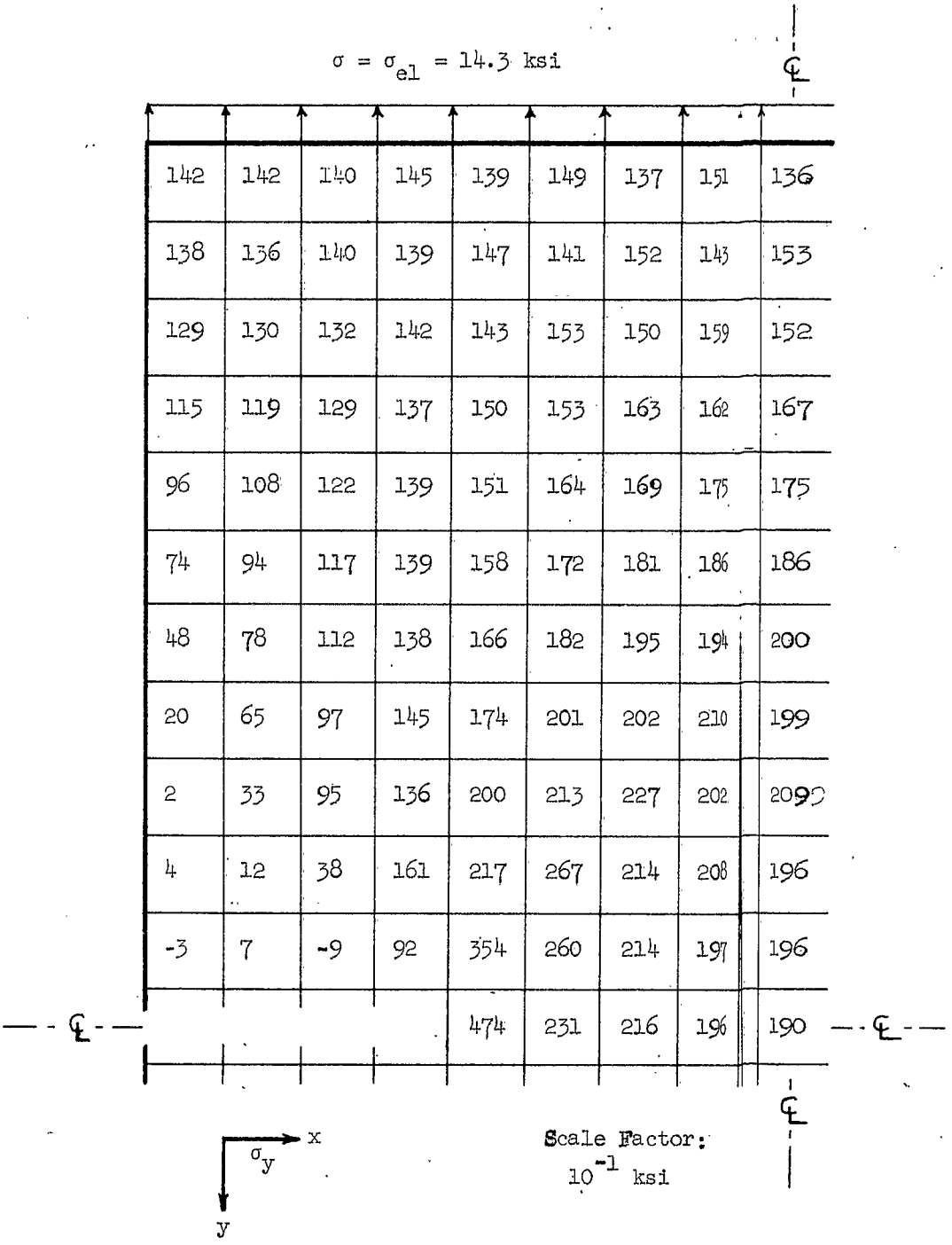

FIG. 20 VERTICAL STRESSES

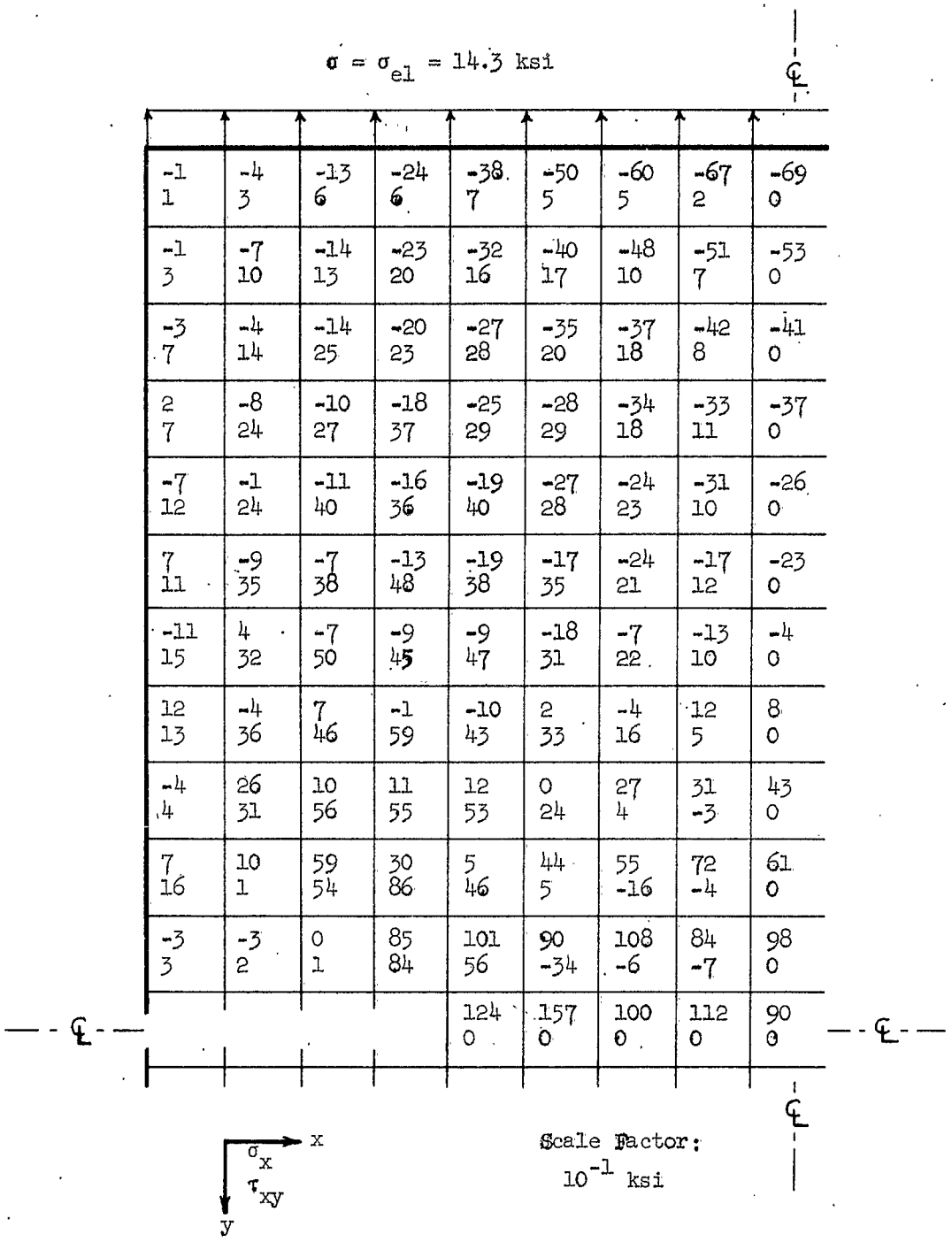

FIG. 21 HORIZONTAL AND SHEAR STRESSES

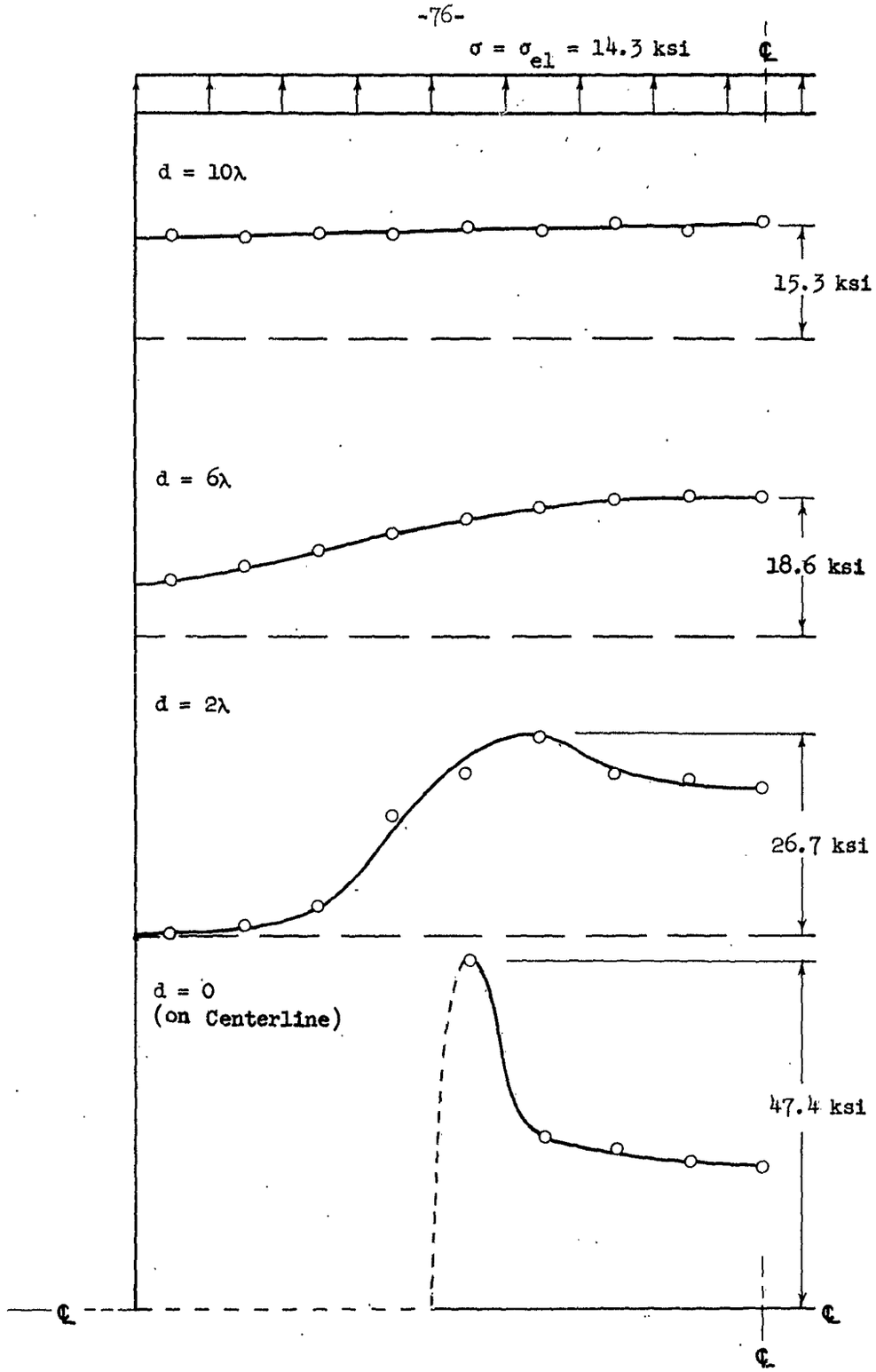

FIG. 22 VERTICAL STRESSES AT VARIOUS DISTANCES ABOVE HORIZONTAL CENTERLINE

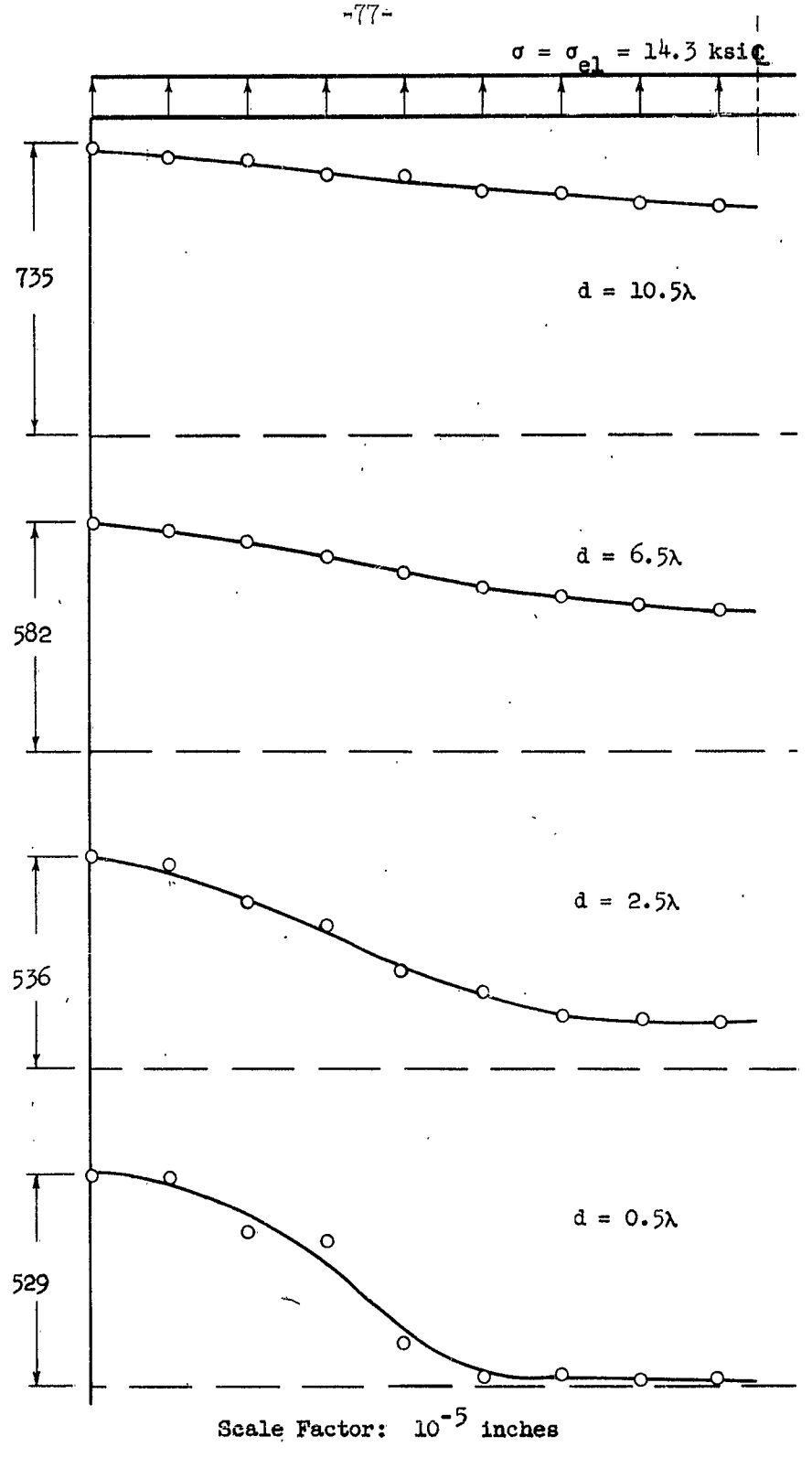

FIG 23 VERTICAL DISPLACEMENTS AT VARIOUS DISTANCES ABOVE HORIZONTAL CENTERLINE

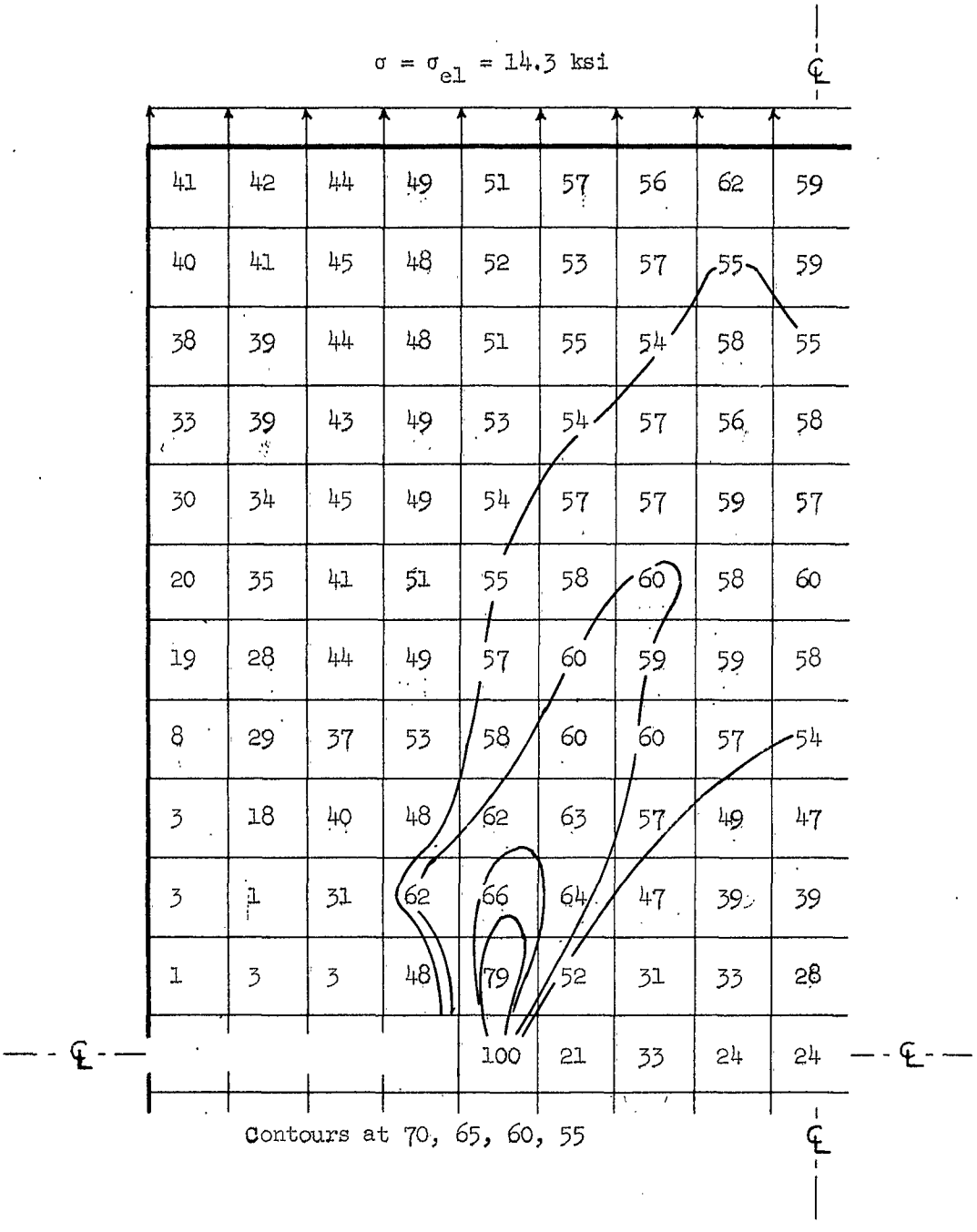

FIG. 24 EQUIVALENT SHEAR STRESS EXPRESSED AS A PERCENTAGE OF ITS MAXIMUM VALUE

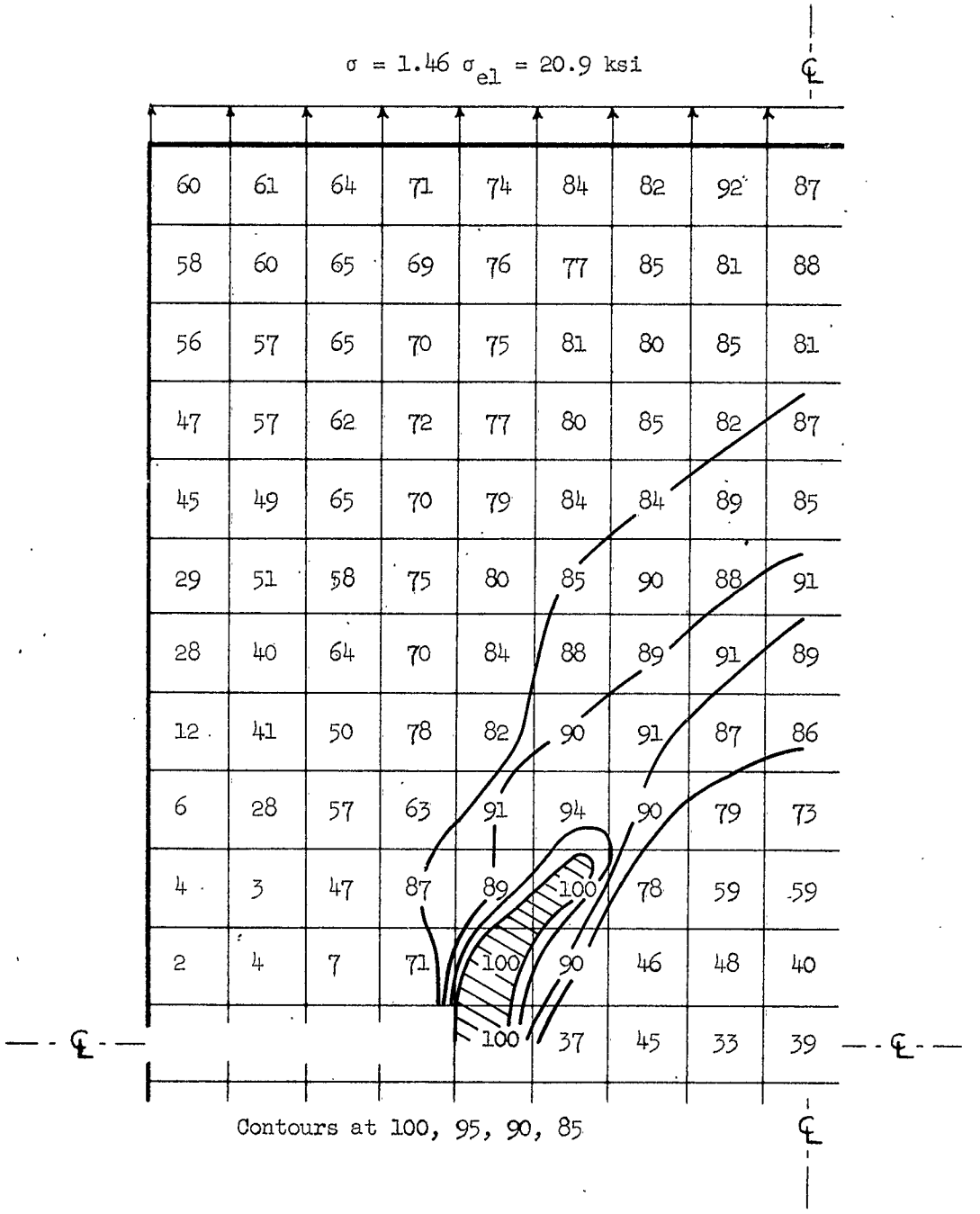

FIG. 25 EQUIVALENT SHEAR STRESS EXPRESSED AS A PERCENTAGE OF ITS MAXIMUM VALUE

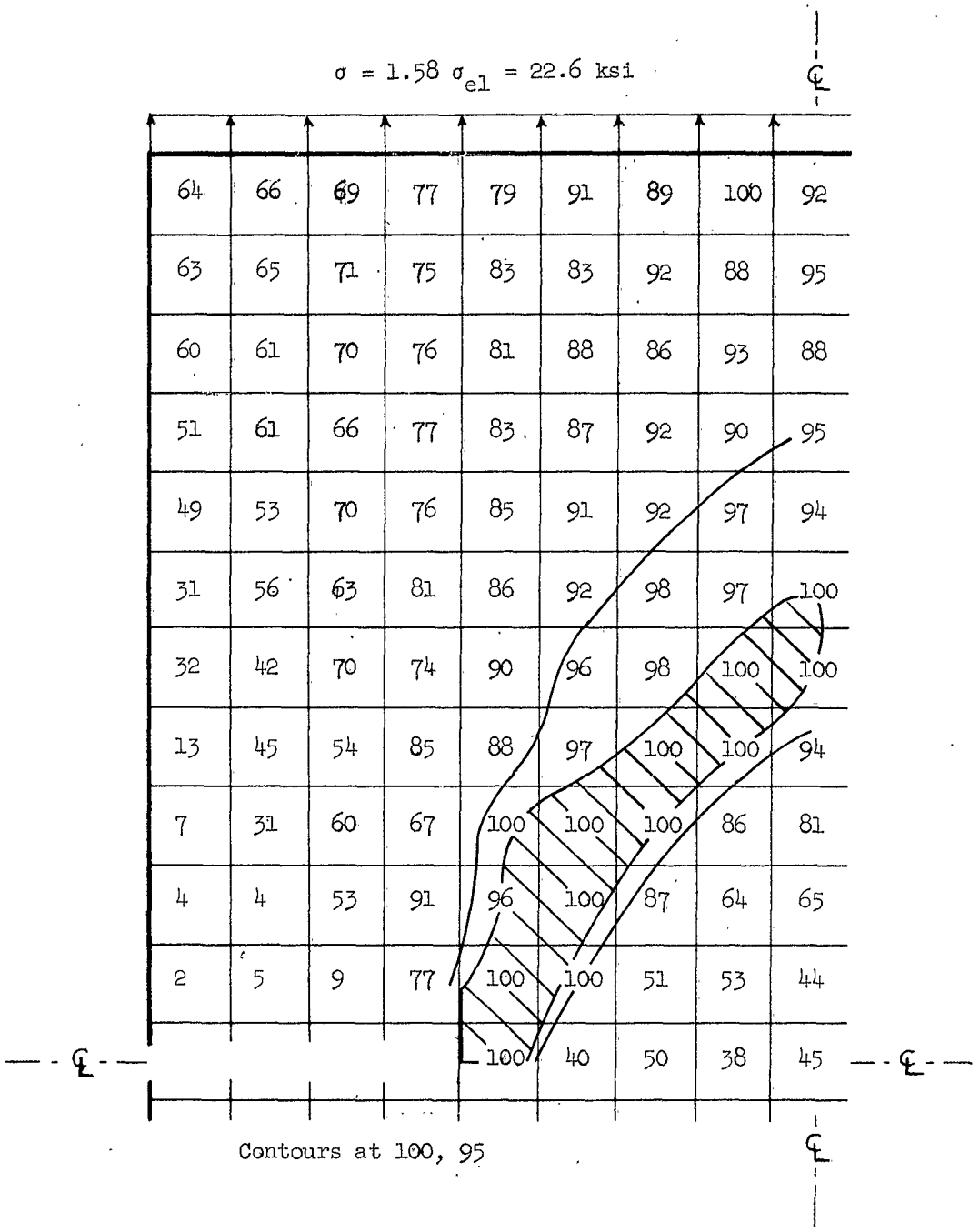

FIG. 26 EQUIVALENT SHEAR STRESS EXPRESSED AS A PERCENTAGE OF ITS MAXIMUM VALUE

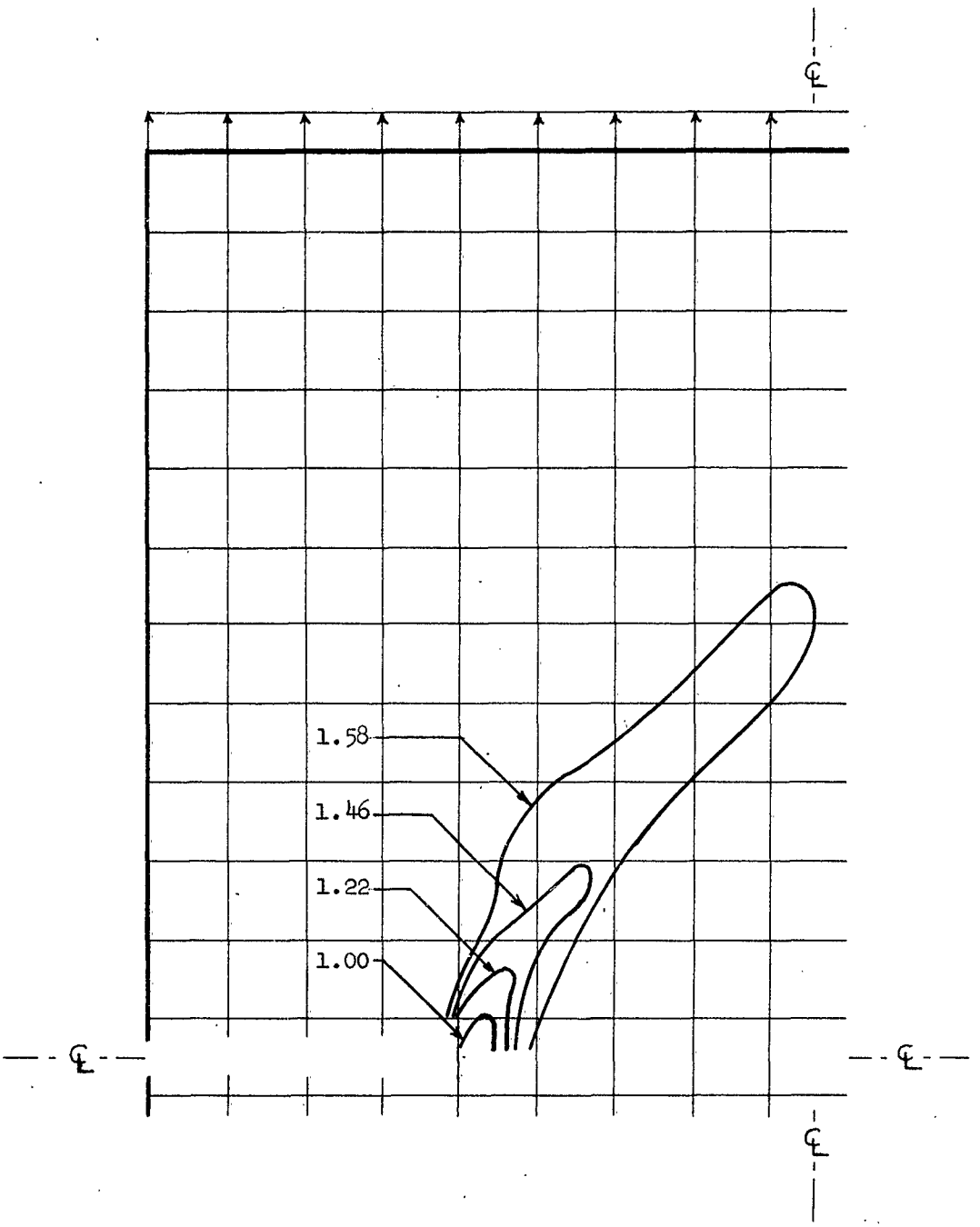

FIG. 27 PROGRESSION OF PLASTIC STRAINING FOR $1.00\sigma_{el}$, $1.22\sigma_{el}$, $1.46\sigma_{el}$, $1.58\sigma_{el}$

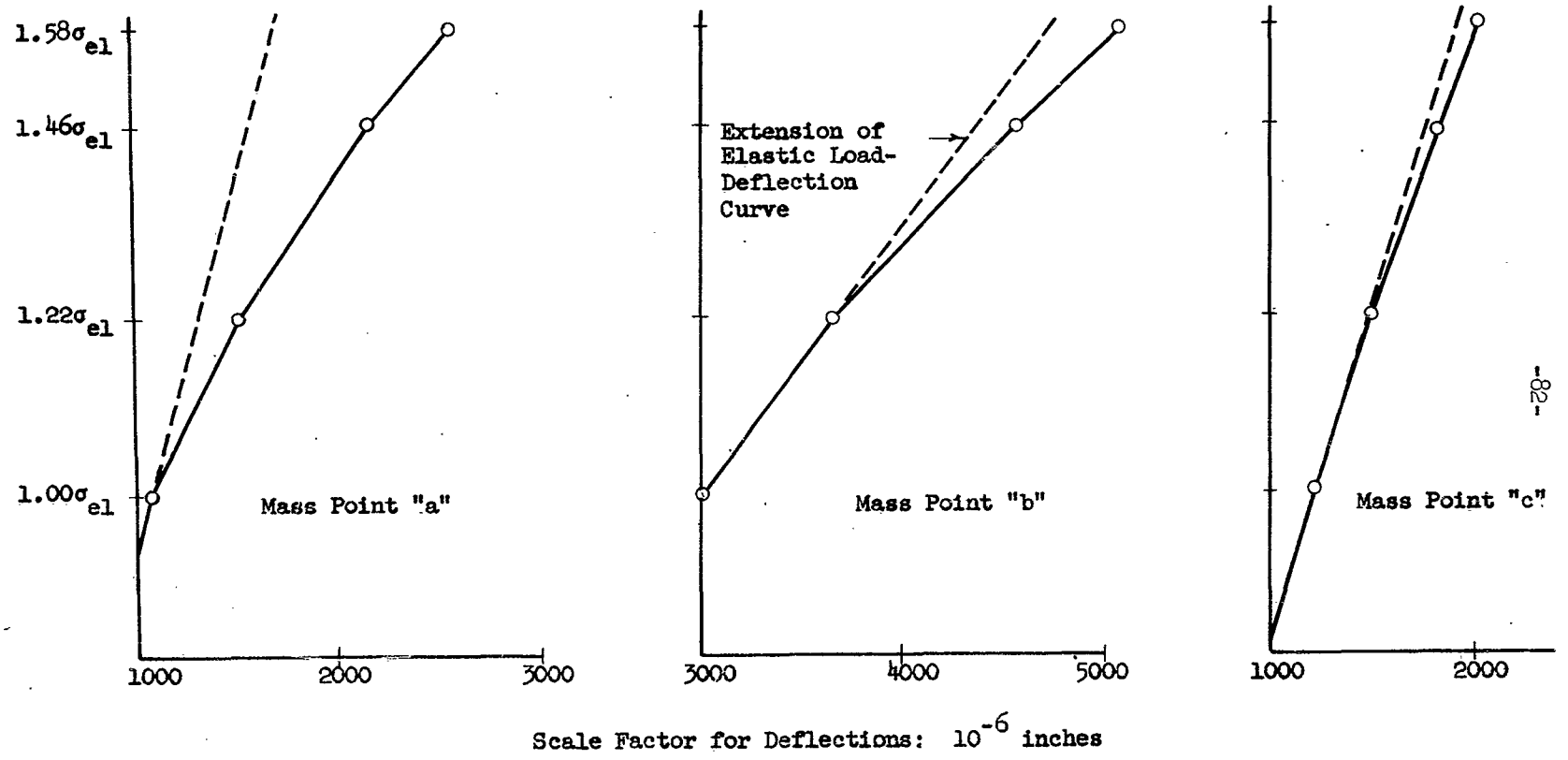

FIG. 28 LOAD-DEFLECTION CURVES FOR VARIOUS MASS POINTS

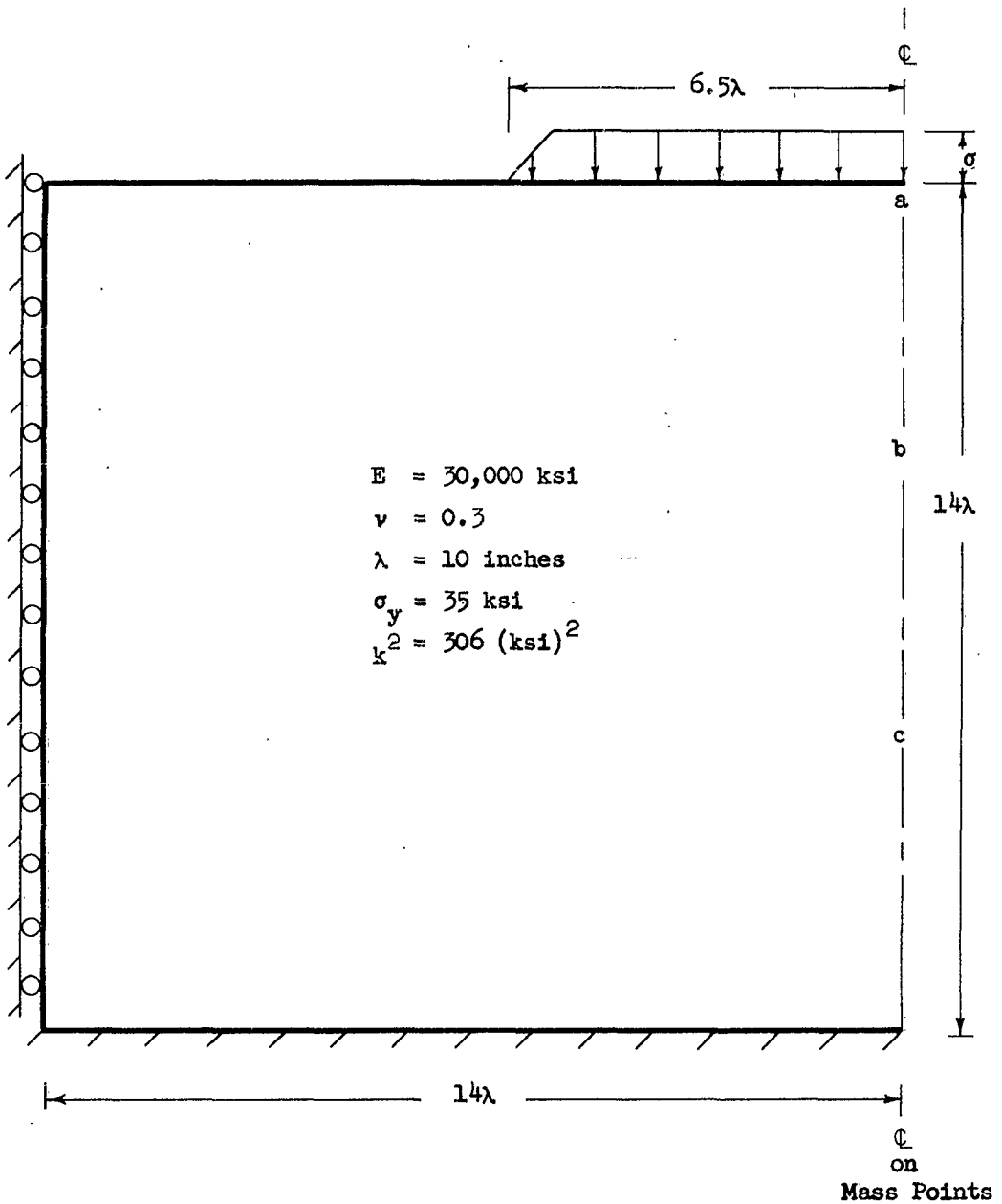

FIG. 29 DIAGRAM FOR PROBLEM 3:
A PARTIALLY LOADED HALF-SPACE

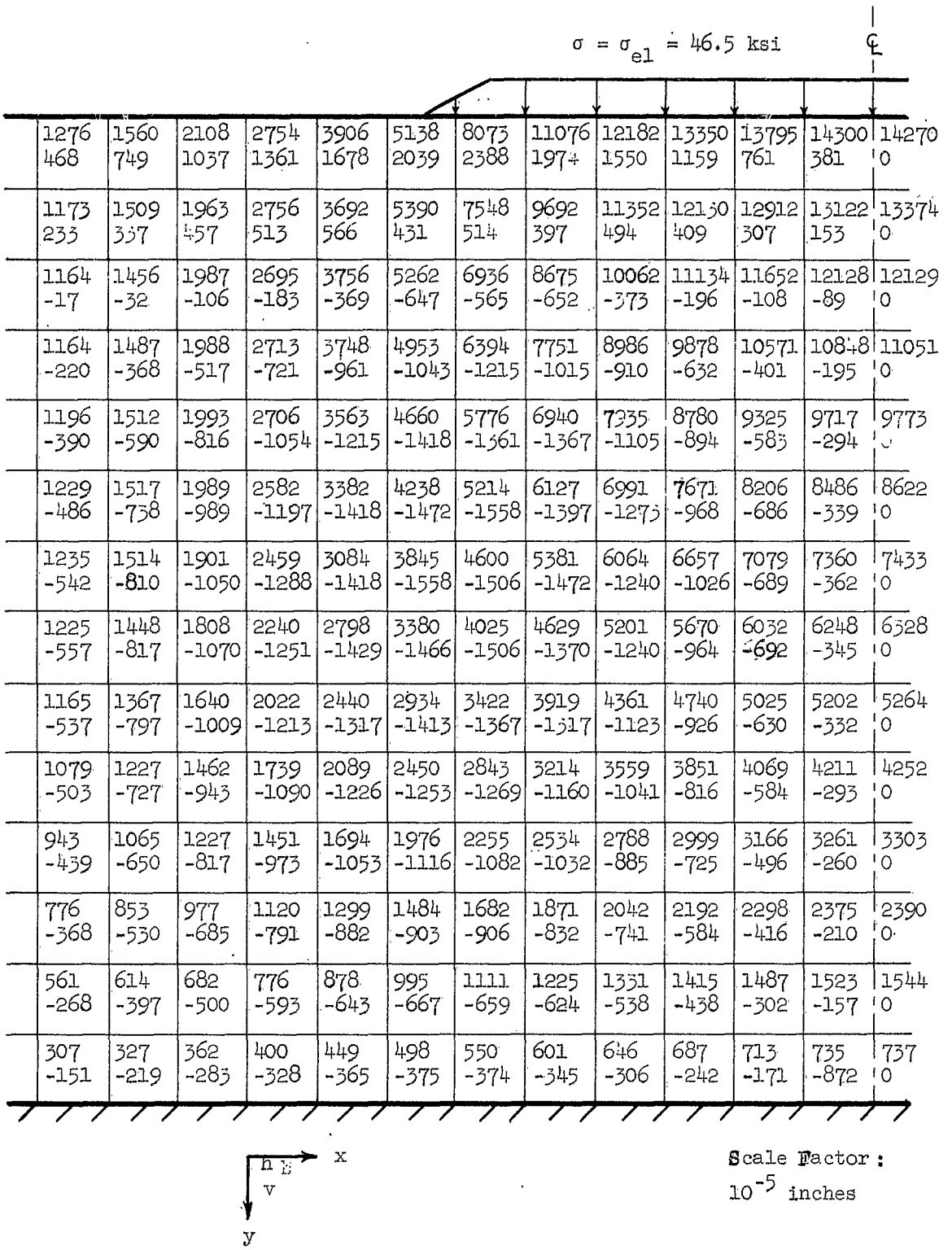

FIG. 30 HORIZONTAL AND VERTICAL DISPLACEMENTS

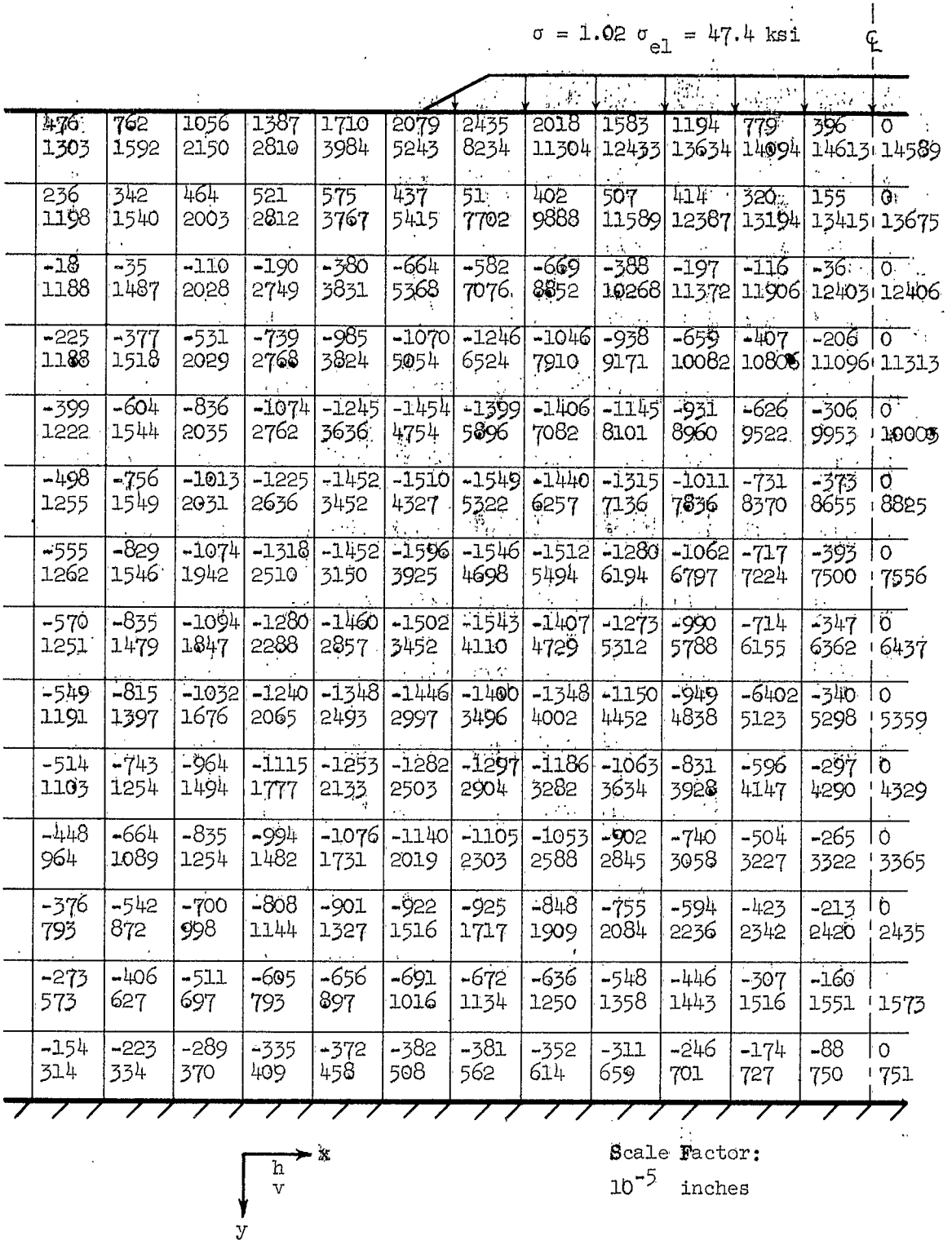

FIG. 31 HORIZONTAL AND VERTICAL DISPLACEMENTS

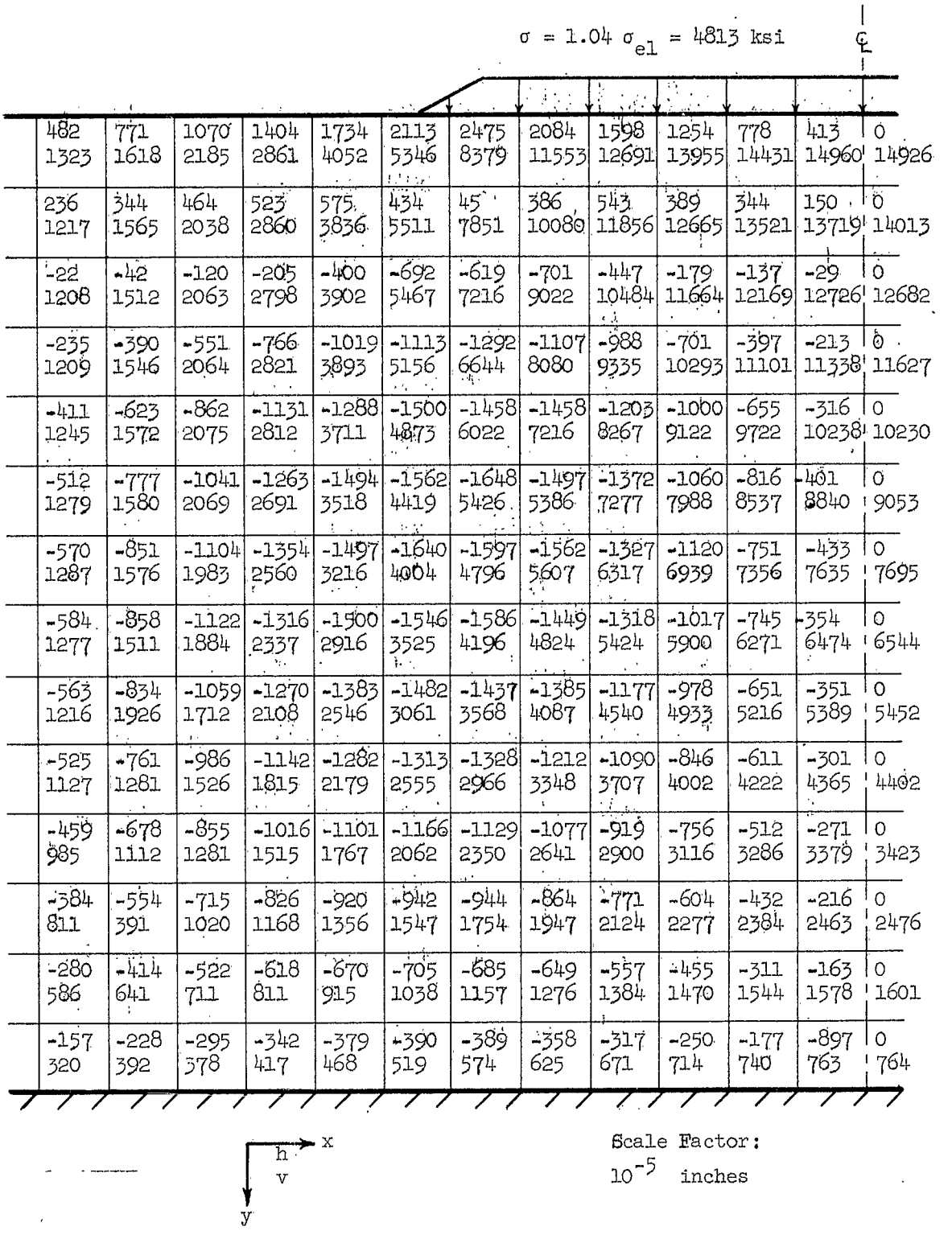

FIG. 32 HORIZONTAL AND VERTICAL DISPLACEMENTS

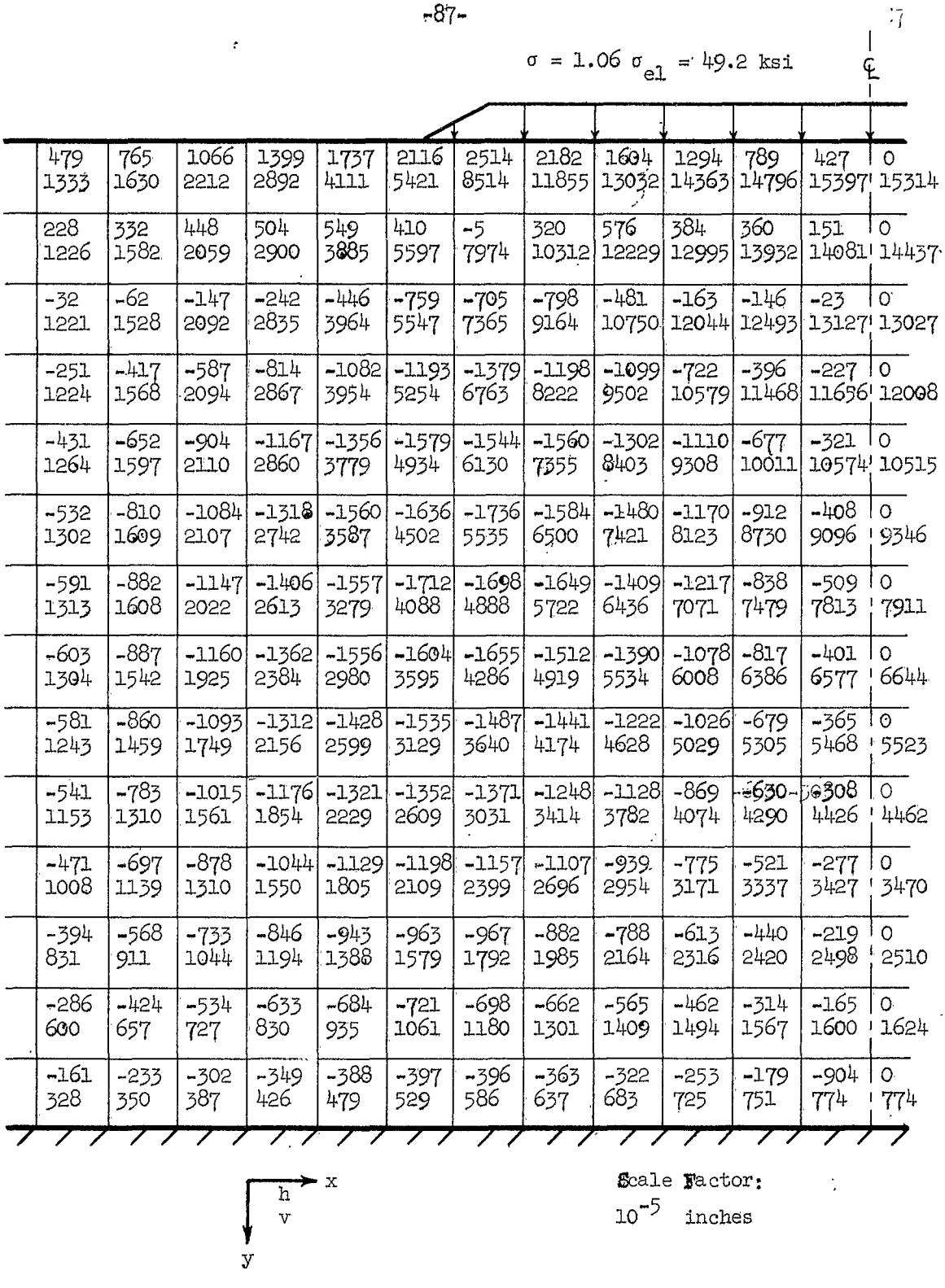

479 1333	765 1630	1066 2212	1399 2892	1737 4111	2116 5421	2514 8514	2182 11855	1604 13032	1294 14363	789 14796	427 15397	0 15314
228 1226	332 1582	448 2059	504 2900	549 3885	410 5597	-5 7974	320 10312	576 12229	384 12995	360 13932	151 14081	0 14437
-32 1221	-62 1528	-147 2092	-242 2835	-446 3964	-759 5547	-705 7365	-798 9164	-481 10750	-163 12044	-146 12493	-23 13127	0 13027
-251 1224	-417 1568	-587 2094	-814 2867	-1082 3954	-1193 5254	-1379 6763	-1198 8222	-1099 9502	-722 10579	-396 11468	-227 11656	0 12008
-431 1264	-652 1597	-904 2110	-1167 2860	-1356 3779	-1579 4934	-1544 6130	-1560 7355	-1302 8403	-1110 9308	-677 10011	-321 10574	0 10515
-532 1302	-810 1609	-1084 2107	-1318 2742	-1560 3587	-1636 4502	-1736 5535	-1584 6500	-1480 7421	-1170 8123	-912 8730	-408 9096	0 9346
-591 1313	-882 1608	-1147 2022	-1406 2613	-1557 3279	-1712 4088	-1698 4888	-1649 5722	-1409 6436	-1217 7071	-838 7479	-509 7813	0 7911
-603 1304	-887 1542	-1160 1925	-1362 2384	-1556 2980	-1604 3595	-1655 4286	-1512 4919	-1390 5534	-1078 6008	-817 6386	-401 6577	0 6644
-581 1243	-860 1459	-1093 1749	-1312 2156	-1428 2599	-1535 3129	-1487 3640	-1441 4174	-1222 4628	-1026 5029	-679 5305	-365 5468	0 5523
-541 1153	-783 1310	-1015 1561	-1176 1854	-1321 2229	-1352 2609	-1371 3031	-1248 3414	-1128 3782	-869 4074	-630 4290	-308 4426	0 4462
-471 1008	-697 1139	-878 1310	-1044 1550	-1129 1805	-1198 2109	-1157 2399	-1107 2696	-939 2954	-775 3171	-521 3337	-277 3427	0 3470
-394 831	-568 911	-733 1044	-846 1194	-943 1388	-963 1579	-967 1792	-882 1985	-788 2164	-613 2316	-440 2420	-219 2498	0 2510
-286 600	-424 657	-534 727	-633 830	-684 935	-721 1061	-698 1180	-662 1301	-565 1409	-462 1494	-314 1567	-165 1600	0 1624
-161 328	-233 350	-302 387	-349 426	-388 479	-397 529	-396 586	-363 637	-322 683	-253 725	-179 751	-904 774	0 774

FIG. 33 HORIZONTAL AND VERTICAL DISPLACEMENTS

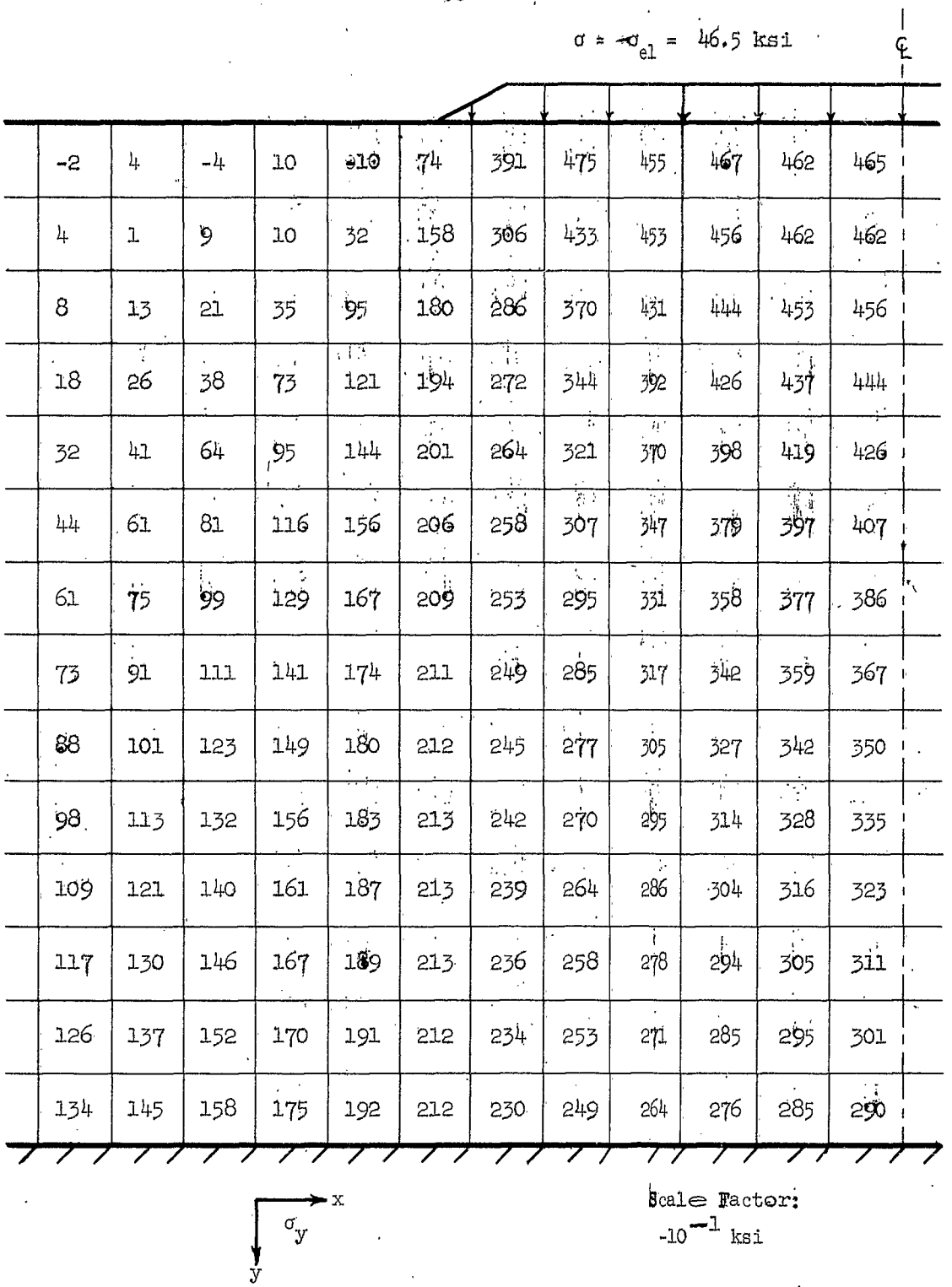

FIG. 34 VERTICAL STRESSES

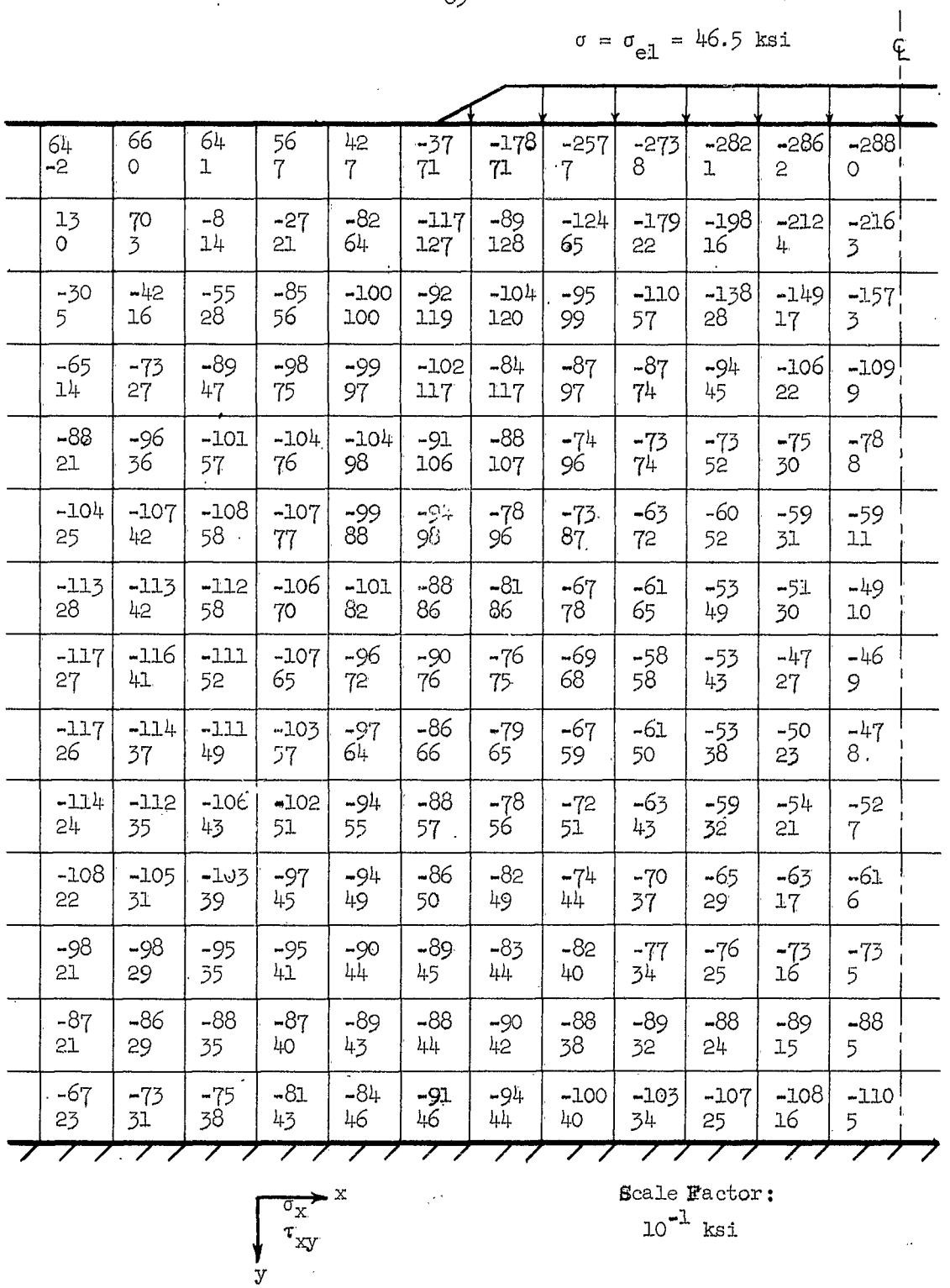

FIG. 35 HORIZONTAL-AND SHEAR STRESSES

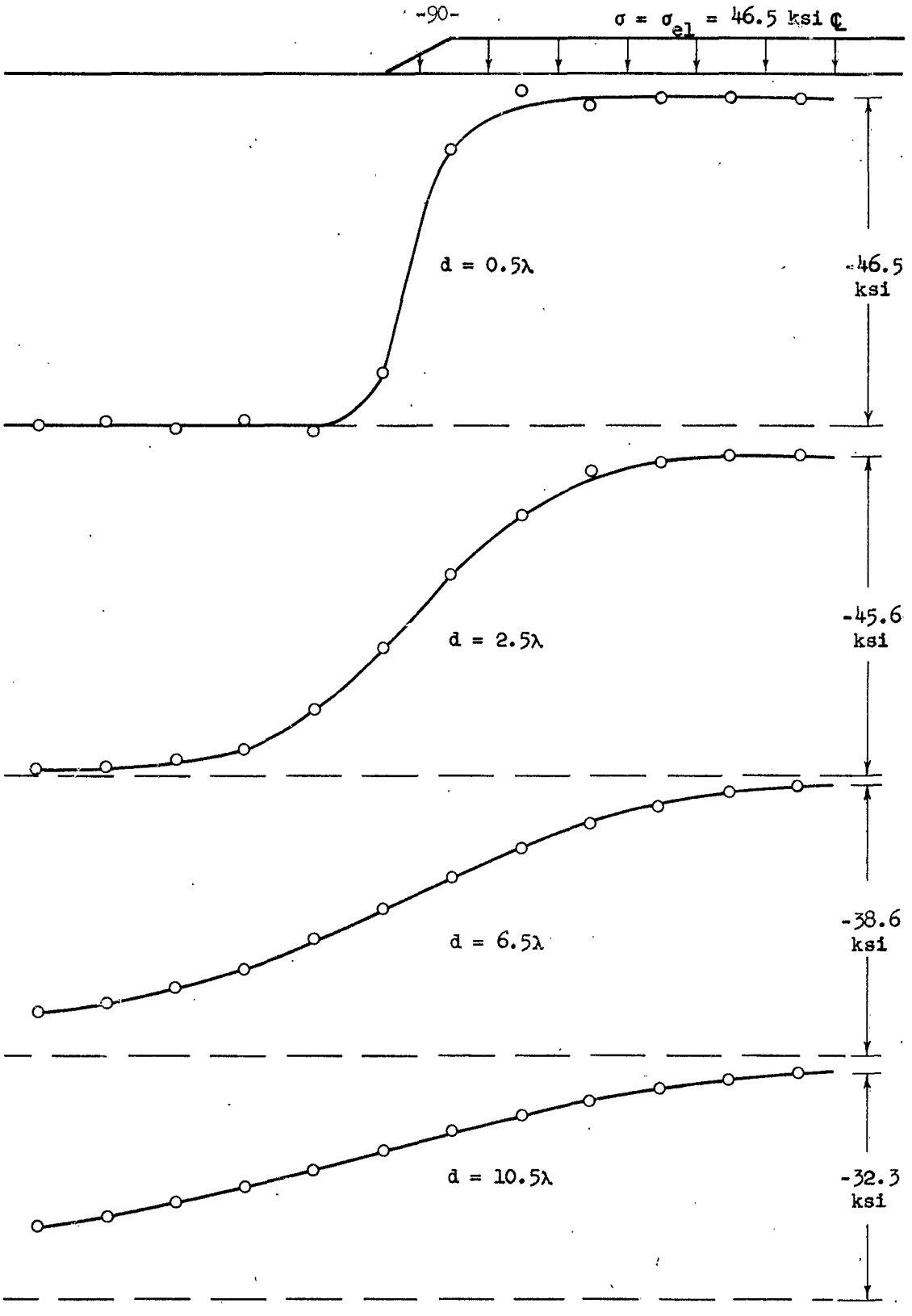

FIG. 36 VERTICAL STRESSES AT VARIOUS DEPTHS

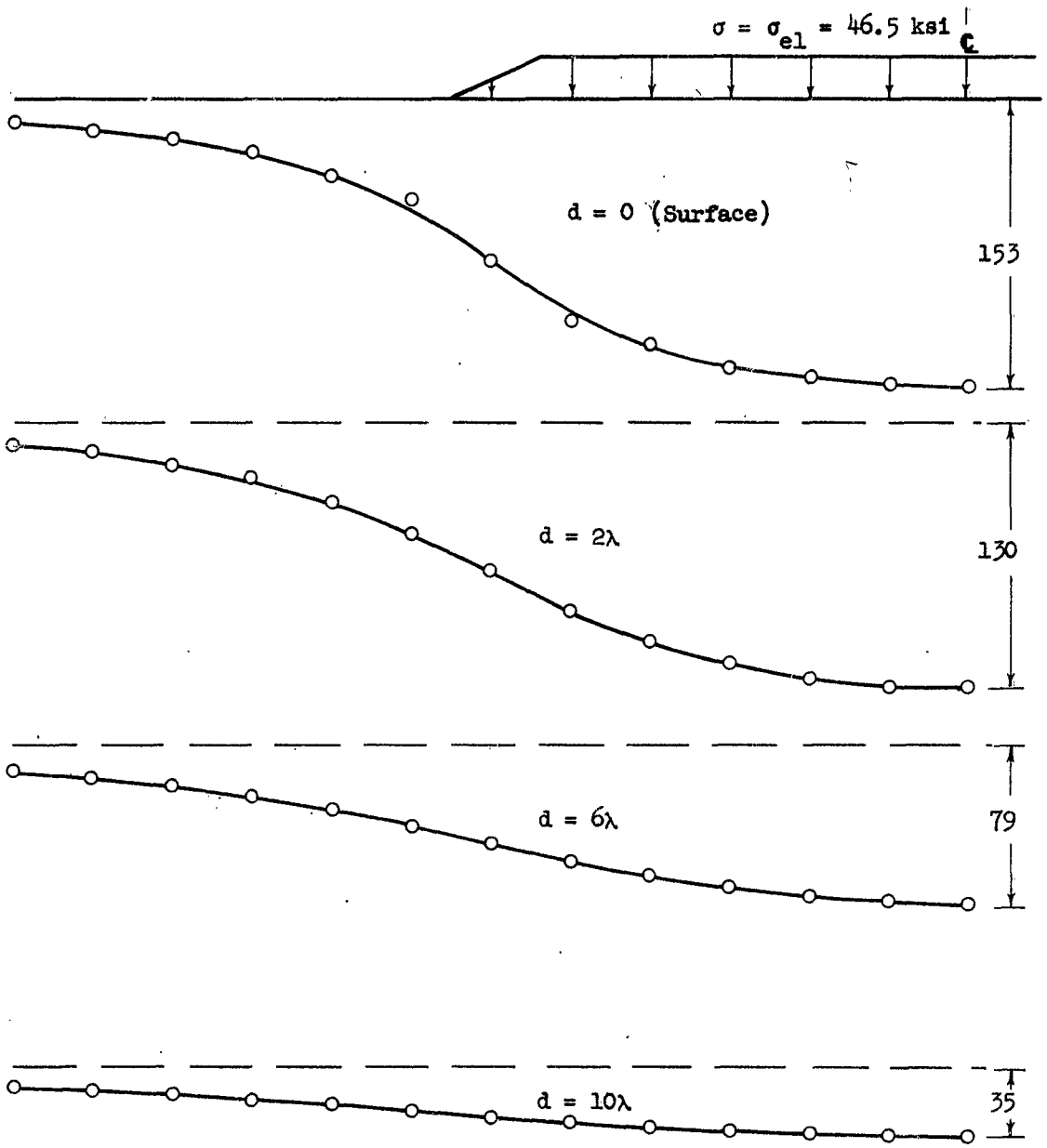

Scale Factor: 10^{-3} inches

FIG. 37 VERTICAL DISPLACEMENTS AT VARIOUS DEPTHS

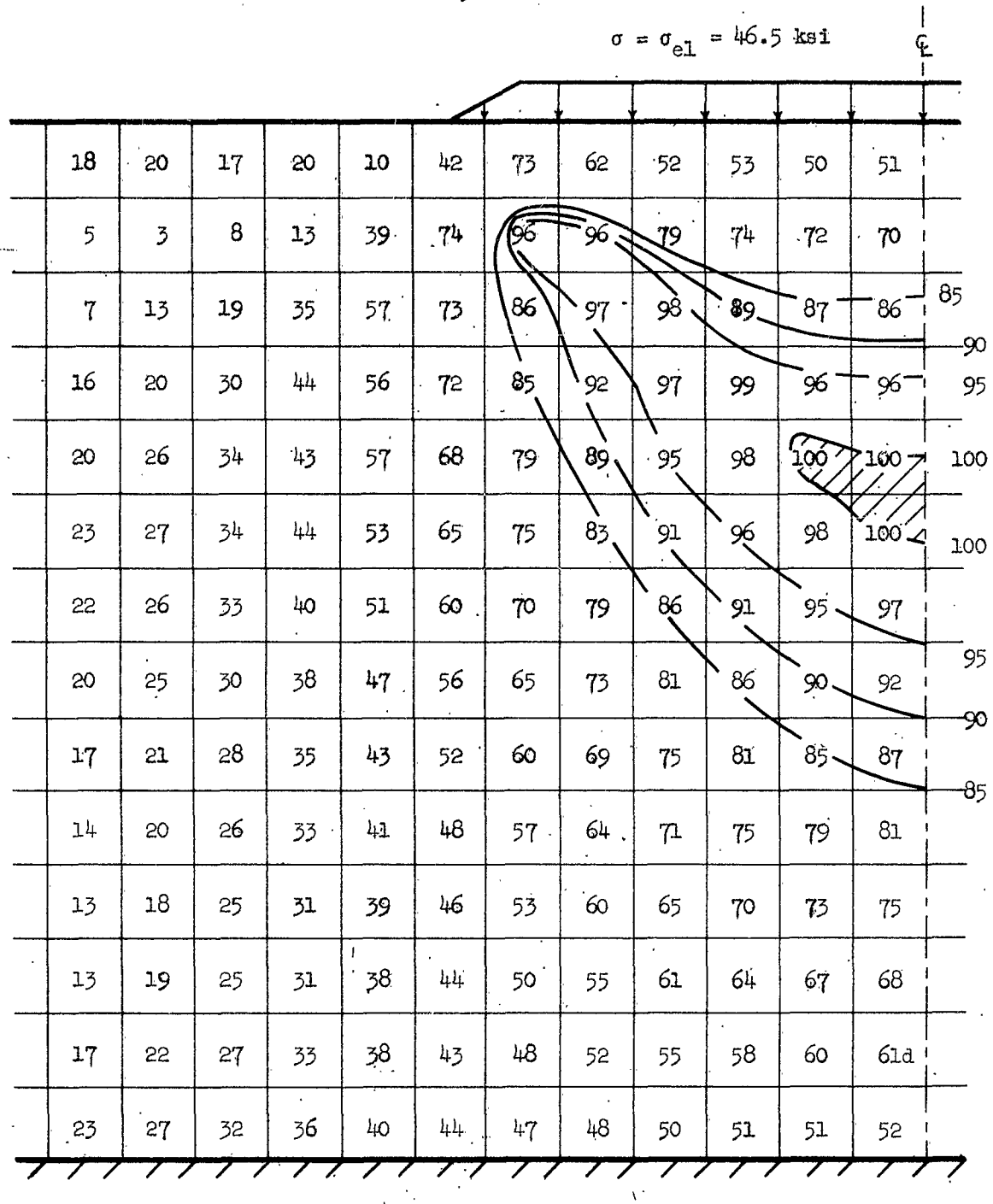

FIG. 38 EQUIVALENT SHEAR STRESS EXPRESSED AS A PERCENTAGE OF ITS MAXIMUM VALUE

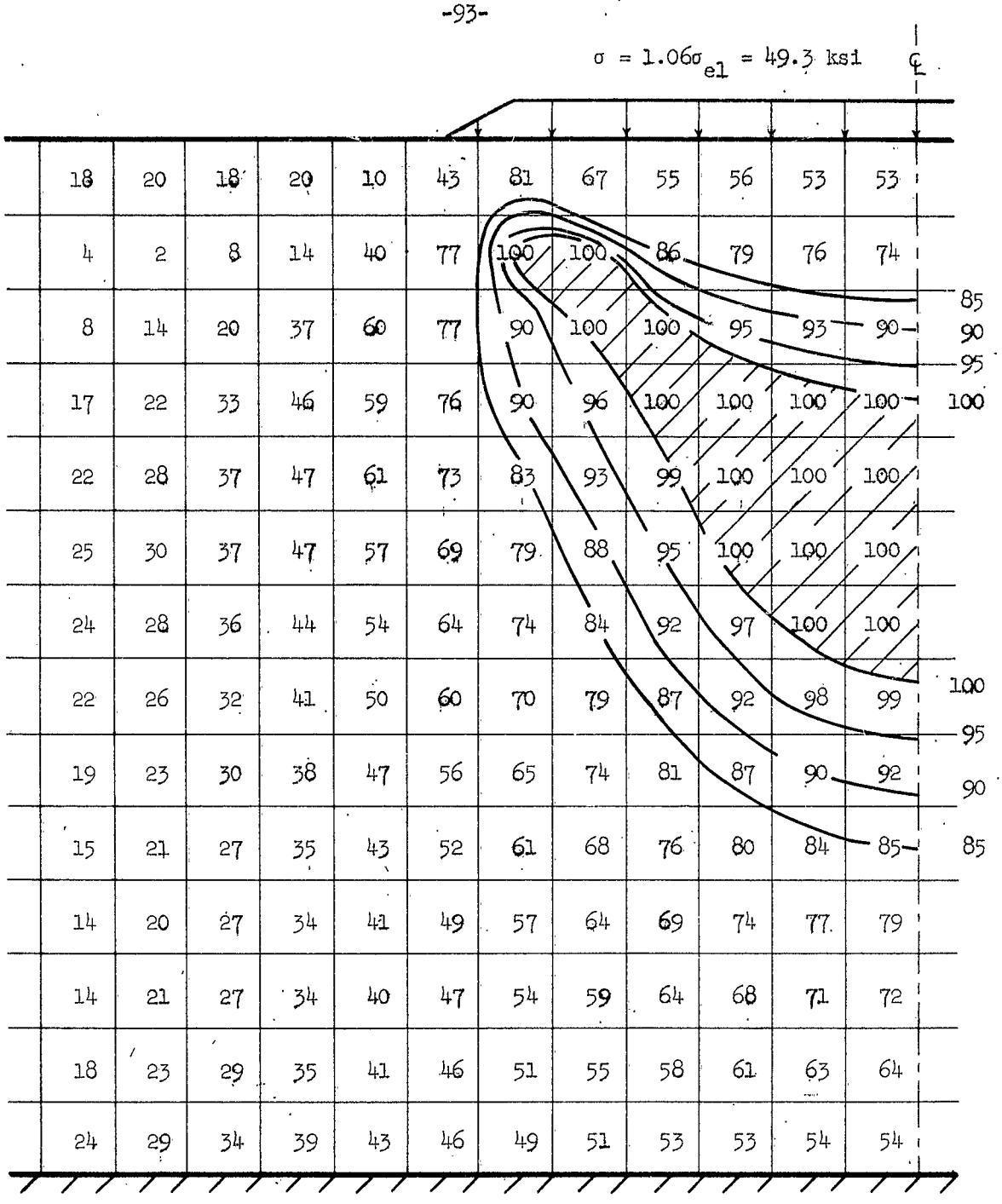

FIG. 39 EQUIVALENT SHEAR STRESS EXPRESSED AS A PERCENTAGE OF ITS MAXIMUM VALUE

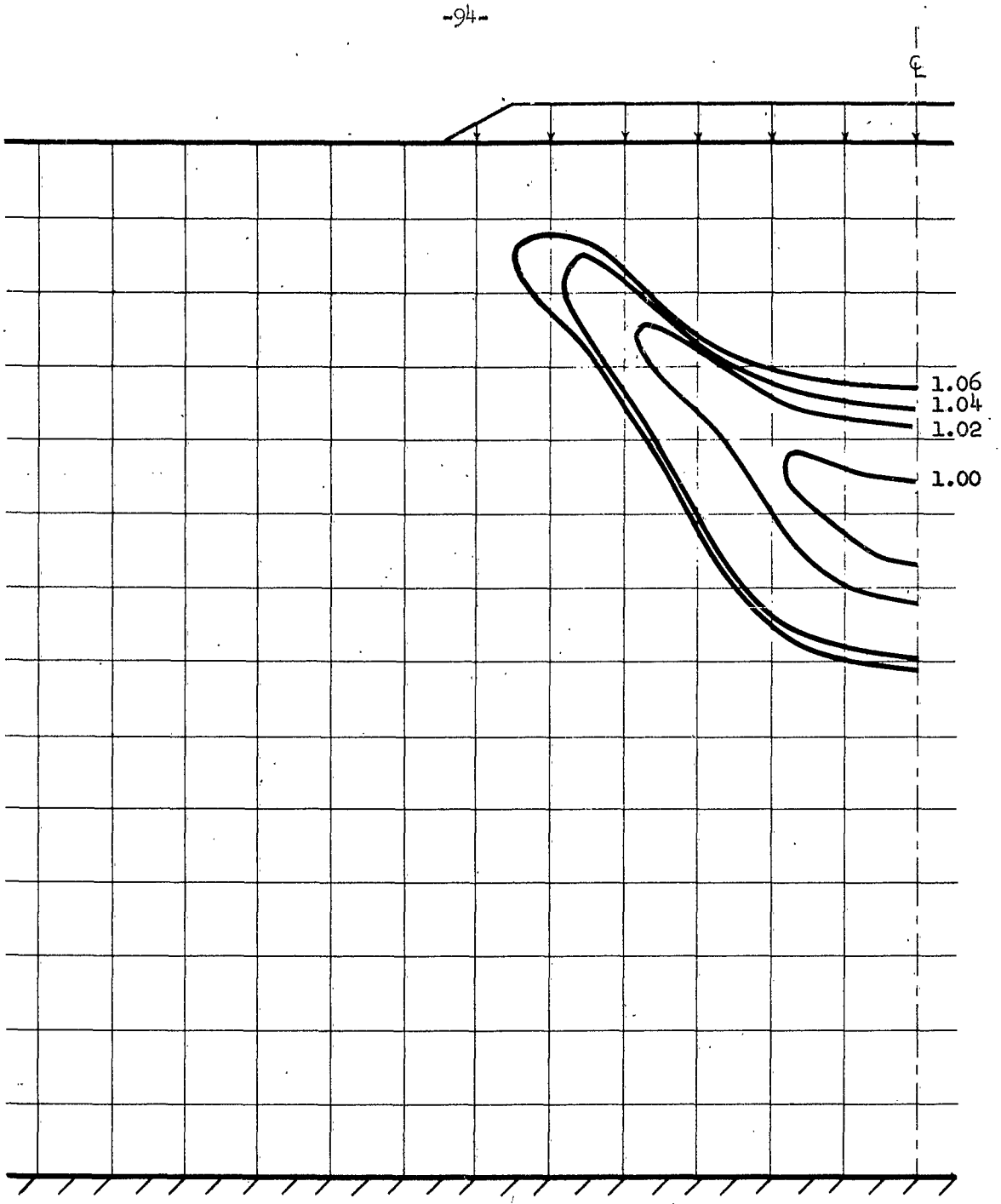

FIG. 40 PROGRESSION OF PLASTIC STRAINING FOR $1.00\sigma_{el}$, $1.02\sigma_{el}$, $1.04\sigma_{el}$, $1.06\sigma_{el}$

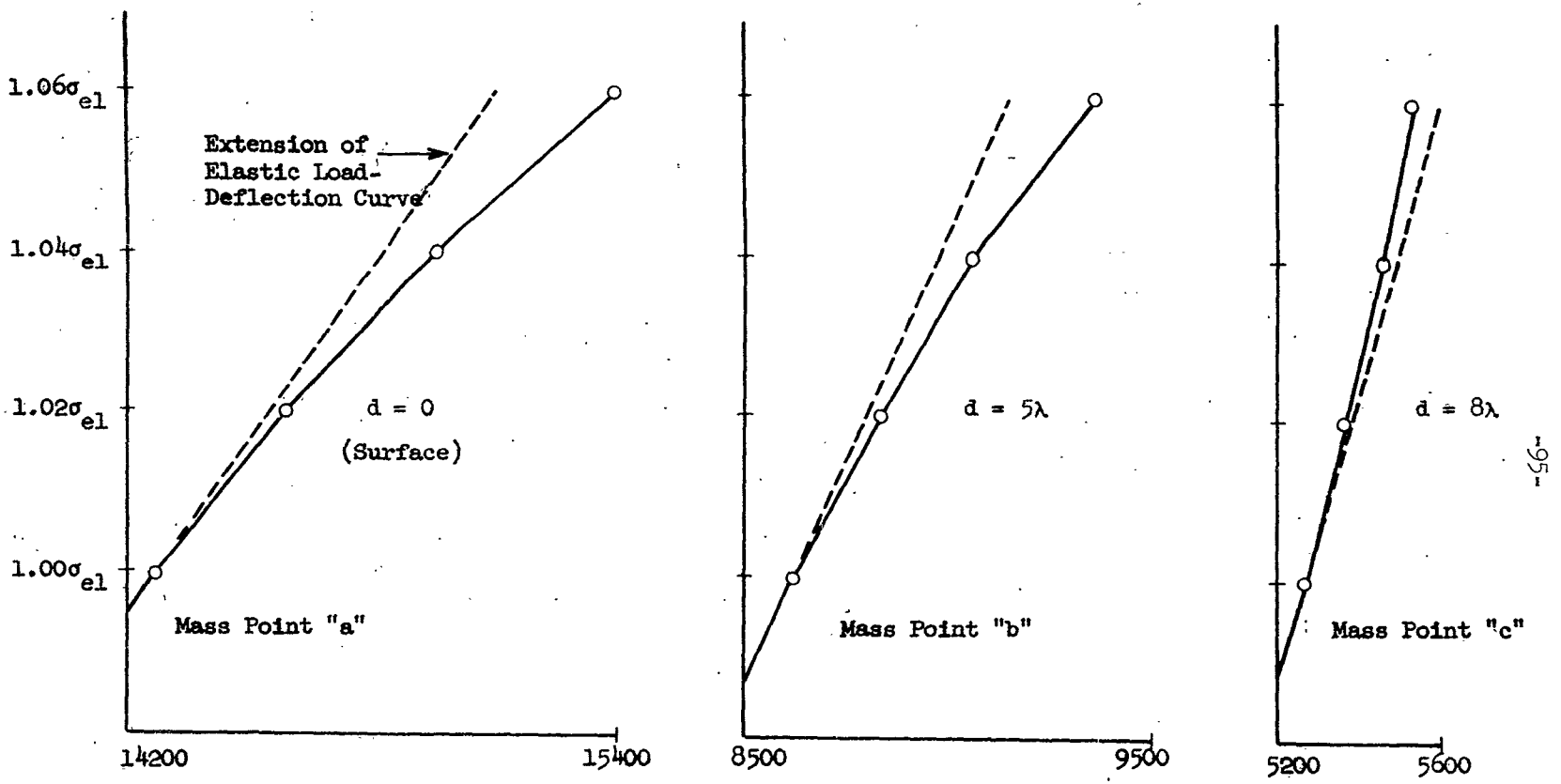

FIG. 41 LOAD-DEFLECTION CURVES FOR CENTERLINE DEFLECTIONS AT VARIOUS DEPTHS